THE EFFECT OF FLOW INDUCED EROSION ON RIVERBANK STABILITY ALONG THE RED RIVER IN WINNIPEG

by

LEANNE FERNANDO

A Thesis
Submitted to the Faculty of Graduate Studies
in Partial Fulfillment of the Requirements for the Degree of

Master of Science

Department of Civil Engineering
University of Manitoba
Winnipeg, Manitoba

August, 2007

THE UNIVERSITY OF MANITOBA

FACULTY OF GRADUATE STUDIES

*****

COPYRIGHT PERMISSION

THE EFFECT OF FLOW INDUCED EROSION OF RIVERBANK STABILITY ALONG THE RED RIVER IN WINNIPEG

A Thesis submitted to the Faculty of Graduate Studies of The University of

Manitoba in partial fulfillment of the requirement of the degree

of

Master of Science

LEANNE T. FERNANDO © 2007

ABSTRACT

A research program was undertaken to quantify the effect of flow induced erosion on the stability of natural river banks along the Red River in Winnipeg, Manitoba. The study correlated the percent decrease in factor of safety to intensity of river flow and duration. Two methods to quantify flow induced erosion were assessed, the first method based on observed erosion and the second on theoretically calculated erosion.

The first method involved aligning annual historical river bank cross-sections and measuring the distance between cross-sections to represent the erosion induced from the flow year between successive cross-sections. Due to the fact there are no sites along the Red River regularly surveyed, the analysis did not provide for a correlation between erosion from a specific flow event to percent decrease in factor of safety. The second part involved the use of theoretical equations to quantify erosion given the river elevation of a specific flow year. The study showed a 1% to 8% decrease in factor of safety from low to high intensity flows and as high as 14.5% for high intensity flows of long duration. Additionally, the evolutionary stability of the riverbank was generated showing the percent decrease each year in factor of safety due to erosion and the years during which failure occurs. The results correlated well to the previous analysis showing a 1% to 5% decrease for low to high intensity flows respectively and as high as 10% for high intensities of long duration.

ACKNOWLEDGEMENTS

I would like to acknowledge the support of my advisor Dr.James Blatz who has provided me with the guidance, advice and encouragement to complete my thesis. It has been a long process but he helped me to persevere. I would also like to recognize the technical assistance I obtained from Shawn Clark and Don Kingerski.

More importantly, I would like to acknowledge my family who provided support every step of the way. In particular, my partner Brent for his patience and understanding, parents Blaise and Pearl for their care and concern, sister Lisa for always listening and brother-in-law Darrell.

TABLE OF CONTENTS

LIST OF FIGURES

LIST OF TABLES

CHAPTER 1: INTRODUCTION

1.1 Importance of Riverbank Research to the City of Winnipeg

The City of Winnipeg has over 240 km of waterfront property with the Red River as the primary waterway that runs through the City. The property along the river is considered to be one of the City's most valuable natural assets. The natural beauty of the river has made waterfront properties prime real-estate for residential landowners, apartment buildings, City parks and public facilities. However, many of these properties have riverbanks that are unstable and have either experienced massive slope failures in the recent past or are currently at severe risk for failure. The direct impact of these failures is significant loss of land which can undermine nearby structures and decrease overall property value.

During the spring/summer of 2005 the Winnipeg Free Press published an article about the abnormally high number of riverbank failures experienced that year, given in Appendix A. The article identified 25 sites that showed extensive slope failures and focused on two private landowners whose properties were severely affected. One of the landowners claimed a 6 m loss of property which undermined a gazebo located near the riverside. In addition, this same property experienced 7 m of land loss following the 1997 flood. The high number of slope failures during the 2005 season was attributed to the abnormally high water levels experienced that summer.

The failures are a significant concern not only from the standpoint of loss of property but also with respect to the high cost associated with stabilizing failed banks. In a report written in 2000 by the City of Winnipeg, 49 City-owned properties were identified as requiring stabilization at a total cost of $36.6 million. In the longer term, the report stated that the cost to stabilize the remainder of the City owned properties to prevent future failures was an additional $41 million. With respect to remediating private properties, landowners are responsible for repairing their own properties with little financial assistance available from the City. Repairs can cost on average $50,000 per property (Winnipeg Free Press article, 2005).

Given the value of this natural asset to the City and citizens of Winnipeg and the high cost associated with remediating failed riverbanks, there is a need to gain a better understanding of the causes of riverbank failure and subsequently design appropriate preventative measures. Several factors contribute towards destabilizing riverbanks, in particular erosion, which has been recognized as the cause of numerous failures. Erosion is viewed as a significant contributor towards instability, although little research has been undertaken to quantify how the effects of erosion reduce stability. The purpose of this research is to quantify how flow-induced erosion affects overall riverbank stability. The research will test the hypothesis:

"Evolutionary stability of natural riverbanks is linked to both intensity and duration of river flows that cause erosion along the lower toe and mid-bank regions"

1.2 Objectives and Organization of Thesis

Objectives of the research include the following:

1. Quantify flow-induced erosion from different flow events along riverbanks of the Red River using:
   - historical surveyed riverbank cross-sections
   - theoretical equations to calculate post-erosion cross-sections
2. Assess the stability of eroded cross-sections and relate percent decrease in factor of safety to flow events
3. Examine the current Winnipeg practice of assuming an annual 10% decrease in factor of safety due to erosion

A brief summary of past riverbank stability research along the Red River is covered in Chapter 1 with an in-depth literature review of river morphology and quantification of flow induced erosion provided in Chapter 2. Details of the two-part modeling study are provided in Chapter 3 and 4 with a discussion of the results and recommendations for future work in Chapter 5. Final conclusions are summarized in Chapter 6.

1.3 Past Research

Slope stability research in Winnipeg has been on-going since the 1960's by a number of researchers. Early studies conducted by Baracos (1960) focused on the correlation between actual and theoretical safety factors for slope stability where factors of safety had been greater than 1.0 for slopes that had experienced failure. An on-going concern was that actual shear strength of clay at failure was much less than laboratory measured undrained shear strengths. Baracos (1960) formulated a method for analyzing slope stability based on modified shear strengths along parts of the failure plane using total stress analysis.

Mishtak (1962) surveyed natural riverbanks in Winnipeg to investigate the slope at which riverbanks were found to be stable, the slopes at which they failed and slopes that they became stable following failure. The ultimate goal of the research was to recommend the slopes at which the Winnipeg Floodway were to be designed and constructed based upon observations of natural riverbanks. Only six riverbanks were determined to be stable of the 141 riverbanks surveyed. Mishtak (1962) noted that practically every bank on the outside of a river bend had previously been affected by an old slide, was actively moving, or had required slope stabilizing measures. His conclusions from the study were that very few riverbanks were found to be stable and those that were stable were at a slope at 6:1 or flatter. This research was followed by Sutherland (1966). The investigation focused on conventional methods of slope stability using laboratory

undrained shear strengths and concluded that these shear strengths should not be applied to Winnipeg clays as they over-estimate stability when applied to the end-of-construction and long term stability condition. An empirical method of maintaining slopes at 6:1 for banks that had no previous sliding and 9:1 for banks where previous sliding was observed was suggested for design.

Full-scale experimental research was initiated with the investigation of slope failures at two sites along the Red River (Baracos 1971). It was the first study that continuously monitored in-situ porewater pressures and slope movements over a long term period. The findings of the study showed that the banks underwent virtually no movement during the spring and summer when the river level was high. However rapid movements occurred after the river level was lowered in the fall and continued at a decreasing rate through the winter. Other factors that were observed to influence the stability included spring snow melt, precipitation and the possibility of leaking water mains and sewers.

This research was followed by Freeman and Sutherland (1974) who studied the stability of slopes in anisotropic clays. They studied the mechanisms of slope failure and in particular failures along non-circular arcs. They concluded that it is not appropriate to use residual shear strengths for the entire length of slip surface because it underestimates the factor of safety. The preceding studies by Baracos (1960, 1971), Mishtak, (1962) Freeman (1974) and Sutherland (1966, 1974), showed that neither undrained shear strengths nor effective stress

strengths could be used to successfully predict slope stability in Winnipeg clay. Instead, it was later shown the parameters required for stabilizing slide areas in Winnipeg are residual shear strengths of c' = 0 and phi' = 8 - 13 degrees, with careful consideration of the worst combination of porewater pressures and river elevation (Baracos 1978).

More recently a research program was undertaken which studied the effects of seasonal variations of the river and upper carbonate aquifer elevations on riverbank stability (Tutkaluk 2000, Tutkaluk *et al*. 2002). Finite element modeling software was used to model the slope stability over a 97 day time period considered the most critical period of stability when the river level decreases and bedrock aquifer levels increase. The factor of safety was quantified continuously over the period and showed a decrease of 13% to 17% at the end of the period. Finally, in 2001 a report was submitted to the Government of Canada compiling studies over a ten year period on the phenomenon of riverbank sliding along the Red and Assiniboine Rivers. Among the major conclusions of the report was that flood conditions on the Red River cause severe lower bank and river bottom erosion and such erosion is a primary cause of the commonly observed deep-seated riverbank sliding (Baracos and Lew 2003).

Baracos and Lew (2003) gave a qualitative assessment of the primary causes of riverbank slides, one of which was erosion due to high river flows. The goal of this research study is to take these observations one step further and quantify

the effect of erosion on bank stability. As Tutkaluk (2000) successfully quantified the effect of seasonal variations of bedrock aquifer and river levels on slope stability, this research will be an extension by combining the latter effects with erosion to quantify the overall effect on slope stability.

CHAPTER 2: LITERATURE REVIEW

2.1 Introduction

The following sections outline theory and background information required to understand the research program described. The first section describes the basic principles of river systems including hydraulics of flow and channel morphology. This is followed by a brief discussion regarding common characteristics of the Red River and frequently observed causes of riverbank instability. Finally, an in depth discussion regarding riverbank erosion is provided that includes theoretical equations and numerical methods to quantify erosion.

2.2 River Systems

Rivers serve two primary purposes (Morisawa 1968):

1. Transport water that drains from the Earth's land surface back to the Ocean.
2. Transport sediment entrained into the water by the shearing action of flow over the bed and banks of the channel.

The climate and geology of a region are the primary factors that determine the characteristics of flow and sediment load (Morisawa 1968). The climate determines the amount of water that precipitates onto the land surface and subsequently the discharge of the river. The geology of the region determines

the composition of the channels bed and banks in addition to the concentration and caliber or grain size of the sediment load. Both the discharge and sediment load are secondary factors that directly influence the morphology of the river.

River morphology is defined as the time-dependent evolution of the longitudinal profile and transverse cross-section of the channel and its associated pattern (Morisawa 1968). The climate and geology are first-order independent variables that determine the second-order variables of discharge and sediment load. The variables collectively interact to determine the third-order morphologic configuration of the river as shown in Figure 2.1. If there is a change in any one of these variables, the river responds by altering its morphology to counteract the effect. It is a process/response system in which a change in any part of the system requires a response that can occur at the location of the disturbance or be transferred downstream to another location in the system (Morisawa 1985). The processes that alter the morphology include erosion or entrainment, transportation of sediment load and deposition (Richards 1982).

2.2.1 Hydraulics of Flow

Sediment entrainment from the bed and banks of a channel is caused by erosion that results from the shear stress of water acting over the cross-section of the channel. Shear stress is directly related to the velocity gradient and fluid viscosity as defined by Equation 2.1 (Knighton 1998). An increase in the velocity gradient corresponds to a subsequent increase to the shear stress.

$$\tau = \upsilon \frac{dv}{dy}$$ Equation 2.1

where,

τ = shear stress

dv/dy = velocity gradient

υ = viscosity

Figure 2.2 shows the velocity distribution of laminar flow in a symmetrical river channel cross-section. The figure shows a parabolic velocity distribution along the channel depth with the velocity decreasing to zero at the channel bed due to frictional resistance between the fluid and channel bed (Knighton 1998). The velocity gradient is at a maximum near the bed and lower bank region. These surfaces experience the greatest amount of erosion because they have the highest shear stress acted upon them. Flow can be described as laminar or turbulent. Laminar flow is characterized by layers of fluid moving overtop of each other in an orderly manner. In comparison, turbulent flow is described as the chaotic movement of fluid which causes greater erosion (Morrisawa, 1968).

The velocity distribution further depends on the configuration of the cross-section. Figures 2.3 and 2.4 show the mean velocity distribution (lines of equal velocity) for different symmetrical and asymmetrical channel cross-sections. In general, the isovels are closer together near the boundaries of the cross-section, with the maximum observed velocity towards the center of the channel due to the

decline in frictional effects from the channel banks (Knighton 1998). Where the isovels are closer together shows the areas where the velocity gradient and therefore shear stresses, are highest. Depending on the channel cross-section, the distribution of isovels may be more closely spaced around the banks as opposed to the bed. In wide shallow sections, the shear stress is greatest at the bed. In narrow deep sections, the shear stress is greatest on the banks which produces greater bank erosion (Knighton 1998). When compared to asymmetrical cross-sections, such as the one shown in Figure 2.4, the velocity distribution becomes skewed. The maximum velocity shifts from the center to the outer edge of the channel as shown in Figure 2.4 (Morisawa, 1985).

When the velocity exceeds a critical value of the Reynolds number defined by Equation 2.2, the flow becomes turbulent. The Reynolds number expressed by Equation 2.2, represents the ratio of inertial to viscous forces and is defined by the density (ρ), mean velocity (V), hydraulic radius (R) and the viscosity (υ). If the Reynolds number is less then 500, the flow is laminar; if it is greater than 2500 the flow is turbulent. Values between these two limits are classified as transitional (Knighton 1998). Flow is often described as chaotic when it reaches the turbulent stage. Roughness of the channel surface generates turbulence when the fluid does not flow smoothly over the bed due to particles that protrude from the bed surface. Turbulence increases the dissipation of energy in the stream (Morrisawa, 1968). As the bed roughness increases, a corresponding

increase in turbulence is observed. Turbulence increases with increasing velocity and bed roughness.

$$R_e = \rho \frac{VR}{\upsilon}$$ Equation 2.2

2.2.3 Sediment Load

The sediment load transported by a river is classified into two main categories, bed load and suspended load. Bed load is described as coarse grained material greater then 0.062 mm in diameter which characteristically roll and slide intermittently along the bed of the channel as the weight of the material is too heavy to be transported in suspension (Knighton 1998). In addition, as the particles protrude from the channel bed, the flow becomes turbulent which results in a greater dissipation of energy. Bed load material is classified as coarse sand and gravel. On the other hand, suspended load is composed of finer particles such as silts and clays which are carried in suspension by the fluid. Once suspended load particles are entrained, little or no energy is required to transport them. In contrast, bed load requires a greater amount of energy to keep the particles in motion. Suspended load actually increases the efficiency of a river by decreasing inner turbulence of the flow thereby reducing frictional energy losses (Knighton 1998).

Transportation of load depends on the energy of the river, which is a function of the river's velocity. The velocity must exceed a minimum value to entrain and transport grains of a given size. If the velocity is lower than this critical value, sediment will drop out of suspension (Knighton 1998). The relationship between entrainment, transportation and deposition in terms of velocity and grain size can be explained through the Hjulstrom Curve shown in Figure 2.5. This curve can be considered conceptual in nature. The curve shows four distinct regions which are erosion, erosion velocity, transportation and sedimentation. The band designated by the erosion velocity, also referred to as the critical velocity, indicates the velocity required to initiate erosion as a function of sediment size in millimetres. For particle sizes above approximately 0.4 mm, the curve shows lower velocities are required to move sand gains compared with clays and silts which require higher velocities because of inter-particle attractions. The critical velocity linearly increases for grains larger than 0.5 mm in diameter which is primarily due to the larger weight of the sediment with increasing grain size and therefore requires greater energy to initiate movement. Grains smaller then 0.5 mm that are typically classified as cohesive also show a linear increase in critical velocity to mobilize the grains. Greater velocities are required to mobilize cohesive materials due to the strong interparticle bonds referred to as electrochemical bonds. Once the fluid velocity increases past the erosion velocity, the soils will actively erode in the designated "erosion" region. The curve further shows that once silts and clays are entrained, they are easily maintained in suspension at a lower velocity than that initially required to entrain

the grains as designated by the transportation region of the graph (Richards 1982). The opposite is true for coarse grained sediment where deposition occurs if the velocity drops below the erosion velocity, designated by the sedimentation region of the graph.

Deposition also results when river flows overtop the riverbanks. The velocity of flow decreases as it spreads across the plain thereby reducing the ability to transport load. Typically coarser sediments are deposited near the edge of the channel whereas finer material are transported farther from the channel. The overtopping of banks and the resulting deposition of sediment build up the floodplain (Morisawa 1968).

2.2.4 Channel Morphology

Time dependent adjustment of a river's longitudinal and transverse cross-section allow the river to transport its discharge and sediment load supplied to it, most efficiently (Morisawa, 1968). This study is known as 'channel morphology'. The secondary factors that directly affect the discharge and type of sediment in the channel are the hydrology and geology of the site (Morisawa 1968). The hydrology determines the amount of precipitation and hence the discharge of the river and the geology determines the soils that make up the bed and banks of the channel. The processes that ultimately transform the shape and pattern of the river are erosion, deposition and transportation of sediment load (Richards 1982). Heavy precipitation for example, increases both the discharge and velocity of the river. As the velocity increases, the shear stress on the bed and banks will also

increase, causing erosion. Erosion of the bed and banks is the river's response to pass the larger discharge by increasing the cross-sectional area available to transport the flow.

The cross-section of the river resulting from the erosion depends on the geology of the bed and banks, where different sediment types respond differently to erosion (Richards 1982). Sand banks are easily eroded and typically produce wide channels with shallow beds. In contrast clay and silt banks are more resistant to erosion and typically produce channels that are deep and narrow with steep side slopes (Richards 1982). On the other hand, if the river bed is bedrock-controlled, erosion will be focused on the banks regardless of the sediment type. The river will overtop its banks when the discharge increases too quickly for the channel to adjust its form. This results in flooding. As the water flows across the land surface, the velocity decreases and sediment is deposited. The deposits are referred to as alluvial deposits which make up the banks and surface of the floodplain. Coarser sediments are typically deposited near the edge of the channel whereas finer sediments are carried further away (Simons and Senturk 1992).

Rivers grow headward with respect to their cross-sectional area as they gain more flow along their channel due to the accumulation of runoff (Morisawa 1968). It is also noted that rivers originate from regions of high altitude and flow down to flatter regions where they finally exit into the ocean (Morisawa 1968). Therefore

the river goes through a metamorphosis in its cross-section and sediment load as it progresses from one type of topography to another.

The sediment load also has a direct impact on the channel morphology based on the concentration and caliber of the load, defined as the grain size of sediment carried by the flow. If the concentration of load increases without a corresponding increase to the discharge, the rivers energy may be insufficient to transport the load resulting in deposition on the bed. Continued deposition will decrease the channels cross-sectional area thereby increasing the velocity of the river to pass the discharge and sediment load. The same applies for an increase in the caliber of the load,. Sediment is deposited out of suspension when the caliber of load increases resulting in the sediment being too heavy to be transported by the flow. The deposition will lead to a decrease in cross-sectional area that results in an increase to the velocity to transport the load (Morisawa 1968).

2.2.5 River Meanders

A meandering river is defined as one that has a distinct pattern of irregular bends along its length (Simons and Senturk 1992). Typical characteristics of these rivers are asymmetrical channel cross-sections along the river's length. These often lead to deep pools of scoured bank material on outer bends opposite bars of deposited sediment on the inner bends (Knighton 1998). Consequently, the thalweg (defined as the deepest points in a channel joined by a line) of a

meandering river is close to the outer edge of each bend and crosses over on the straight sections between bends (Morisawa 1968).

Similar to the thalweg, streamlines of maximum velocity move downstream, crossing over from one bank to the other. Streamlines behave similar to the thalweg in that they converge at the outer edge of the bends and diverge at the inner sides. The resulting acceleration of velocity due to converging streamlines increases the ability of the flow to transport particles and consequently the banks are more subject to erosion. Velocity is decelerated when streamlines diverge, resulting in deposition due to a loss of ability to transport sediment (Morisawa 1968). Erosion and deposition in meanders can also be explained in terms of maximum and minimum turbulence. Erosion takes place where turbulence is maximum and deposition results where turbulence is minimum (Morisawa 1968). Turbulence is expressed by the Reynolds number which is a function of velocity. The turbulence increases as the velocity increases and *vice versa*. The increase in velocity can be explained through the hydraulics of flow by converging and diverging streamlines, as already explained. The morphological nature of river meanders is that they will continue to erode at outside bends until the channel again intersects the river downstream. This leaves an isolated section of the former channel, often seen as an oxbow lake (Simons and Senturk 1992).

The reason why rivers meander is of interest. Many researchers have studied the meander behaviour and put forward explanations, though none have been

officially accepted. Shulits (1941) proposed that rivers meandered to lengthen their course as a way to decrease channel gradient. He suggested the channel gradient is a function of grain size comprising the bed and the river will adjust its slope to transport the material it must carry. As the caliber of load increases, the gradient must steepen to have enough energy to transport the load. Therefore a coarse grained bed load requires a steep gradient whereas a fine grained suspended load requires a shallow gradient. If the slope exceeds the energy required to transport the grains on the bed, the river will meander to lengthen its course to decrease its gradient and total energy.

Schumm (1960) related meandering rivers to those that generally had higher concentrations of silts and clays in their bed and banks. He also observed that meandering sections of a river tended to have deep, narrow cross-sections whereas wide, shallow sections were straighter and contained greater bed load. He concluded that meandering was the result of a large proportion of load carried as suspended load.

Friedkin (1945) conducted flume experiments to understand the initiation of meandering in a channel. The experiment started with an initially straight channel subjected to constant discharge but no additional sediment load. The conclusion of the experiment was that the stream naturally developed meanders. Local erosion of the channel banks initiated the meandering pattern and once the initial bend was formed, the meandering was transmitted downstream creating

more bends. Using a variety of materials for the channel, he also found that fine grained materials were more resistant to erosion which created deeper channels with gentler gradients; whereas coarse grained materials produced banks that were easily eroded and resulted in wide and shallow channels with steeper gradients.

2.2.6 Equilibrium

Do rivers attain states of equilibrium where they no longer erode or deposit? Such states are unlikely due to the dynamic factors that control the morphology of rivers. If one of these variables is modified, the river will respond with a change to its morphology. However, some researchers have proposed the idea of dynamic equilibrium which is a fluctuating or changing balance. This theory follows that parts of the river are continuously adjusting to maintain an equilibrium with their environment (Richards 1982).

2.3 Characteristics of the Red River

The Red River originates in the southern part of North Dakota and Minnesota at the confluence of the Ottertail and Bois de Sioux Rivers. From this point, the river meanders northward over a distance of 885 km to Lake Winnipeg (Red River Basin Investigation (RRBI) 1953). The river originally became established between 8200 and 7800 ^{14}C yr B.P. when Glacial Lake Agassiz receded northward, allowing the Red River to erode a shallow valley in the lacustrine glacial lake deposits. The river eroded a 15 m deep and 2500 m wide channel with a gentle gradient of 0.0001 (Brooks *et al*. 2005).

The drainage area of the river is 287,500 km^2 of which 163,000 km^2 or 57% is drained by the Assiniboine River which is the major tributary to the Red River. Of the remaining 124,000 km^2, 102,000 km^2 is from the U.S. and 22,000 km^2 is within Canada (RRBI 1953). The river carries predominantly a suspended sediment load composed 90% of silt and clay regardless of the sediment concentration and river discharge (Brooks 2000). The minimum and maximum sediment concentrations range from 10 to 20 mg/L during December and February and 500 to 1900 mg/L from April to July (Brooks 2002). The sediment load is representative of deposits that make up the bed and banks of the channel.

2.3.1 Annual Flows and Elevations

Continuous records of flow and elevation have been recorded since 1912 at the Emerson International Gauging Station at the international boundary between Canada and the United States approximately 140 km from Winnipeg. The record shows that flows and elevations on the Red River peak during the spring months of April to May in response to the winter snowmelt runoff and spring precipitation. Secondary peak flows are also common to the region and are generated by high rainfall events from June to October. Outside of the peak flow periods of the year, Public Works Canada regulates the elevation of the Red River within the City boundaries with the use of the St.Andrews Lock and Dam (SALD). SALD is operated each year after the spring peak inflows subside to 223.7 m. The river is

maintained at this elevation through the summer and fall to facilitate boat navigation as a result of outcrops of bedrock approximately 50 km downstream of Winnipeg, known as Lister Rapids. The dam is opened at the beginning of November to allow the river elevation to subside to its natural elevation of 221.9 m to accommodate the following year's spring inflows.

A review through historical flow records from 1912 shows the mean annual discharge has been 110 m^3/s with the highest discharge recorded at 3770 m^3/s in 1997 (Manitoba Water Resources 2005). The bank full discharge of the Red River is 600 m^3/s and has a 2-year return period (Brooks 2003). Exceeding the bank-full discharge results in a state of flood to the City of Winnipeg which has been exceeded 49 times or 53% over a 92 year record (Manitoba Water Resources 2005). Flooding is common along the Red River due to the shallowness of the valley with insufficient capacity to contain high flows (Brooks and Nielsen 2000). Consequently the banks are frequently overtopped.

Floods are typically associated with spring snowmelt; however prolonged periods of rain in the late spring and early summer can also result in flood conditions (RRBI 1953). Floods rise and fall slowly over a period of up to 4 to 6 weeks (Brooks 2003). This behaviour is a result of the low valley gradient of the region. The flat topography further increases the flood hazard when the river overtops its banks as the flows spread across the prairie surface, inundating a large area many kilometers wide as observed with the flood of 1997 (Brooks 2000). From

the historical flow records and tree-ring dating, the largest floods of the Red River have been in 1826 (5350 m^3/s), 1852 (3770 m^3/s), 1950 (2670 m^3/s), 1979 (2620 m^3/s) and 1997 (3740 m^3/s) (Manitoba Water Resources 2005, Brooks *et al*. 2003). The flood of 1997 was the largest Red River flood in southern Manitoba since 1852. It inundated an area of 2000 km^2 and up to 40 km wide between the Canada/U.S. boarder and Winnipeg (Brooks 2003).

To mitigate the flood risk to the City, the Red River Floodway was constructed and put into operation in 1968. The floodway is an excavated channel that diverts the Red River around the City of Winnipeg. It has a design capacity of 1700 m^3/s though it successfully carried a discharge of 2110 m^3/s in the flood of 1997 (Brooks and Nielsen 2000). Due to the Floodway, the flows at Emerson are not representative of those through the City of Winnipeg. The alternative gauging station is at James Street Pumping Station inside the City of Winnipeg. Daily flows and elevations have been recorded at this station since 1948.

2.3.2 River Pattern

A common characteristic of the Red River is its meandering morphology. Meanders within the City of Winnipeg are particularly evident at Kingston Crescent, St.Vital Park, King's Park and Crescent Wood. Through the interpretation of aerial photographs over the past 130 years, researchers have concluded that the meanders are relatively inactive. A single pattern of ridge and swale topography is identified on the floodplain, which indicates the meanders

have undergone a single sequence of expansion (Brooks 2003). Ridges and swales are typical features of meandering rivers which are similar to ripples of sediment on the floodplain surface. They are formed by sedimentation on the inner bank of a meander and basically mark past positions of the river channel on the floodplain (personal communication with Brooks 2006).

At a select meander along the Red River, average rates of channel migration were initially 0.35 m/year between 7900 and 7400 cal years B.P., followed by a decrease to 0.18 m/year between 7400 and 6200 cal years B.P. Since this time the migration has varied between 0.04 and 0.08 m/year (Brooks 2003). The resulting increase in valley cross-sectional area since 1000 years B.P. is approximately 2% and 0.7% as observed at the two sites studied, essentially very low lateral migration rates are observed. In comparison to timescales over several centuries, the widening of the valley cross-section is very low to negligible (Brooks 2003).

2.3.3 Lake Agassiz Soils

The soils in the Winnipeg area are what used to be the bed of Glacial Lake Agassiz which formed between 13,500 and 8,000 years BP and covered the greater part of Manitoba (Quigley 1980). The Lake was formed when the Wisconsin continental glacier blocked the natural drainage to the northern Arctic Ocean through the Hudson's Bay (Graham and Shields 1985). Rivers continued to bring water from the south and west which combined with melted water from the glacier and local rainfall to form glacial Lake Agassiz. There is evidence that

this great lake stood over 150 meters deep above the present City of Winnipeg (Macdonald 1937). At maximum extent the Lake was the largest lake in North America, covering an area of over 521,000 km^2 although its maximum size at any one time was 208,000 km^2 (Baracos *et al*. 1983). Initially Lake Agassiz drained southward into the Mississippi river system. As the ice retreated north, the Lakes drained successively northwards into Lake Superior and then into the Hudson Bay. Lakes Winnipeg, Manitoba and Winnipegosis and the Red Lakes in Minnesota are what remain of Lake Agassiz (RRBI 1953).

The Wisconsin glacier went through a series of advances and retreats during which layers of till were deposited over the basin as a heterogeneous mass of clay, sand, gravel and boulders, to a maximum depth of 90 meters in some areas (RRBI 1953). Lacustrine clay was deposited overtop of the till during the existence of Lake Agassiz where sediment transported into the lake by rivers were spread over the lake bottom (RRBI 1953). Clay covers the till to an average depth of 9 to 13 meters and is found at depths varying from zero to 20 meters (Baracos *et al*. 1983). The lacustrine deposits are high plastic clays, which have the ability to hold large quantities of moisture and consequently exhibit high swelling and shrinkage characteristics (RRBI 1953).

2.3.4 Soil Stratigraphy

Present day analysis of the Lake Agassiz deposits classifies them into two main categories, an upper complex zone and a silty clay unit (Baracos and Kingerski

1998). These deposits are underlain by till and bedrock. In the areas of riverbanks, alluvial deposits overly the Lake Agassiz deposits.

2.3.4.1 Upper Complex Zone

The upper complex zone makes up the top portion of the soil stratigraphy averaging a depth of 1 m to 4.5 m and represents late post-glacial events such as flooding, deposition and erosion in addition to recent depositional environments from vegetation growth and human activity (Baracos *et al*. 1983, Baracos and Kingerski 1998). These activities have modified the near-surface deposits characterizing them as complex due to their stratigraphy that consists of discontinuous thin layers of silt, silty clay and clay (Baracos and Kingerski 1998). The silty clay and clays are highly plastic and exhibit a nuggety structure from repeated freeze-thaw cycles involving shrinkage upon drying and swelling upon wetting (Baracos and Kingerski 1998). The silt is in discontinuous interlayers up to 3 m thick and can vary in thickness over a short distance (Baracos *et al*. 1983). The base of the complex zone is delineated by a layer of lacustrine silt.

2.3.4.2 Silty Clay Unit

The silty clay unit underlies the complex zone and ranges in thickness from zero to 21 meters with an average thickness of 9 to 12 meters (Baracos and Kingerski 1998). The unit is divided into two distinct layers based on the soil colour, although both layers are considered to be a part of a single depositional sequence as there is no difference in clay fraction or mineralogy (Baracos *et al*.

1983). The upper clay ranges in thickness from 1.5 to 6 meters and exhibits a brown to mottled grey-brown colour. The lower clay is described as grey with deposits that are coarser and more bedded than the upper layer with alternating layers of clay-rich and silt-rich sediments (Baracos *et al*. 1983). The unit also contains fissures, joints, uncemented silt inclusions and rock fragments that approach boulder size. The change in colour of the upper unit is due to oxidation (Baracos *et al*. 1983).

2.3.4.3 Till

Underlying the glaciolacustrine clay is till that ranges in thickness from zero to 10 meters. The tills were deposited during numerous advances and retreats of the Wisconsin glacier (Baracos *et al*. 1983). The tills are a heterogeneous mixture of clay to boulder-sized particles, in which the clay content decreases with increasing depth into the till unit. There are two distinct layers to the till unit and they exhibit different properties. The upper portion is classified as soft whereas the lower portion is considered hard. The two units differ in terms of their clay and moisture content and this influences the strength of each unit. The upper units are classified as having a greater clay and moisture content resulting in a lower strength as compared to the lower units which have a very high unconfined compression (Baracos and Kingerski 1998). The lower till units exhibit an undrained shear strength that approaches the strength of weak concrete (Baracos and Kingerski 1998). Therefore, it is common for end bearing piles to be founded on the lower tills. Both units are still classified as soils regardless of their strength properties (Baracos *et al*. 1983).

2.3.4.4 Bedrock

Clay and till deposits are underlain by 76 to 230 meters of Paleozoic limestone and dolomite bedrock (Render 1970). The upper 15 to 30 m of this bedrock is characterized by a major aquifer referred to as the Upper Carbonate aquifer. The aquifer is highly fractured, jointed and contains bedding planes that provide the high degree of permeability (Render 1970). The upper 7.5 m of the carbonate rock is the zone of highest permeability which experiences the greatest amount of flow (Render 1970). The aquifer is confined overtop by the low permeability clay and till deposits and below by the low permeability (Baracos and Kingerski 1998). The aquifer has been a major source of groundwater to the City of Winnipeg for the past 130 years (Render 1970). During this period over 200 commercial and municipal wells have been installed. Due to increased consumption during the 1900's, a large drawdown cone of the aquifer resulted under the City of Winnipeg (Render 1970). The groundwater has been used for irrigation and domestic use but primarily for commercial and industrial cooling due to the constant low temperature of the groundwater (Render 1970). More recently, groundwater usage in the City has been declining. This is primarily due to the fact some major industrial companies have closed down and those that still use the aquifer for heating and air conditioning purposes, return the water to the aquifer after it has been used (Tutkaluk, 2000).

2.3.5 Riverbank Stratigraphy

The banks of the Red River are overlain by alluvial sediments deposited by the river during high flows and flooding. The deposits are a mixture of sand, silt and

clay exhibiting little to no coarse grained materials (Brooks 1993). The fine texture of the alluvium reflects the fine grain size of the Lake Agassiz clay plain, which represents the majority of eroded sediment transported by the river (Brooks 1993). All sections of the Red River, referring here to the outside and inside bends, transitions and straight sections, are all subjected to erosion and deposition (Baracos and Lew 2001). Erosion is strongest where flow velocities are highest. During flood events, erosion is active in the lower parts of the slope and the bed (Figure 2.3 and 2.4). In contrast, where velocities are lowest, (near the top of the slope, among vegetation, or where the river has overtopped its banks) the velocity cannot support the suspended load and deposition occurs (Baracos and Lew 2001). Further erosion can be induced when trees and vegetation are undercut from fluvial and ice action. Exposed tree roots interfere with the flows causing increased turbulence that undercut the bank further (Baracos and Lew 2003).

A study conducted by Brooks (2005) measured the thickness of the 1999 flood deposits along the upper slope of the outside bends of both low and steep angled slopes. In the study reach, the bank was overtopped to a depth of 0.5 m by the 1999 peak spring flow, resulting in the deposition of sediment behind the crest and on the upper slope. Deposition was measured along both low-angled slopes defined as having gradients less steep than 11° and steep-angled slopes with gradients between 23° and 27°. The study concluded that overbank deposits aggraded up to a thickness of 21 cm for low-angled slopes and generally thinned

with increasing distance from the river. Within 30 meters from the channel's edge, the thickness of deposits varied from 3 to 21 centimeters. At distances greater than 50 meters from the channel, the thickness decreased to five centimeters or less. Sieve analysis of overbank deposits showed that the sediment was 60 to 80 percent silt particles. Similarly, the deposits on steeper slopes were silt-sized particles and thinned with increasing distance from the controlled summer water level. However, the overall thickness of the deposits was observed to be thinner in comparison with those on the low angled slopes. Thicknesses of the deposits ranged from 7 cm to less then 0.1 cm. The majority of the deposits were along the lower several meters of the bank and were deposited as water levels withdrew to the controlled summer levels. The study also concluded that deposition on the banks of inside bends was minor in comparison to the accumulation on the outside bends (Brooks 2005). This is contrary to common meander theory where deposition is more pronounced on inside bends.

2.3.6 Riverbank Stability and Failures

Instability of riverbanks is observed to be seasonal and related to a combination of porewater pressures, river elevation and bedrock aquifer elevation (Baracos 1978, Tutkaluk 2000, Baracos and Lew 2003). High porewater pressures within the banks arise during the spring and summer due to infiltration of snowmelt and heavy rains. The result is a decrease in shear strength available to mobilize the failure surface through the bank. However the failure is often delayed due to the raised river elevation maintained by Public Works

Canada through the summer and early fall with the use of St.Andrews Lock and Dam (SALD) (Baracos and Lew 2003). The force of the river water acting over the lower bank, acts as a counter-balancing force to the high porewater pressures within the bank (Baracos and Lew 2003). In addition, the riverbanks experience greater stability during the summer due to increased consumption of the groundwater which decreases porewater pressures along the clay-till interface. In the fall, consumption of the groundwater decreases and the gates at SALD are opened to lower the river elevation in preparation for the following year's spring inflows. This combined effect with the increased porewater pressures that remain elevated from the spring due to the low permeability of the clay (Baracos 1978, Baracos and Lew 2003), commonly result in riverbank failures in the fall which continue at a decreased rate through the winter.

Another factor that adds to the instability of the banks is the effect of erosion at the lower parts and deposition at the higher parts of the riverbanks due to high flows and ice forces. The high flows that arise during the spring and summer exert shear stresses on the banks that cause soil particles to be entrained into the flow, also known as erosion (Thorne 1982). The erosion causes the banks to become unstable because the forces supporting the weight of the upper bank are reduced (Baracos and Lew 2003). However, the banks typically do not fail until the full effects of both the river and aquifer are observed in the fall (Baracos 1978). Ice scour is another factor that removes large amounts of soil from the bank during the spring ice break-up. Ice attaches to the frozen soil and when

detached lifts the riverbank materials,which allows them to be carried away by the flow. As the ice sheets flow down the river, they impact the bank removing large chunks of bank material and exposing tree roots. Trees located close to the channel cause an increase in local turbulence. This leads to more erosion of the banks (Baracos and Lew 2003). The accumulation of annual sediment can produce appreciable loading on the bank and add to instability and eventual failure. Deposition of sediment is common along upper portions of the bank submerged by spring flows. Trees and vegetation also promote sediment deposition by reducing flow velocities. In some locations the deposition over several years can result in appreciable loading. Riverbanks will become more unstable if the loading adds to the forces causing sliding or it can experience greater stability if the sediment is deposited at the bottom of the slope (Baracos and Lew 2003). Alternatively to soil removal is the deposition of sediment along the mid-bank to crest regions of the riverbanks after elevated flows.

It is important to note that failure of riverbanks is not confined to the outside of bends but also occurs along inside bends, straight and transition sections of the Red River (Baracos and Lew 2003). These failures are common under high flow conditions and are explained through the change in thalweg location under low-stage and high-stage flows as shown in Figure 2.6. Under low-stage flows the thalweg encroaches on the outer banks of the river bends whereas high-stage flows short-circuit the meander pattern and flow over rather than around the bends. Consequently, the high flows scour both the outside, inside and straight

sections as the thalweg cuts across these areas (Baracos and Lew, 2003, Simons and Senturk 1992).

Instability of riverbanks depends on a number of factors that combine to cause the banks to fail (Baracos and Lew 2003). Once the banks fail, soil moves towards the lower bank and toe or directly into the channel. Removal of the material from this point is entirely dependent on the flows of the river. The amount of material accumulating at the toe depends on the frequency of bank failure and how easily the material can be removed by the flow. Where the flow is able to remove all debris, the toe continues to erode, thereby increasing the slope angle and inducing further bank failures. Riverbank equilibrium is a balance between supply and removal at the base. This would result in no change to the slope angle. Conversely, if the flow is unable to remove the debris, the failed material accumulates at the toe and acts like a buttress. This action, also known as basal endpoint control, tends to protect the intact bank from erosion and increases bank stability. The decreased slope angle and extra weight at the toe to support the upper bank (Thorne 1982).

Basal endpoint control has a significant effect on the sustained stability of riverbanks. Once a failure occurs the new configuration of the bank is one that is more stable then the former. The bank can maintain this stable position for a period of time if the flows are not great enough to erode the deposited material away. However, if the flows are large, the bank will continue to be unstable.

Also the material can be progressively eroded by the flows over a number of years until the riverbank fails. This process may explain the common occurrence of riverbanks along the Red River maintaining stability over a long period and then suddenly failing. Basal endpoint control plays an important role in maintaining the stability of the bank (Thorne 1982).

Riverbank slides have been observed to be deep seated and retrogressive. Deep-seated slides can extend to the clay-till interface and over an 80 meter distance from the summer's water's edge (Baracos and Kingerski 1998). Sliding is limited to material above the till due to the lower shear strength of this material (Baracos and Lew 2003).

2.4 Erosion

Erosion is the process by which soil particles are removed from the bed and banks of the channel and entrained into the flow of the river (Richards 1982). Erosion depends on a number of factors that include the intensity of flow (river elevation), soil characteristics of the bed and banks, geometry of the channel, ice effects and characteristics of the fluid. Quantifying the amount of soil eroded from the bed and banks of the channel under a given river flow is of interest. To calculate this value three variables are required:

- Fluid shear stress
- Critical shear stress

- Erosion rate

Various researchers have proposed different methods for calculating the above quantities. The following sections provide an overview of selected methods.

2.4.1 Fluid Shear Stress

Fluid shear stress is defined as the force per unit area in the direction of flow (Chang 1988). The shear stress distribution in a steady and uniform two-dimensional flow in a channel can be explained by Figure 2.7. The figure shows all of the forces acting on a unit volume of water described by ABCD within the channel. The x-axis is in the direction of flow along the slope of the channel defined by S with the z-axis perpendicular to the flow (Chang 1988). The forces and stresses acting on the unit volume include the hydrostatic forces on AB and CD, shear stress τ acting on BC and the x-component of the fluid weight W_x in the unit volume. All forces act in the x-direction. If the flow is uniform the hydrostatic forces are equal and opposite and hence the remaining force W_x (= WS) must be counterbalanced by the shear force.

$$WS = \tau\, Pdx$$

$$\gamma \forall S = \tau\, Pdx$$

$$\gamma AdxS = \tau\, Pdx$$

$$R = A/P$$

where,

τ = fluid shear stress

P = wetted perimeter

A = Area

$\forall$ = Volume

Isolating the above equations for τ produces Equation 2.3. This equation is the average shear stress exerted on the bed of the channel. R is defined as the hydraulic radius of the channel and γ is the unit weight of the soil.

$\tau = \gamma RS$ Equation 2.3

The equation was further expanded by Olsen and Florey (1952) in a finite difference analysis to describe the shear distribution along the bed and banks of straight trapezoidal channels. The graphical distribution is shown in Figure 2.8(a) where shear stresses are a maximum along the bed and a minimum at the top of the bank. For this particular cross-section of side slope 2:1, the maximum shear on the bed is 1.37γRS and on the bank is 1.08γRS approximately one third from the bed. This research was furthered by the Highway Research Board (1970) where the coefficients of maximum γRS were adjusted for the bed and bank as a function of the ratio of channel width (b) to water depth (D). Values for the coefficient of maximum shear stress were also provided for channels of different side slopes. The graphs in Figures 2.8(b) and 2.8(c) show for a channel of side

slope 2:1, as the b/d decreases the coefficient for γRS approaches 1.0. However, as b/d increases the coefficient can be as high as 1.4.

2.4.2 Critical Shear Stress

A particle will be set in motion if the applied forces on the particle exceed the resisting forces on the particle (Richards 1982). The resisting forces of the particle depend on the characteristics of the soil. Non-cohesive soils such as sands and gravels resist erosion by gravitational forces through their submerged weight (Richards 1982). The Shields curve shown in Figure 2.9 is commonly used to determine the critical shear of non-cohesive soils, based on the diameter of the particle. The curve is based on a series of flume experiments of water flowing over flat sand beds and offers a range of critical shear stresses for particles of 0.1 mm to 10,000 mm in diameter with shear stresses ranging from 0.1 Pa to 10 Pa. This curve has been modified by several researchers to further expand the use of the curve to a larger range of particle diameters. The curve is however limited to providing the critical shear stress on the bed of the channel (Morisawa 1968). In 1953, Lane proposed an equation to quantify the critical shear on the side slopes of channels. The reasoning for the method was that particles on a stream bed are subjected to a tractive force acting in the direction of flow whereas particles on a side slope are additionally subjected to a gravitational force parallel to the slope which causes the particles to roll down into the channel. Therefore, the critical shear stress of the bed is multiplied by a value K which represents the ratio of the tractive force necessary to start motion

on a side slope to that required to start motion on the bed. The value for K is given by Equation 2.4:

$$K = \cos\phi\sqrt{1-\frac{\tan^2\phi}{\tan^2\theta}} \qquad \text{Equation 2.4}$$

where,

θ = soil friction angle

ϕ = side slope angle

The critical shear for cohesive soils cannot be estimated from the Shields curve as gravity forces do not solely control the soil behaviour. Instead, the resisting forces are related to physical and chemical surface effects such as soil particle bonding and soil interaction with the pore and eroding fluids (Arulanandan *et al*. 1980). Among the first research was a chart developed by Alizadeh (1974) and revised by Heinzen (1976) as shown in Figure 2.10, which can be used to determine the critical shear stress (τ_c) given the soil sodium adsorption ratio (SAR) calculated by Equation 2.5, dielectric dispersion and total salt concentration of the eroding fluid expressed in milliequivalents per liter (meq/l).

$$SAR = \left(Na^{+}\right)\frac{\sqrt{\left(Ca^{++}\right)+\left(Mg^{++}\right)}}{2} \qquad \text{Equation 2.5}$$

The dielectric dispersion provides a quantitative measure of the soil fabric in terms of particle arrangement and pore spaces in the soil (Mitchell and Soga 2005). It measures the decrease in dielectric constant as a function of the soil structure defined by the type and amount of clay particles, water content, pore fluid composition and fabric. The magnitude of the dielectric dispersion can be used to characterize clays as it takes into account the compositional and environmental factors of the clay-fluid system (Arulanandan *et al*. 1975). Sodium adsorption ratio measures the pore fluid salt concentration by measuring the sodium, calcium and magnesium cations adsorbed on the soil surface. The surface of clay soils are negatively charged and therefore attract positively charged particles also known as cations. The charged surface and the distribution of cations attracted to the surface is termed the diffuse double layer (Barbour and Fredlund 1989). Repulsion of clay particles is caused when cations from overlapping double layers repel each other enough to overcome the attractive van der Waal's forces between particles. If the cations are bound tightly to the clay surface the diffuse double layer will be thinner causing a greater attraction between clay particles. Such effects leads to flocculation of clay particles and shrinkage of the soil (Mitchell and Soga 2005). Cations with higher valence such as Ca^{+} and Mg^{+} are more tightly bound to the clay surface whereas Na^{+} has among the lowest valence and promotes dispersion of the soils. Therefore a high value of SAR relates to a high degree of deflocculation or erosion.

This research was furthered by Arulanandan *et al.* (1980) who performed erosion experiments to measure the critical shear stress and compare these results to those predicted by Alizadeh (1974) and Heinzen's (1976) chart. The research involved selecting 30 soil samples from stream bank sites across the United States where half of the samples were from sites exhibiting erosion and the other half from stable sites. Undisturbed and disturbed samples were both collected along with 3 gallons of river water at each site for the eroding fluid in the experiment. Re-circulating hydraulic flume erosion tests were performed on the undisturbed samples. The flume was 8 ft long, 6 inches wide and 12 inches deep. Fluid was circulated through the flume with the soil sample inserted into the flume bed. A hole was cut in the flume bed so that the sample was supported just below the hole. A schematic is shown in Figure 2.11. A pitot tube was used to measure the velocity head of the flow which was used in an empirical equation by Preston (1954) to approximate the bed shear stress for when particle movement was observed. Equation 2.6 was used to calculate the shear stress (Arulanandan *et al*. 1980) which was only valid for shear stresses less than 14.6 dynes/cm^2.

$$\log\frac{\tau_o d^2}{4\rho v^2} = -1.396 + \frac{7}{8}\log\frac{(p_t - p_o)d^2}{4\rho v^2} \qquad \text{Equation 2.6}$$

where

$$4.5 < \log\frac{(p_t - p_o)d^2}{4\rho v^2} < 6.5$$

τ_o = bed shear stress (dynes/cm^2)

d = outside diameter of pitot tube (cm)

ρ = mass density of fluid (gm/cm^2)

ν = kinematic viscosity of the fluid (cm^2/sec)

p_t = total head measured (dynes/cm^2)

p_o = static head measured (dynes/cm^2)

To obtain an accurate measurement of the velocity head, the pitot tube was placed along different locations of the soil surface in order to calculate an average shear stress distribution across the surface. Each test was conducted for a duration of 2.5 minutes and after each test the soil sample was removed from the apparatus and weighed. The same procedure was repeated for increasing flows with a graph of weight loss versus shear stress produced. The point at which the weight loss increased from zero represented the critical shear stress.

Further to this, tests on remolded samples were undertaken in a rotating cylinder apparatus as shown in Figure 2.12. The apparatus consisted of a hollow plexiglass cylinder supported axially on a shaft rotated by an electric motor. Soil samples were placed inside the rotating cylinder and the chamber between the rotating cylinder and sample was filled with the eroding fluid. The outside cylinder was electrically rotated. This created a shear stress on the fluid contained within the cylinder and subsequently produced a shear stress on the

soil sample. As the cylinder was rotated, a shear force reading was recorded directly by measuring the total force exerted by the fluid on the sample surface area. Arulanandan *et al*. (1980) compared τ_c measured to predicted critical shear stress results shown in Figures 2.13 and 2.14 for undisturbed and disturbed samples respectively, with the measured τ_c on the x-axis and the predicted τ_c on the y-axis. A straight line was drawn on both charts with a 1:1 slope. The measured and predicted results are the same if they fall on the straight line. Results above the line indicate the predicted values are too high and vice versa if below. It was determined that the chart yielded predicted values for τ_c that were less than measured values for both undisturbed and remolded samples. The lower critical shear stress results of Alizadeh (1974) and Heinzen's (1976) chart are suggested to be related to the eroding fluid used in their experiment which was distilled water.

The experiments conducted by Arulanandan *et al*. (1980) further proved that the salt concentration of eroding fluid significantly influenced the erosion of soil samples. As the salt concentration of the river water decreased, the critical shear stress decreased. Therefore, the more concentrated the water is with material such as suspended solids, the higher the critical shear stress to initiate erosion. This is explained through the concept of osmotic pressure (Arulanandan *et al*. 1980), which decreases when there is a decrease in the salt concentration gradients between the eroding fluid and pore fluid. Therefore, critical shear stresses are much higher for soils in distilled water as opposed to soils with an

existing suspended load due to the higher salt concentration gradients with distilled water. Since the critical shear stress increases as the salt concentration of the eroding fluid increases, Arulanandan *et al*. (1980) suggested that the chart proposed by Alizadeh (1974) and Heinzen (1976) (Figure 2.10) should give a reasonable estimate of the critical shear stress for a natural undisturbed soil subject to hydraulic shear stress from river water.

Another similar method for determining the critical shear stress is proposed by Briaud *et al*. (2001) which involves the measurement of critical shear stress through use of the Erosion Function Apparatus (EFA) shown in Figure 2.11. The experiment involves obtaining a sample of soil using a standard ASTM Shelby tube. One end of the tube is positioned in a circular opening at the bottom of a pipe of rectangular cross-section. A piston pushes the soil from the sampling tube into the rectangular pipe until it protrudes 1 mm. A flow of a given velocity is run through the pipe and the time and velocity required to erode the soil is measured. The process is repeated for increasing velocities with the shear stress calculated using Equation 2.7.

$$\tau = \frac{1}{8} f \rho v^2 \qquad \text{Equation 2.7}$$

where,

τ = shear stress

f = friction factor obtained from a Moody chart

ρ = density of water

ν = mean flow velocity in pipe

Tap water can be used to run the tests, however Briaud *et al*. (2001) suggest that the chemistry of the water influences the erodibility of cohesive soils, therefore to duplicate actual site conditions it is best to use the river water or at least duplicate the water chemistry. According to results given by Briaud *et al*. (2001) the values of τ_c for fine grained soils vary between zero and 5 Pa.

2.4.3 Erosion Rate

The final quantity required to quantify erosion is the erosion rate. The erosion rate is the volume of soil scoured during a period of time once the critical shear stress is surpassed. Given the erosion rate, one can back-calculate to determine the quantity of erosion in metres and estimate the bank retreat from this value. Erosion rates for cohesive soils can be calculated using an excess shear stress approach proposed by Partheniades (1965) given by Equation 2.8.

$$\varepsilon = k(\tau_o - \tau_c)^a \qquad \text{Equation 2.8}$$

where

k = erodibility coefficient

τ_o-τ_c = Excess shear stress

a = an exponent often assumed equal to 1.0

The value of *k* is determined experimentally. According to experiments completed on almost 200 soil samples at stream sites from Nebraska, Iowa and Mississippi *k* was estimated as a function of τ_c given by Equation 2.9 (Hanson and Simon 2001).

$$k = 0.1x10^{-6}\tau_c^{-0.5} \qquad \text{Equation 2.9}$$

The Briaud *et al*. (2001) method for erosion rate is based on Equation 2.10 where h is the height of sample eroded which is a standard 1 mm for all tests and t is the amount of time required to erode the sample to be flush with the bottom of the pipe.

$$\dot{z} = \frac{h}{t} \qquad \text{Equation 2.10}$$

The final output is a curve which shows the shear stress on the x-axis and the erosion rate on the y-axis. The point on the curve where the erosion rate first increases from the zero point corresponds to the critical shear stress. Briaud *et al*. (2001) states the erosion rate will vary from 0.3 to 30 mm/hr and the erosion rate of fine grained soil is thousands of times slower than the erosion rate of coarse-grained soils.

Osmann and Thorn (1988) also propose an equation for erosion rate based on the experimental results of Arulanandan *et al.* (1980). Arulanandan *et al.* (1980) produced a graph of rate of change of erosion rate versus measured critical shear stress shown in Figure 2.15. Osmann and Thorne (1980) developed Equation 2.11 to describe the behaviour of this graph (Figure 2.15) in the transition region for τ_c greater than 0.6 Pa. It is assumed that soils with critical shear stresses less than 0.6 Pa will behave as cohesionless soils. The final erosion rate is defined by inserting Equation 2.11 into Equation 2.12, where τ_c is in dynes/cm^2 and dW is in m/min.

$$R = 223 \times 10^{-4} \tau_c e^{0.13 T_c} \qquad \text{Equation 2.11}$$

$$dW = \frac{R}{\gamma}\left(\frac{\tau - \tau_c}{\tau}\right) \qquad \text{Equation 2.12}$$

Once the erosion rate is obtained, the quantity of eroded riverbank can be calculated by performing a back calculation. Given a period of time over which the shear stress of the river has been greater than the critical shear stress, the bank retreat in meters can be calculated by multiplying the erosion rate by the period of time.

2.4.4 Critical Shear Stress and Erosion Rate Related to Soil Properties

Briaud *et al*. (2001) attempted to formulate a relationship between τ_c and erosion rate using standard soil properties. Briaud *et al.* (2001) postulated that a correlation existed between erodibility and soil properties but after extensive literature review dating back to 1960, no widely accepted correlation could be found. Briaud *et al.* (2001) infers that if a correlation exists, it must involve several parameters and require many tests on clay samples to validate the relationship. Due to the complexity of the correlation, Briaud *et al.* (2001) recommends the EFA (Figure 2.11) to directly measure the two variables for any type of soil, which can then be used in a scour prediction analysis.

Arulanandan *et al*. (1980) states that the main property governing the erosion of clays is the ratio of dissolved sodium ions to cations of calcium and magnesium in the pore water, represented by SAR. Arulanandan *et al*. (1975) has also correlated SAR to erosion rate and τ_c as shown in Figure 2.16. Soils with SAR values greater than 10 exhibit high rates of erosion as shown by the steep lines and lower critical shear stress. The other main factor is the concentration of dissolved salts in the eroding fluid, which if low causes the soil to have a greater susceptibility to erosion (Arulanandan *et al*. 1975) as shown in Figure 2.17. Arulanandan *et al.* (1975) further states that erosion is a surface phenomenon where mechanical soil properties such as shear strength, moisture content and plasticity index do not accurately describe the state of the soil at the surface.

Whereas SAR less than 10 shows τ_c as high as 38 dynes/cm^2 or 3.8 Pa with a gradual erosion rate.

2.4.5 Numerical Methods to Quantify Erosion

Several numerical models exist for channel width adjustments which consider the hydraulics of flow, sediment transport of bank material and bank stability. However, no one model has been capable of representing all physical processes and mechanisms involved with channel adjustments. Most of the models show sophisticated solutions to describe the hydraulics of flow and sediment transport. However the models lack in ability to analyse riverbank stability. The models also make assumptions that are not necessarily accurate as to how failed bank material is deposited in the channel or carried away by the river flow. The existing models have not been subjected to rigorous evaluation in terms of their ability to replicate laboratory data or simulate field situations. These limitations show the need for laboratory and field data in order to evaluate and fine tune the models (Darby 1998).

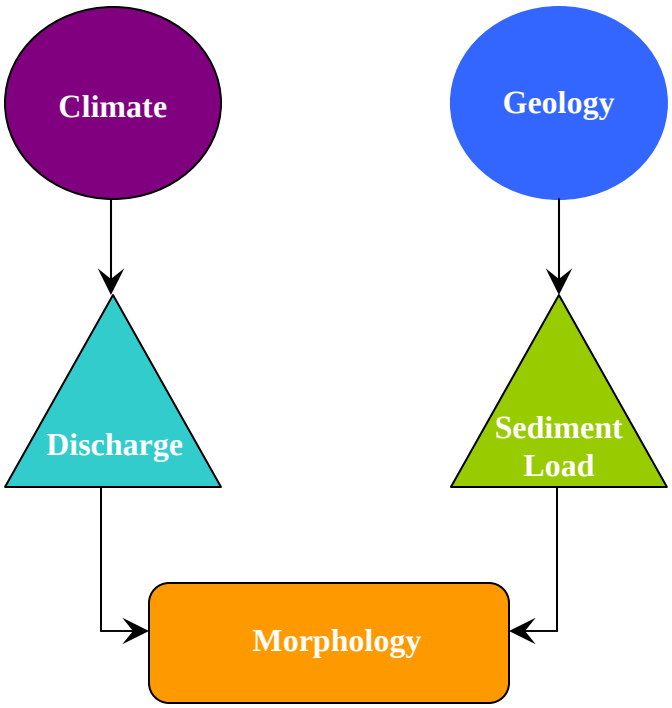

Figure 2.1: Variables affecting the morphology of a river (based on ideas from Morisawa 1985)

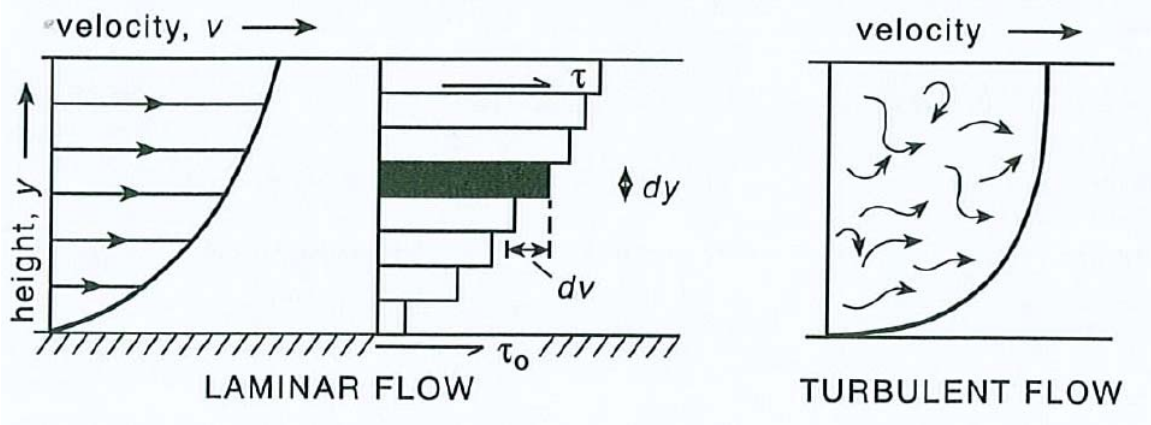

Figure 2.2: Average velocity (μ) distribution at the center of a channel under laminar and turbulent flow conditions (after Knighton 1998 - used with permission from Oxford University Press obtained April 16th, 2007)

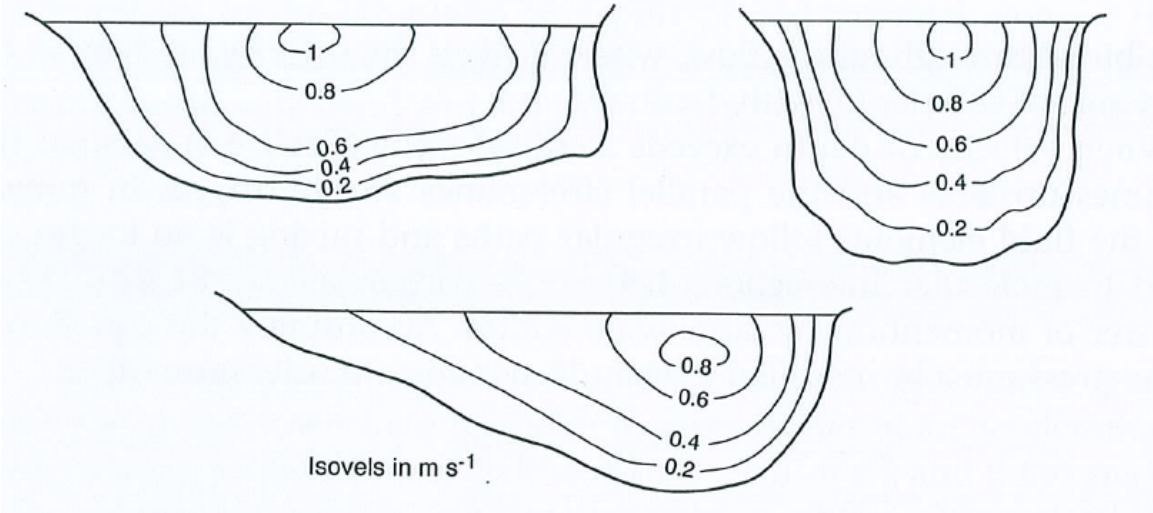

Figure 2.3: Velocity isovels in different channel cross-sections
(after Knighton 1998 - used with permission from Oxford University Press obtained April 16th, 2007)

Figure 2.4: Velocity and turbulence distribution in a symmetrical channel (a) and asymmetrical channel (b) (after Morisawa 1968)

Figure 2.5: Hjulstrom Graph for erosion, transportation and deposition of sediment as a function of grain size (after Knighton 1998)

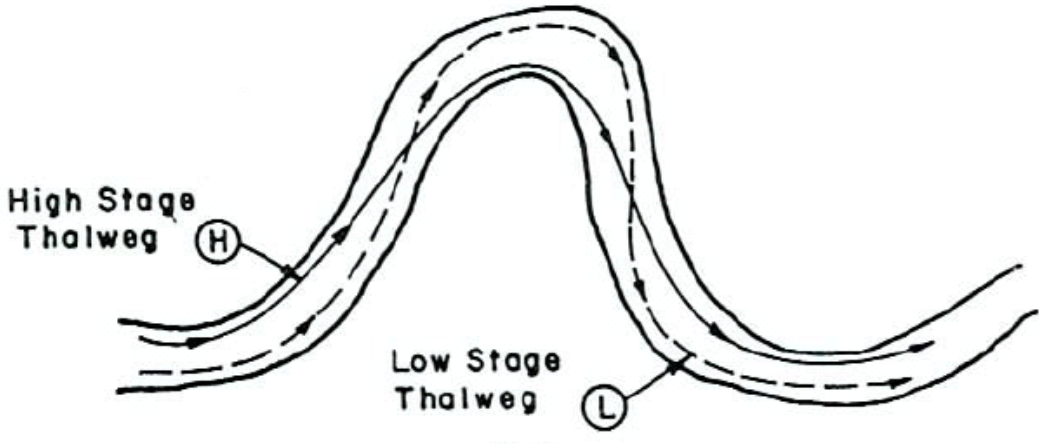

Figure 2.6: Location of thalweg at low and high stage flows
(after Simons and Senturk 1992 - used with permission from May Jo Simons obtained July 25th, 2007)

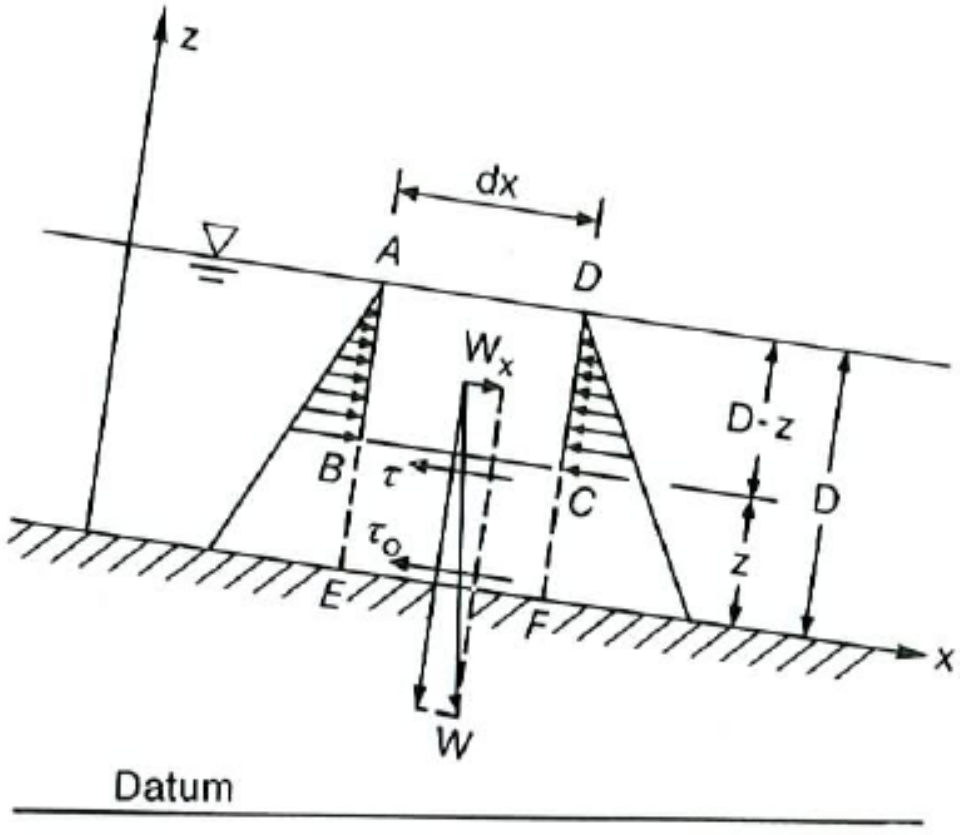

Figure 2.7: Schematic of forces acting on a unit volume of flow
(after Chang 1988 - used with permission from Howard H. Chang obtained on July 23rd, 2007)

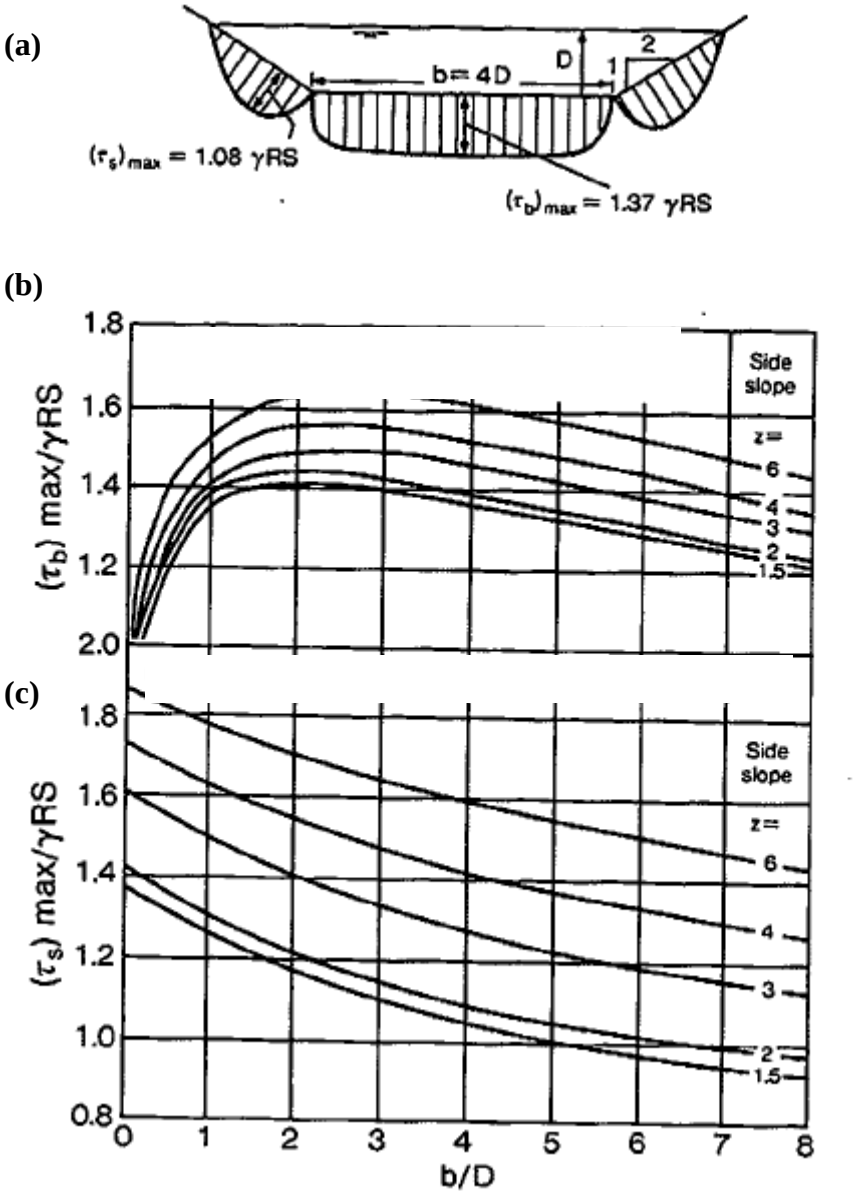

Figure 2.8: Distributions of boundary shear stress in a trapezoidal channel (a) with coefficients for maximum shear on bed (b) and banks (c) as a function of b/D (after Chang 1988 - used with permission from Howard H. Chang obtained July 23rd, 2007)

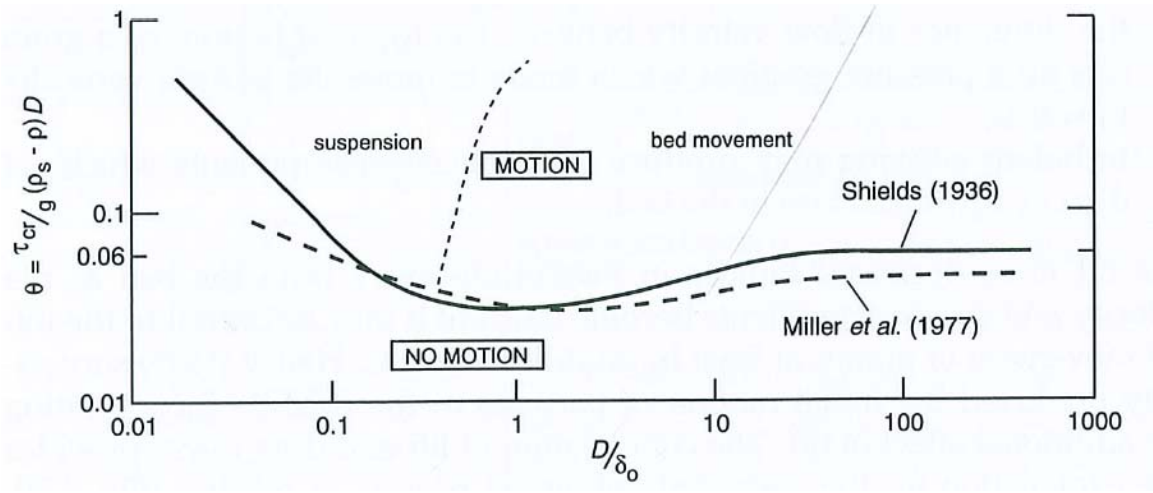

Figure 2.9: Shields Diagram for determining the critical shear stress of cohesive soils (after Knighton 1998 - used with permission from Oxford University Press obtained April 16th, 2007)

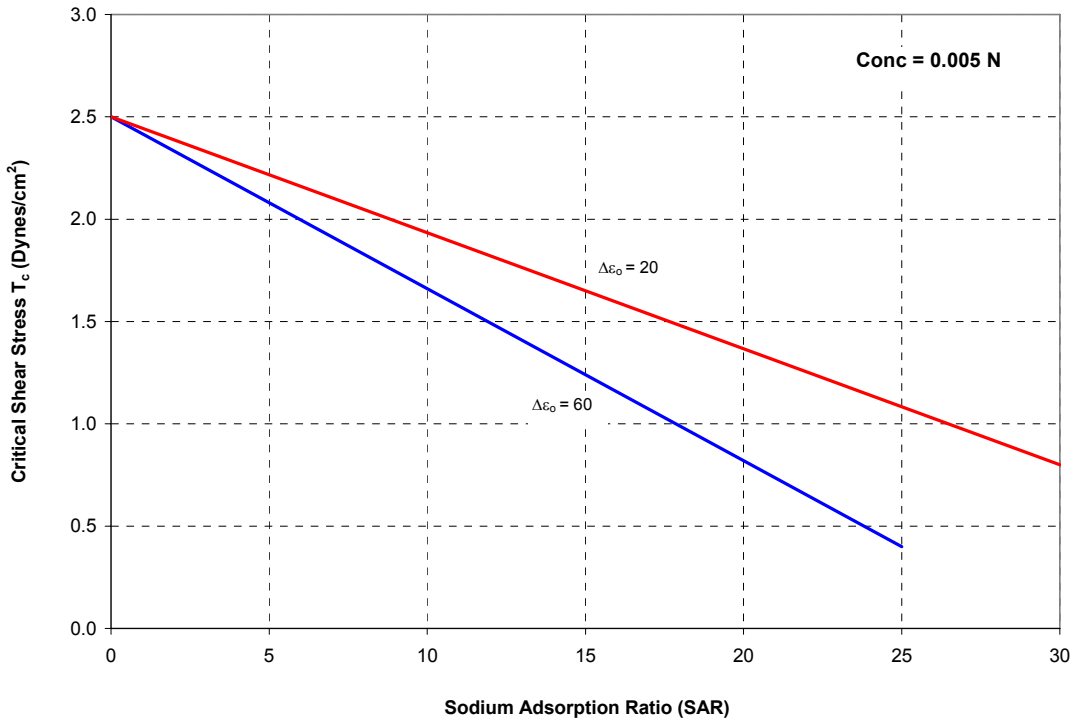

Figure 2.10: Critical Shear Stress as a function of SAR, $\Delta\varepsilon_o$ and CONC (based on data from Arulanandan *et al*. 1980)

Figure 2.11: Representation of laboratory recirculating hydraulic erosion flume (after Arulanandan *et al*. 1980)

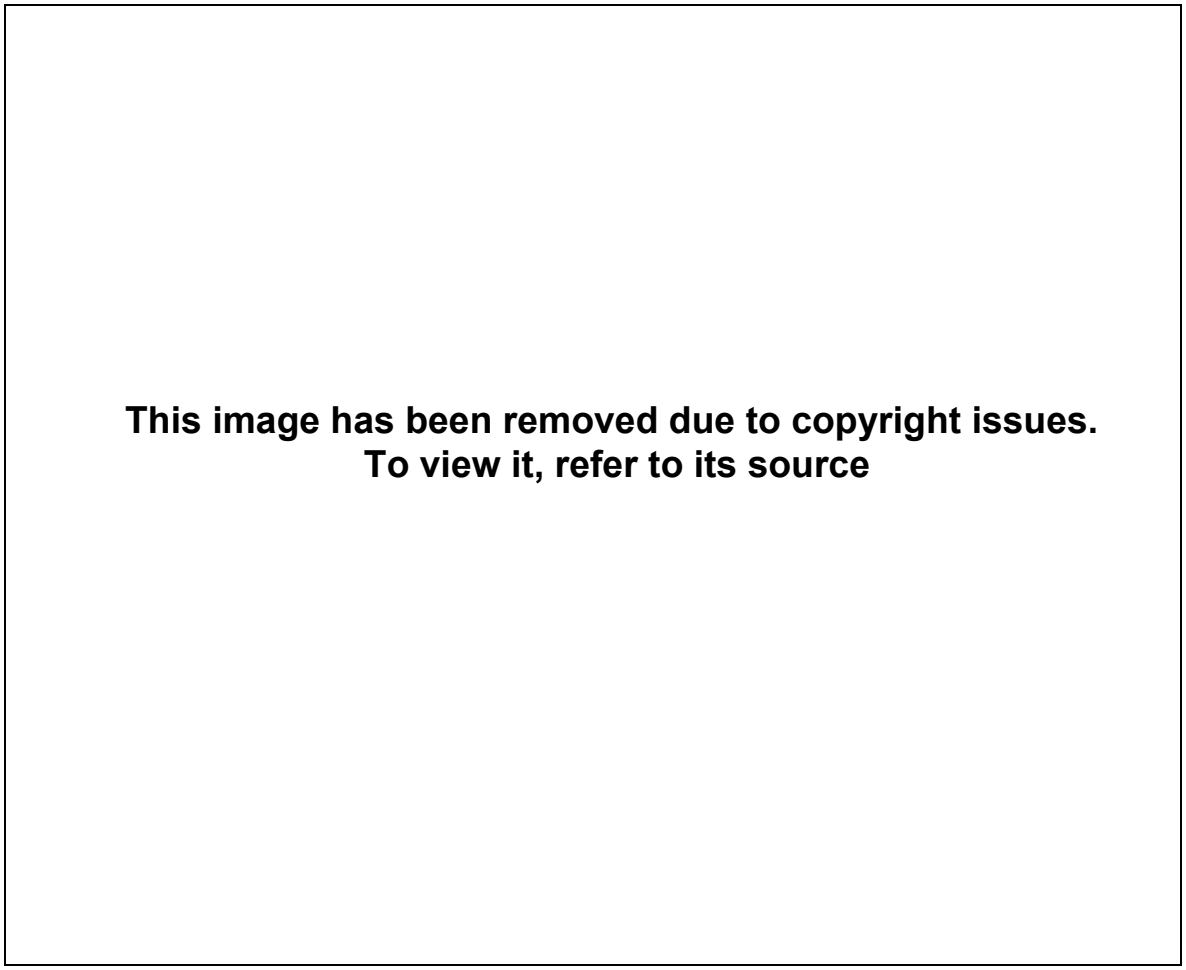

Figure 2.12: Cross-Section through rotating cylinder apparatus
(after Arulanandan *et al*. 1980)

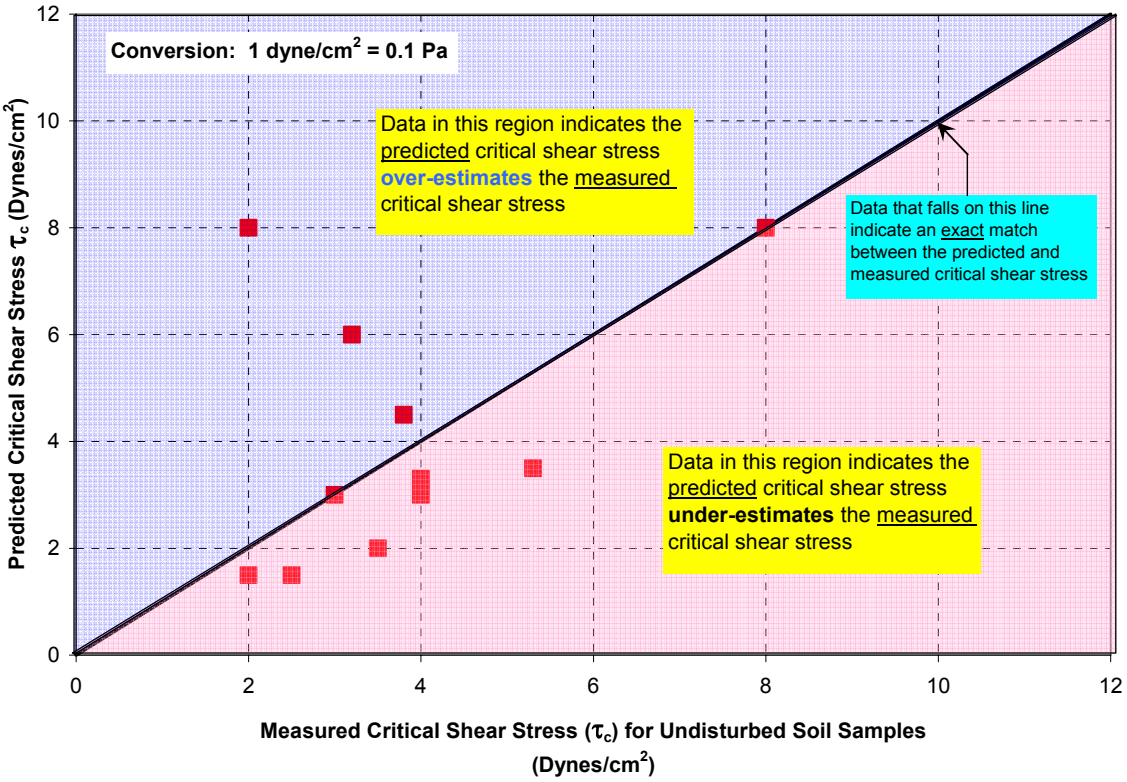

Figure 2.13: Predicted critical shear vs. measured critical shear for undisturbed soil samples (based on data from Arulanandan *et al*. 1980)

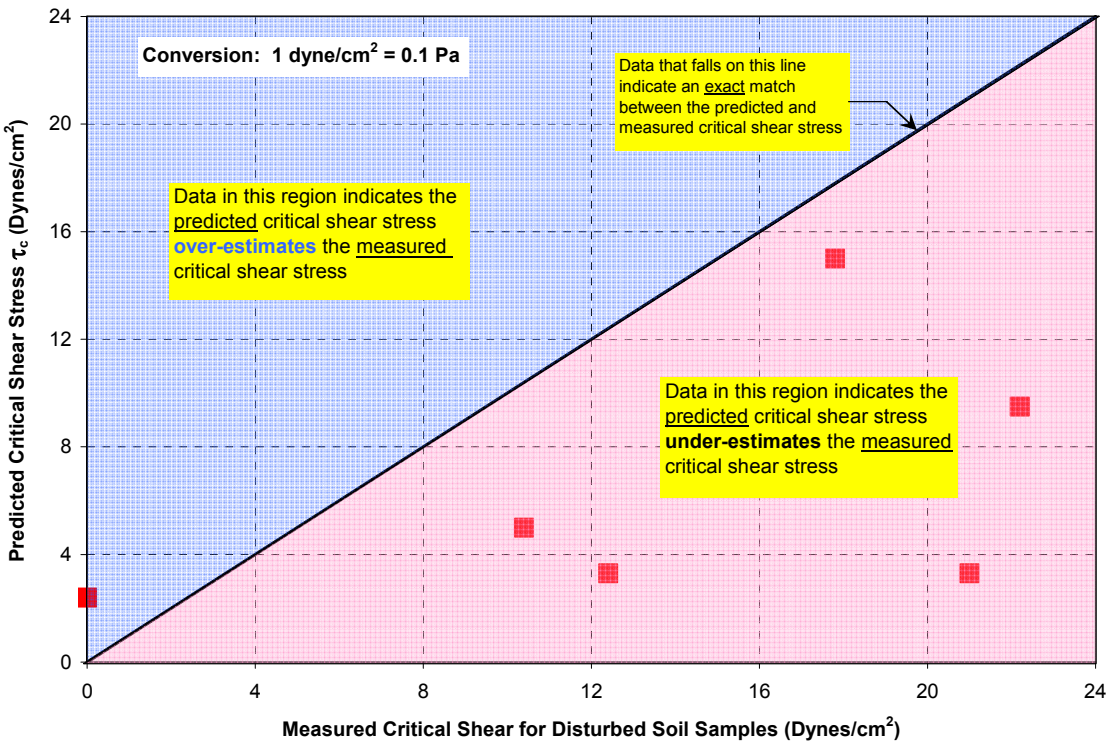

Figure 2.14: Predicted critical shear vs. measured critical shear for disturbed soil samples (based on data from Arulanandan *et al*. 1980)

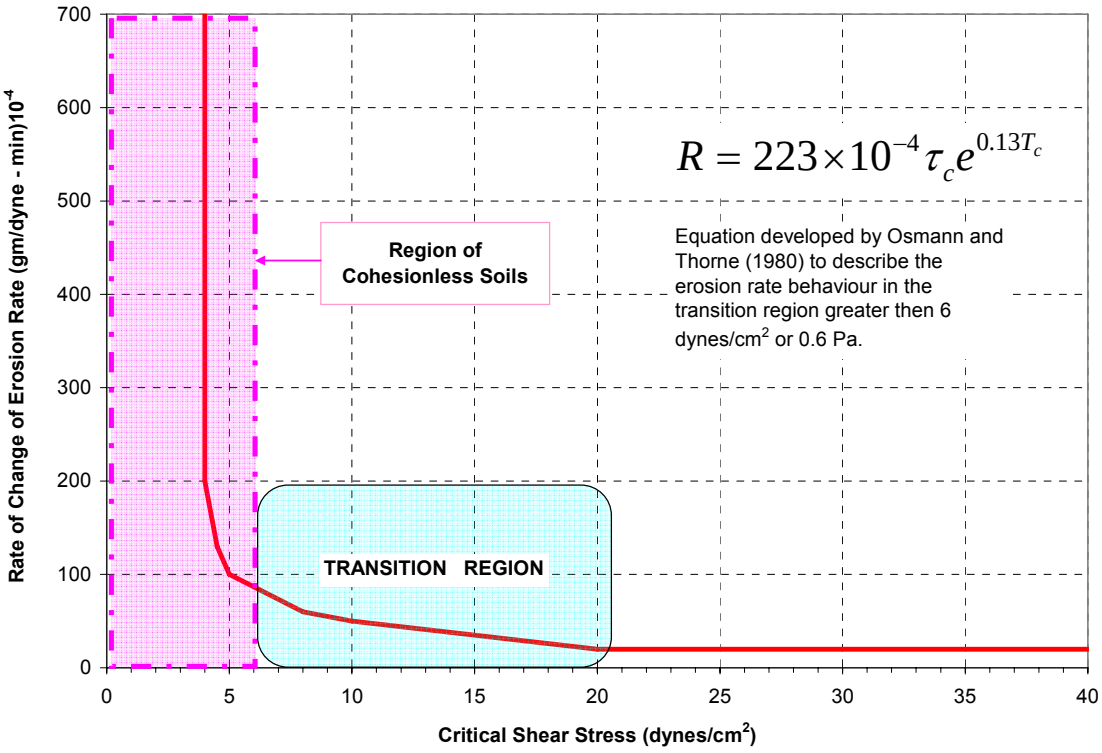

Figure 2.15: Rate of change of erosion rate vs. critical shear stress for undisturbed soil samples (based on data from Arulanandan *et al*. 1980)

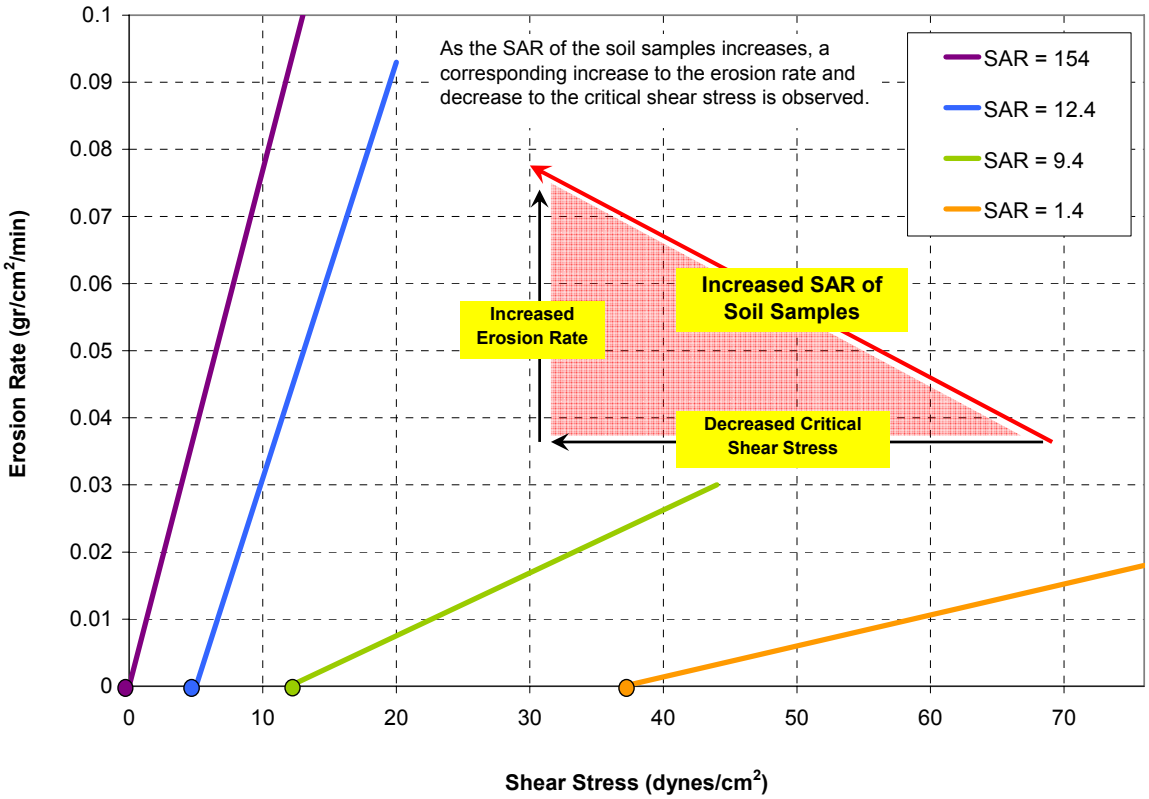

Figure 2.16: Effect of Sodium Adsorption Ratio (SAR) and Eroding Fluid Concentration (CONC) on Erosion Rate and Critical Shear Stress (based on data from Arulanandan *et al.* 1975)

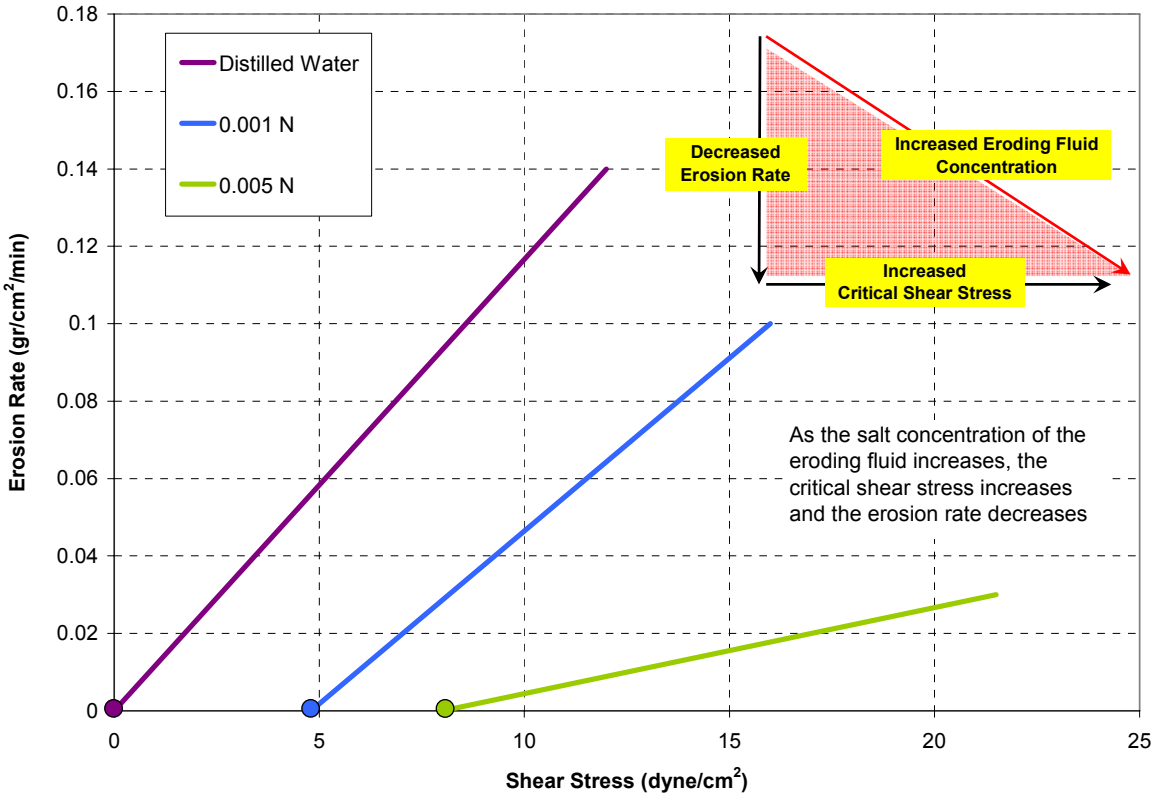

Figure 2.17: Effect of Eroding Fluid Concentration (CONC) on Erosion Rate and Critical Shear Stress (based on data from Arulanandan *et al.* 1975)

CHAPTER 3: OBSERVED EROSION

3.1 Introduction

Researchers have stated that erosion is a contributor to riverbank instability (Baracos and Lew, 2003). As river flows increase, greater erosion occurs, which causes greater instability. However, none of the research has quantified the decrease in factor of safety due to erosion from annual river flow. Local Winnipeg consulting practice generally assumes the annual decrease in stability due to erosion is approximately 10%, although this value has never been validated and seems excessive. The goal of this research is to quantify erosion from yearly flow events and relate the intensity and duration of the flow events to the percent decrease in factor of safety. The research involves the following steps:

- Obtain consecutive yearly riverbank cross-sections at a specific location along the Red River.
- Align the cross-sections in reference to a common datum
- Measure the horizontal distance at the toe of the bank between consecutive annual cross-sections. This quantity represents the yearly erosion due to that years flow event.
- Model the riverbank cross-sections from consecutive years using a numerical slope stability model to quantify the factor of safety for each cross-section. The percent decrease in slope stability is calculated based on the difference between the factors of safety.

3.2 Riverbank Cross-Sections

Erosion due to a given flow event can be quantified by comparing the riverbank cross-sections between consecutive years. The horizontal difference between the two cross-sections represents the erosion from the given flow event or a major movement caused by erosion from a number of flow events. Since the majority of erosion is concentrated at the toe of the bank it is necessary to have riverbank cross-sections that are surveyed below the water line, to the bottom of the channel. A search through historical to present day information at the City of Winnipeg Waterways Department was undertaken to obtain riverbank cross-sections along the Red River. Through this search it was determined that there are no sites continuously monitored or surveyed on an annual basis along the Red River. The information is limited to cross-sections from 1912, 1951 and numerous reports of remediated riverbanks from 1978 to 2005 which include cross-sections of failed riverbanks prior to remediation.

The data from 1912 contain topographic maps for select areas of the Red River which include areas of Kingston Crescent, St.Vital Park and Alexander Dock. The surveys are shown in imperial units at a scale of 1 inch = 200 feet. The cross-sections are spaced approximately 75 m apart. As the surveys were completed in 1912, they do not show the same level of present day urbanization. For example, Perimeter Rd. and River Dr. which run through St.Vital Park had not been developed in 1912. The next set of data was from 1951 which involved an extensive survey of the Red River from Emerson to Lockport compiled for the

Red River Basin Investigation (RRBI). In 1951 an extensive study of the Red River was undertaken due to the flood of 1950 that resulted in 1838 km^2 of land that was inundated and approximately 22 million dollars in costs to the City of Winnipeg for flood fighting, rehabilitation and relief (Rutherford and Baracos 1953, RRBI 1953). The study, which followed with construction of the Red River Floodway, was undertaken to determine better flood protection measures for the City of Winnipeg. The data are on topographical maps in the form of contours as well as complete river channel cross-sections approximately every 115 meters and given in imperial units at a scale of 1inch = 100 feet on the x-axis and 1inch = 10 ft on the y-axis. The data are a little more extensive than the 1912 data with the addition of graphed river channel cross-sections. However, the cross-sections are not as closely spaced as the 1912 maps. The remainder of the data is in the form of reports submitted to the City of Winnipeg completed by various consulting groups for remedial works along different sections of the Red River. The reports span from 1975 to 2005 and include remedial works to both residential and City owned properties such as Kingston Crescent, Lyndale Drive, Chruchill Drive, St.Vital Park and King's Park. Most of the reports include a cross-section of the riverbank prior to remediation, however not all reports include cross-sections that extend past the waterline showing the configuration of the riverbank toe which is the primary area for erosion. These cross-sections will be referred to as the present day cross-sections.

3.2.1 Site Selection

The criteria for site selection are as follows:

- The site must be present in the 1912, 1951 and present day cross-sections.
- Present day cross-sections are limited to those that extend below the waterline to the toe of the cross-section. Toe of the cross-section is defined as the location where the riverbank transitions to the riverbed. The location of this point is subjective.
- Each cross-section must have a common datum to reference when aligning the cross-sections.
- Study site must be a location along the Red River prone to yearly erosion, preferably an outside bend or transition. Erosion can be observed along all stretches of the river but is expected to be more pronounced on the outside bends and transitions.

The location selected for study that satisfied these criteria was Kingston Crescent which is a distinct location in Winnipeg that appears as a peninsula with the Red River outlining the perimeter as shown in Figure 3.1. At this location the river has as sharp meander that is approaching the stage of an oxbow lake which is evidence that this area has experienced significant erosion. The exact location within the area selected for study is on the south side of Kingston Crescent at an outside bend of the river where the peninsula is the narrowest. The present day

cross-section for this location is from 2001 and was completed for a dyke assessment study.

3.2.2 Aligning Riverbank Cross-Sections

In order to align the cross-sections from 1912, 1951 and 2001, all cross-sections had to be in the same units and scale and referenced to a common datum. The datum for aligning the cross-sections had to be defined based on a common coordinate system. The x-coordinate was defined as the location along the length of the river. This point was aligned by estimating the closest cross-section from the 1951 and 1912 maps to the 2001 site. A surveyed cross-section does not exist at the exact location of the 2001 site on the 1951 and 1912 maps. However the closest cross-section to the site was selected. The y-coordinate was defined at the edge of the road closest to the river. The road appeared on each map and it was assumed that its location had not moved since 1912. Further to this, all cross-sections required the same orientation with the riverbank on the left side looking upstream into the page. This required the 1951 cross-section to be mirrored in order to have the same orientation as 1912 and 2001 cross-sections.

Microsoft Excel was used to align the cross-sections by adjusting the coordinates. The construction of aligning the cross-sections is shown in Figures 3.2 through 3.5, with the final assembly given in Figure 3.6. In general, when aligning the cross-sections, it was assumed the riverbank had to retreat

horizontally from past to present day cross-sections. Therefore the 1912 cross-section extended the furthest horizontally followed by the 1951 cross-section then 2001.

As shown in Figure 3.6, the erosion at the toe from 1912 to 1951 is approximately 26 m and from 1912 to 2001 it is 39 m. At the bank crest the erosion from 1912 to 2001 shows approximately 24 m. If the amount of erosion at the toe between 1912 and 2001 is divided by the total number of years the averaged result is approximately 0.44 m per year. However, this quantity is not a true representation of the amount of erosion per year as erosion is flow dependent, with more erosion occurring during high flow years and less during low flow years. This quantity represents the average erosion rate per year over an 89 year period.

3.3 Slope Stability

Assessing the stability of a riverbank is traditionally based on a limit equilibrium method used to calculate the factor of safety of the slope. The factor of safety (FS) is the ratio of maximum available resisting moments ($M_{R\text{-}MAX}$) to the disturbing moments (M_D) developed by gravity and other disturbing forces (FS = $M_{R\text{-}max}/M_D$). A value of 1.0 or close to 1.0 represents a failed slope or a slope that is approaching failure. In local Winnipeg practice, typically the F.S of a stable slope along the Red River is designed to be 1.3.

The factor of safety is traditionally calculated using a limit equilibrium method which is based on assuming a failure surface through the slope and then formulating the equilibrium equations for the disturbing and resisting forces acting on that surface. The disturbing forces and moment are a result of the weight of the soil mass and piezometric conditions in the soil. Resisting forces and moments are due to the shearing forces mobilized along the failure surface. However, in using this method there are several problems with solving the forces and moments. These include:

- difficulties determining the center and weight of the sliding mass
- mobilized shear resistance varies along the slip surface
- seepage forces vary within the soil mass and along the failure surface and are typically unknown

To overcome these problems, the sliding mass is divided into a number of slices and then the forces and moments of each slice are summed. As the number of slices increase, the approximation of the factor of safety improves. However, dividing the mass into slices presents more problems as the number of forces acting is greater than the number of equilibrium equations available to solve the system of unknowns. To solve this problem assumptions have to be made about three of the unknowns, one being the inter-slice forces. A number of methods have been proposed which make different assumptions about the unknowns and

which equilibrium condition (force, moment or both) is/are satisfied. The best known limit equilibrium (LE) methods that have been proposed include:

- Ordinary or Fellenius (1936)
- Simplified Bishop (1955)
- Janbu's Simplified (1954)
- Janbu's rigourous (1956)
- Spencer's (1967)
- Morgenstern-Price (1965)

The reader is referred to Tutkaluk (2000) who presented detailed discussions on each of these methods in terms of the assumptions, equilibrium conditions satisfied and recommended method for riverbanks along the Red River. Factors of safety calculated with methods such as Morgenstern-Price and Spencer, that satisfy all conditions of equilibrium, are not significantly affected by the assumptions of the method. With respect to force equilibrium methods which satisfy only force equilibrium, the factor of safety is significantly affected by the assumptions made for the interslice forces. Consequently, the force equilibrium methods do not produce factors of safety that are as consistent as methods that satisfy all conditions of equilibrium.

A fairly recent development which is becoming more routinely used for solving slope stability problems, involves the incorporation of finite element (FE) stress and seepage analysis into limit equilibrium. The FE analysis provides an alternative to the assumptions that the LE analysis needs to make regarding interslice forces. In general both solutions (the original LE solution and the solution with interslice forces calculated by FE) produce similar factors of safety for the sliding mass however the FE solution presents more options and advantages over LE. The FE method involves discretizing the soil mass into elements and nodes and then solving the stress-strain constitutive equations at the nodes of each element to determine the stress distribution within the soil mass. Since FE makes use of stress-strain constitutive equations to solve the stresses in the soil mass, the stresses are much more realistic as compared to those solved in LE (Krahn 2003). This further allows the ability to calculate local factors of safety within the sliding mass which can help to design more effective and economical remedial measures to best support the slope (Krahn 2003). The graphical capabilities of FE also allow for a better understanding of the failure mechanism.

Ultimately the accuracy of the analysis can only be as good as the accuracy of the soil properties and boundary conditions defined in the analysis. Therefore some may argue that the solution of an FE analysis does not present greater accuracy over LE solutions if there are several assumptions with the defined soil

properties and porewater pressures. Further to this, FE is still a relatively new technique for analysis and more use is required to gain greater support.

3.4 Stability of Erosion Cross-Sections

The method selected to analyse the stability of the erosion cross-sections was finite element analysis combined with limit equilibrium. The program selected for the analysis was Geostudio which is a product of Geoslope International[1]. Geostudio offers a variety of finite element numerical soil models, three of which were integrated to assess the stability of the erosion cross-sections. The models used were SEEP/W, SIGMA/W and SLOPE/W. The methodology for analyzing the cross-sections with all three programs is shown in Figure 3.7.

Finite element analysis involves dividing the problem into smaller pieces, solving for the solution at each piece and finally reconnecting the pieces to represent the solution to the global problem (Krahn 2004). Dividing the problem into smaller pieces is referred to as discretizing the domain or meshing and the individual pieces are called finite elements. A detailed discussion of the finite element program is covered by Tutkaluk (2000) and therefore details of how the program is used will not be covered here.

[1] Canadian company based in Calgary, Alberta

3.4 1 SEEP/W Model

The slope cross-sections were initially set up in SEEP/W, a program used to model seepage through porous media. Details for setting up the SEEP/W model are shown in Figure 3.8. The cross-sections were sketched just as they were set-up in Figure 3.6 and then the soil mass was discretized into elements, with the soil properties and boundary conditions of the problem input into the model. The problem was defined as a steady state analysis with four distinct soil layers. The stratigraphy of the site was obtained from the City of Winnipeg Report[2] for which a soils investigation was undertaken at the site. The stratigraphy consists of approximately 9.4 m of silty clay of alluvial origin, 1.3 m of lacustrine clay and 3.7 m of glacial till overlying bedrock. In addition, a weak clay layer of 0.6 m thickness was modeled overlying the glacial till. The inclusion of this soil layer was based on Tutkaluk (2000) who suggested that composite slip surfaces common to Red River can be modeled in SLOPE/W by specifying a weak clay layer just above the till. Tutkaluk (2000) modeled a weak clay layer of 0.6 m thickness therefore this same condition was applied.

The four soil layers were modeled with three different hydraulic conductivity functions. The weak clay layer was assigned the same hydraulic conductivity function as the lacustrine clay. As there was no laboratory testing completed to

[2] KGS Group, 2001. "Kingston Crescent/Row Community Ring Dike - Geotechnical Design Report", Winnipeg.

produce hydraulic conductivity functions, the functions were obtained from Tutkaluk (2000). The soil properties used in the analysis are shown in Table 3.1 (after Figure 3.14), with the model cross section shown in Figure 3.11. The boundary conditions defined included the groundwater level, the river level and the bedrock aquifer elevations. The worst case boundary conditions were selected for the analysis which occur during the fall when the river level decreases and the aquifer level increases. The fall river level was selected as 219 m obtained from the City of Winnipeg report, whereas the aquifer and groundwater elevations were obtained from Tutkaluk (2000) as there were no piezometers or aquifer monitoring wells at the study location to state the exact elevations of the groundwater and aquifer. The aquifer elevation was defined as 223.70 m and the groundwater 4 m below the ground surface. A detailed summary of the steps taken to set up the seepage model is shown in Figure 3.8.

3.4.2 SIGMA/W Model

The stress model was defined after the seepage model with the use of SIGMA/W. The author arbitrarily chose to follow this order for setting up the models however it is acceptable to define the models in the opposite order. Details for how the SIGMA/W model was set-up are shown in Figure 3.9. The model was defined using a linear-elastic constitutive relationship and effective stress analysis. The soil properties were defined for each soil layer as shown in Table 3.1 (after Figure 3.14), which include the alluvial clay, silty clay, weak clay layer and till. The properties include the unit weight, cohesion and angle of

friction. Soil properties for the alluvial clay for cohesion and angle of friction were given in the 2001 consultant report to the City of Winnipeg. The properties for the lacustrine clay and glacial till were defined according to the properties defined in Tutkaluk (2000). The unit weights of the soils were defined according to those used in local Winnipeg practice. The unit weight of the soil was applied as a body load in the analysis and the lateral earth pressure coefficient was defined as 1.0. The boundary conditions defined for the stress anlaysis was an X-displacement of zero on the left and right edges of the model and an X-Y displacement of zero along the base of the model. The flow chart in Figure 3.9 graphically shows all major inputs to the model under the two menu headings Key-In and Draw for the SIGMA/W model.

3.4.3 SLOPE/W Model

After the seepage and stresses of the model were solved they were imported into the SLOPE/W model to analyse the slope stability. Details for how the SLOPE/W model was set up are shown in Figure 3.10. The model uses a Mohr-Coulomb strength analysis with the soil properties such as unit weight, which are the same as the seepage and stress models. Figure 3.10 shows a flow chart outlining the major inputs to the model. The models were run sequentially for each of the riverbank cross-sections, and the factor of safety was calculated as shown in Figure 3.12. The final results showed a decreasing trend in factor of safety from 1912 to 2001 as shown in Figure 3.13 which gives the percent decrease in factor of safety as a function of the cross-section year.

The decrease in factor of safety from 1912 to 1951 was 11% and from 1951 to 2001 was 14%. The overall decrease over the 89 year period was 23% or 0.26% per year on average. The decreasing trend is explained by the increasing gradient of the cross-sections from 1912 to 2000 due to erosion. Steeper slopes are less stable than flatter slopes and hence produce lower factors of safety. It is important to recognize that riverbanks are dynamic systems which are continuously eroding and failing as a result of different flow events. As the riverbank erodes, the factor of safety decreases until failure is induced. Once the riverbank fails it attains a stable configuration which raises the factor of safety above that prior to failure. The cross-sections from 1951 and 2000 are snap-shots in the riverbanks history and it may simply be a coincidence that the factors of safety for both years follow a decreasing trend from 1912. It seems likely that between these years the bank did fail and subsequently attained a factor of safety greater than the value it had in 1912. Erosion then caused the factor of safety to decrease again. This cyclic behavior is examined in the following section and in Chapter 4.

3.5 Evolutionary Stability of a Riverbank

Figure 3.14 shows idealized failure cycles induced by erosion. The x-axis shows the time period in years and the y-axis shows the factor of safety. The riverbank initially begins at a stable configuration with a factor of safety well above 1.0. Over time, the factor of safety decreases due to decreasing stability caused by

erosion. Eventually the factor of safety drops to 1.0 and the riverbank fails. After failure, the factor of safety increases above 1.0 since the slope has moved to a more stable configuration. Depending on this new configuration, the factor of safety can be greater or less than the initial factor of safety at the beginning of the previous cycle. This is an on-going discontinuous process over the history of a riverbank. Figure 3.14 is an idealization showing four such cycles. The collection of cycles describes the evolutionary stability. The percent decrease in factor of safety due to flow years of different intensity and duration is of interest. This study recreates the evolutionary stability, although the lack of yearly historical surveyed cross-sections clearly limits the precision of the analysis.

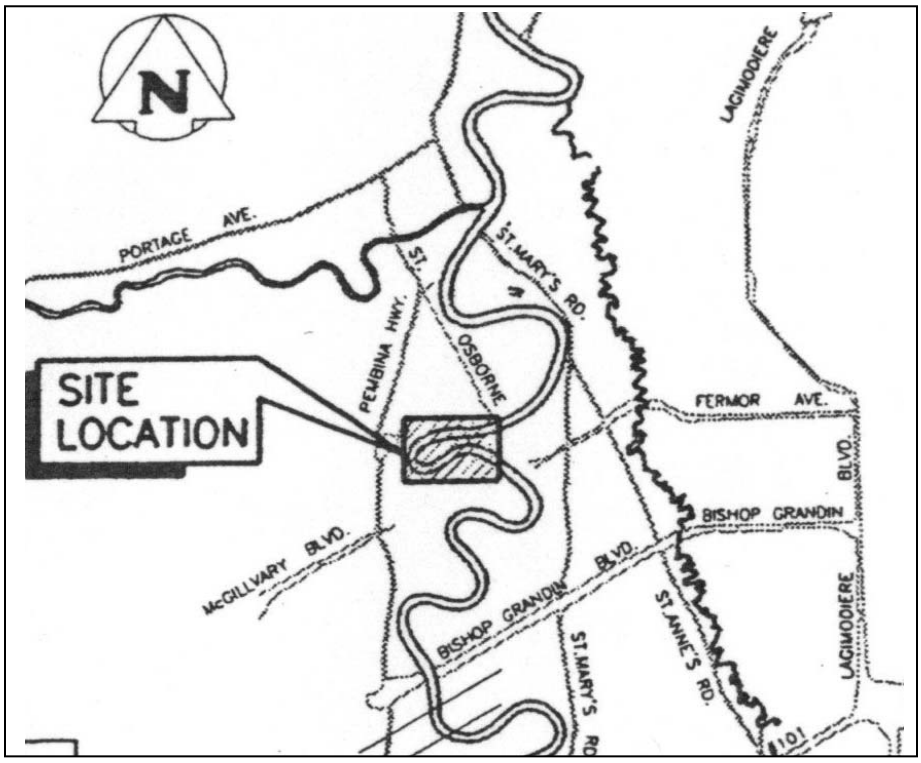

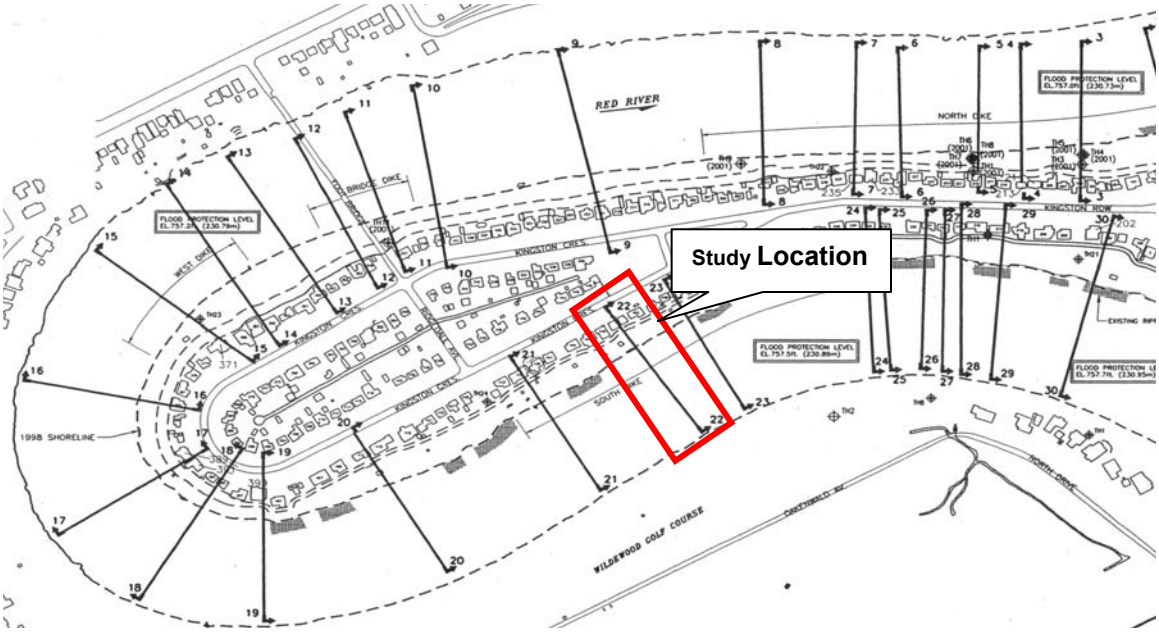

Figure 3.1: Location of study site - Kingston Crescent (after KGS Consultants, 2001 - used with permission from Rob Kenyon, P.Eng. of KGS Consultants obtained July 24th, 2007)

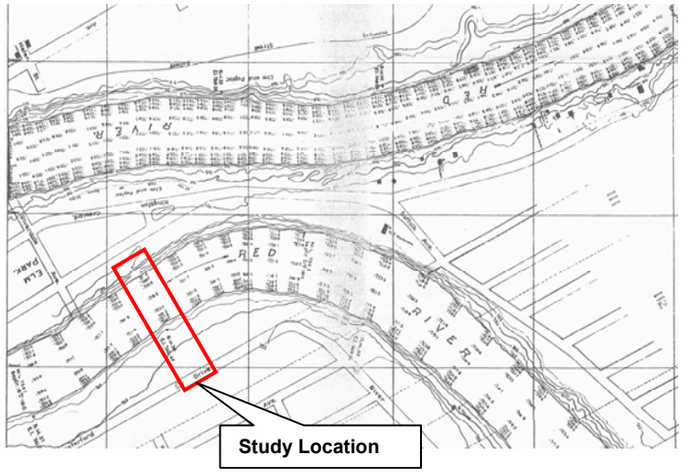

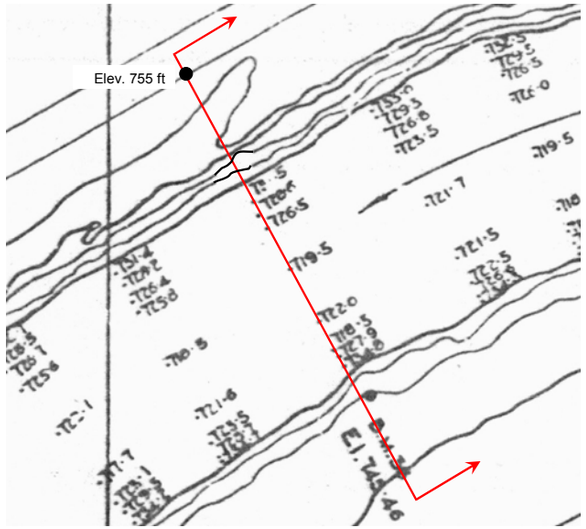

The distance between contours and surveyed elevations is measured in inches and converted to feet. Drawing scale is 1 inch = 200 ft. Surveyed elevations are shown in feet which are read off the map and entered into an excel spreadsheet

x (in)	x (ft)	y (ft)
0.0	0	755
0.3	59	755
0.6	114	755
0.6	129	755
0.7	145	750
0.8	161	745
0.9	176	740
1.0	192	732
1.1	212	729
1.3	251	727
1.4	282	720
1.8	353	722
2.3	455	719
2.4	486	728
2.5	510	735
2.6	529	740
2.8	557	745
2.9	584	750
3.6	725	755

1912 cross-section is plot in Excel using the above data points

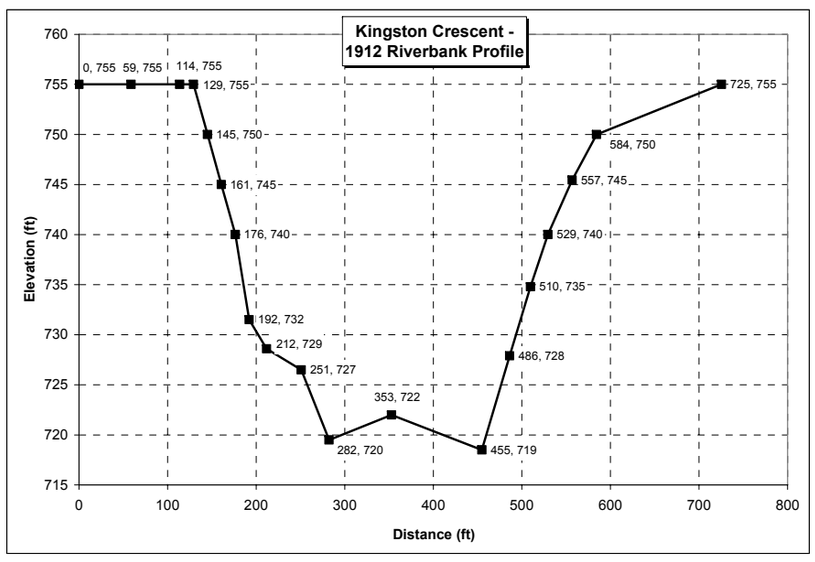

Final Cross-section is converted from imperial into metric units

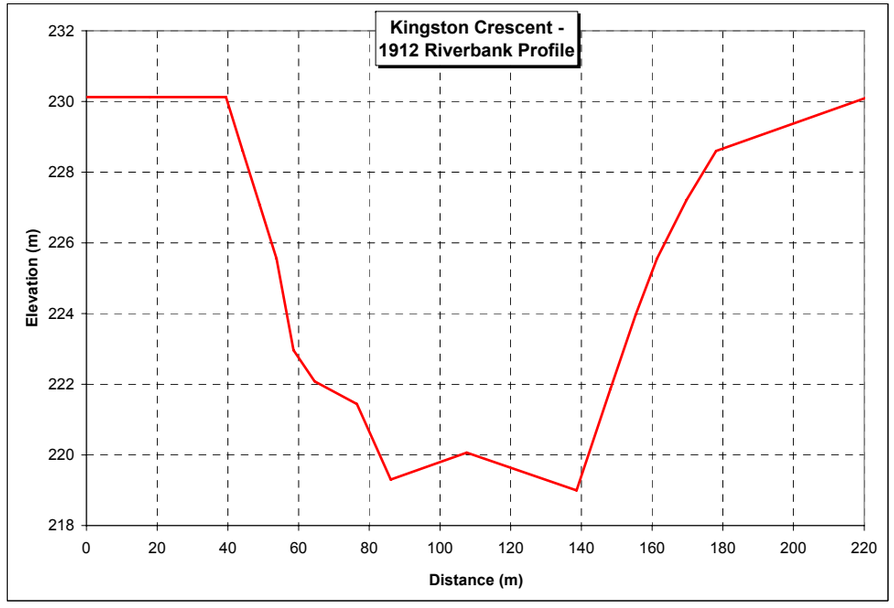

Figure 3.2: Methodology for aligning 1912 riverbank cross-section

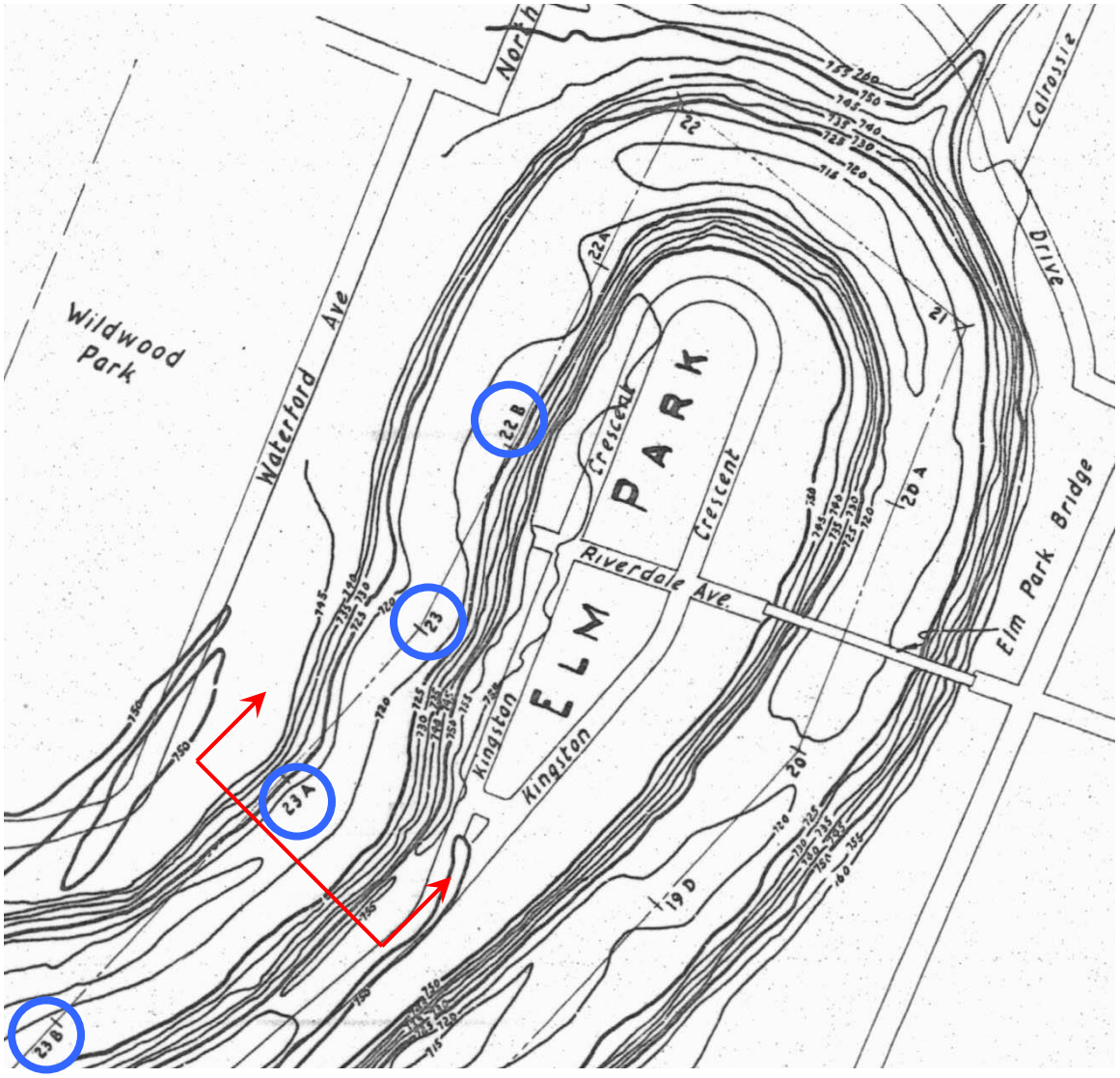

Figure 3.3: Plan view of surveys obtained in 1951 - cross-section 23A selected for study (after RRBI, 1953 - used with permission from Eugene Kozera, Manager of Water Control System Management at Manitoba Water Stewardship, obtained July 23rd, 2007)

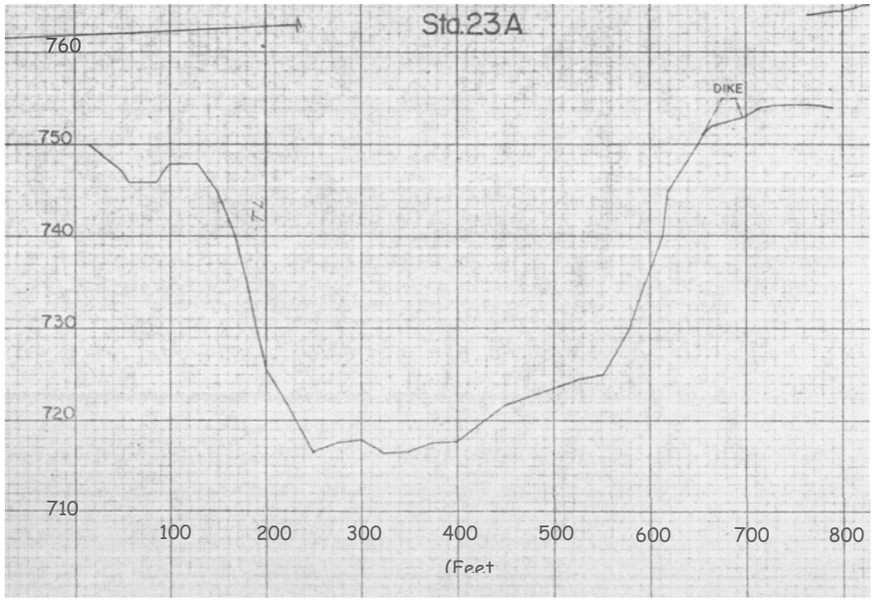

Original 1951 RRBI cross-section (left) is re-created in Microsoft Excel (right) by picking off the data points at all transitions on the original cross-section. View of the cross-section is looking downstream.

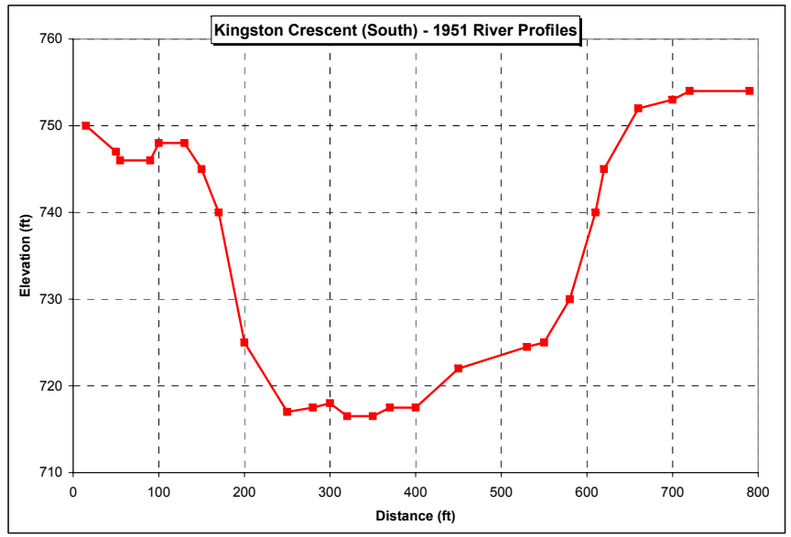

x (ft)	y (ft)
15	750
50	747
55	746
90	746
100	748
130	748
150	745
170	740
200	725
250	717
280	717.5
300	718
320	716.5
350	716.5
370	717.5
400	717.5
450	722
530	724.5
550	725
580	730
610	740
620	745
660	752
700	753
720	754
790	754

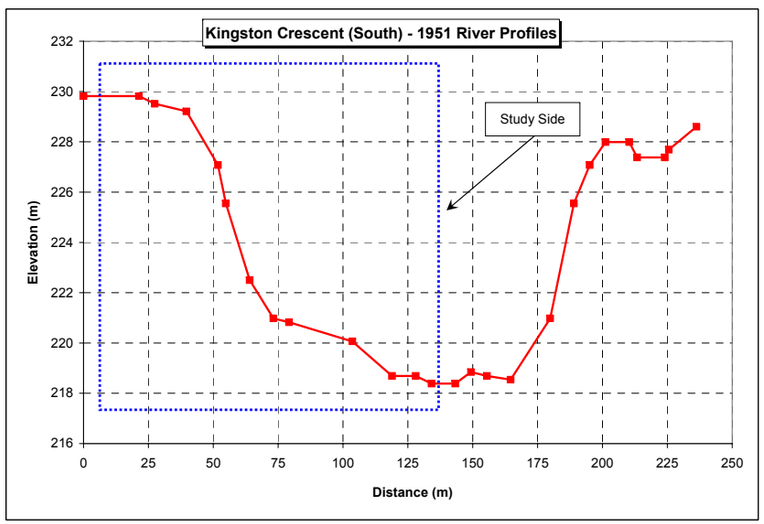

Cross-section is mirrored to have the same orientation (upstream view) as the 1912 and 2000 cross-sections

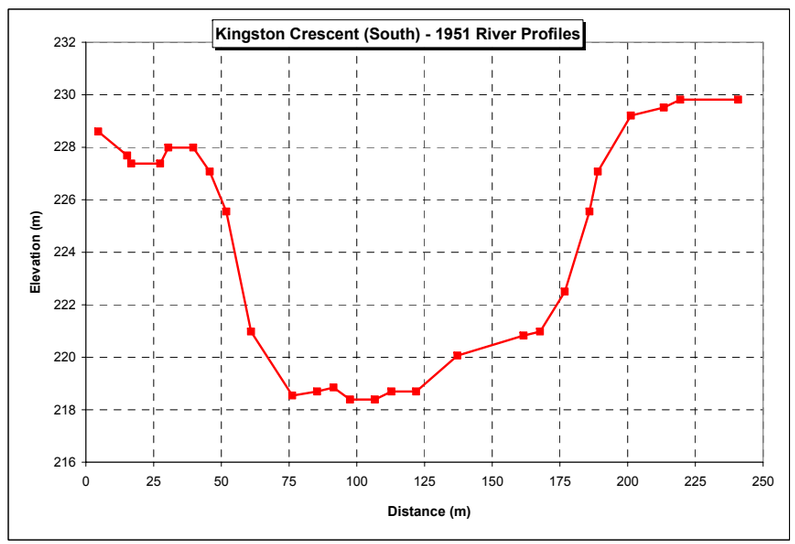

x (m)	y (m)
5	229
15	228
17	227
27	227
30	228
40	228
46	227
52	226
61	221
76	219
85	219
91	219
98	218
107	218
113	219
122	219
137	220
162	221
168	221
177	223
186	226
189	227
201	229
213	230
219	230
241	230

Figure 3.4: Methodology for aligning 1951 riverbank cross-section

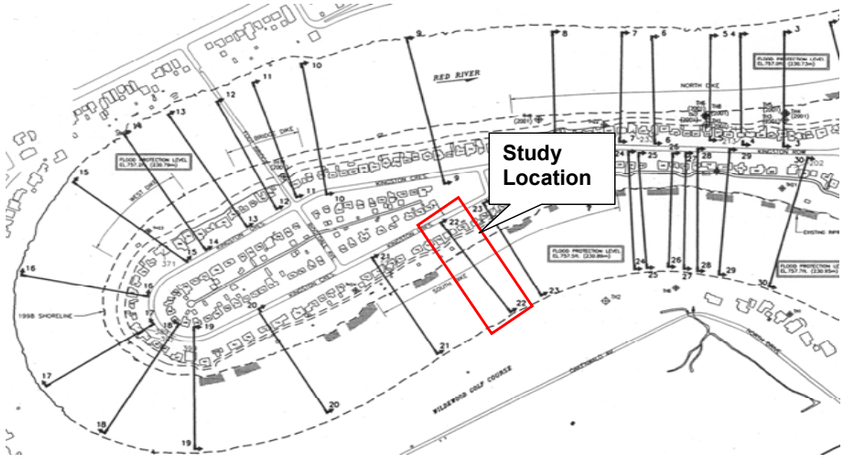

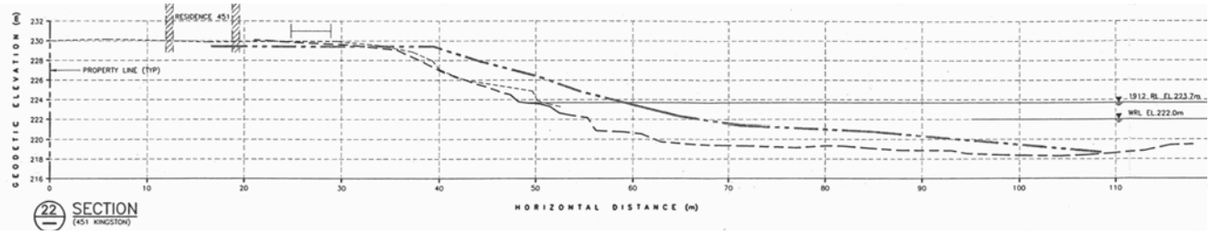

x (m)	y (m)
0	230
21	230
36	229
42	226
47	224
49	224
51	224
52	223
56	222
56	221
61	220
63	220
80	219
94	219
100	218
106	218
116	220
118	220

The 2001 cross-section is from a consultants report for which they have generated a survey of the riverbank and superimposed the 1912 cross-section on top of it. The 2001 cross-section is the most receded cross-section. All transition points of the 2001 cross-section are entered into an excel spreadsheet and a duplicate cross-section is produced.

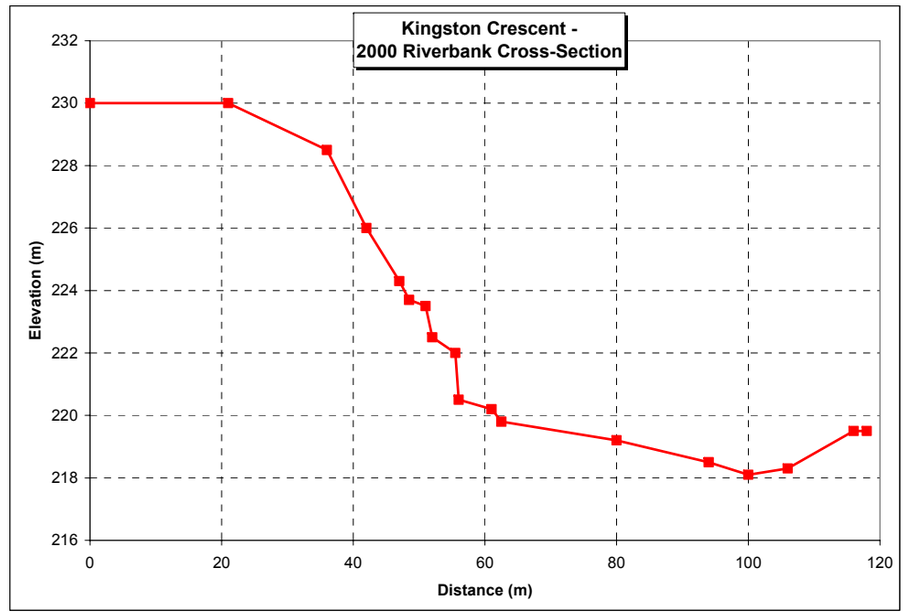

Figure 3.5: Methodology for aligning 2001 riverbank cross-section

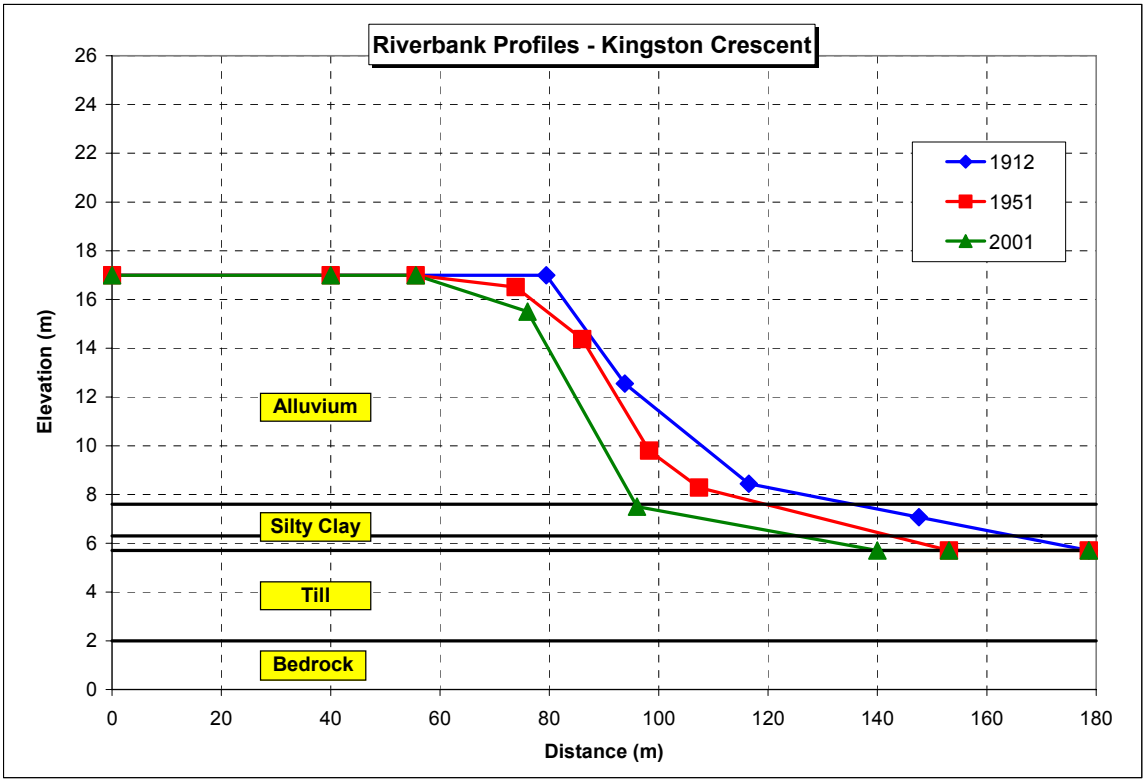

Figure 3.6: Aligned historical riverbank surveys for Kingston Crescent

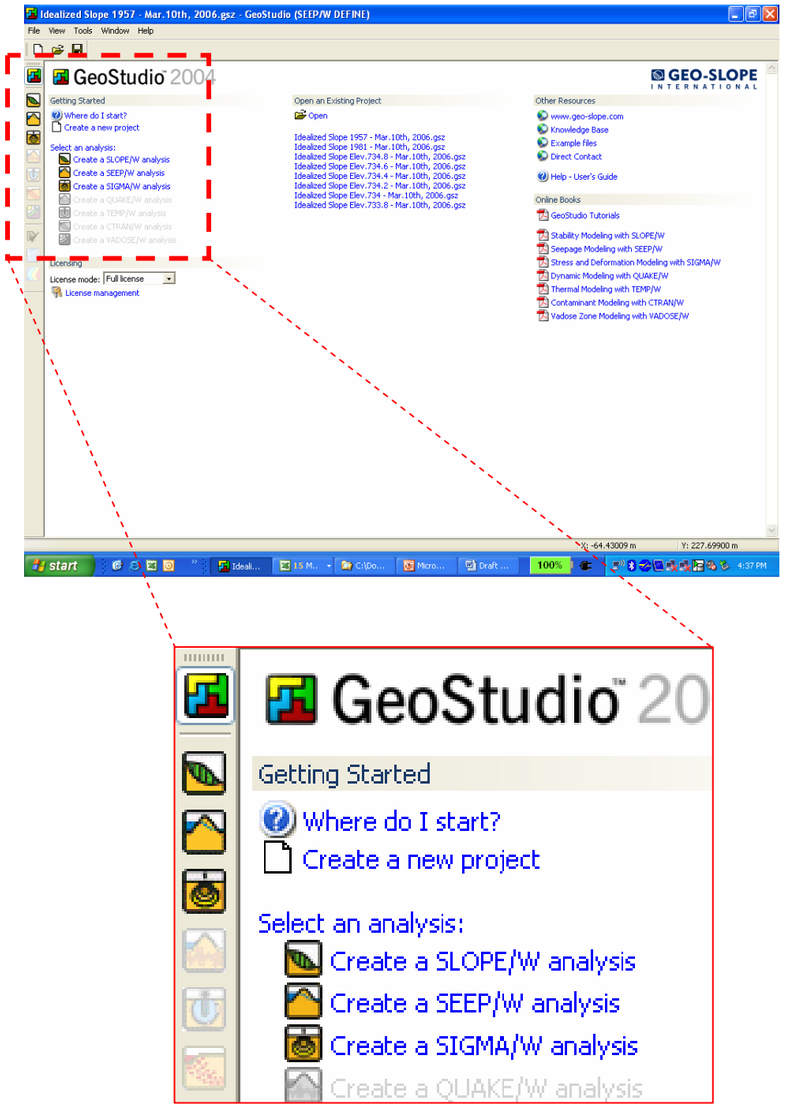

SEEP/W

– Define:

- Material properties - soil stratigraphy
- Hydraulic conductivity
- K-ratio - measure of soil anisotropy

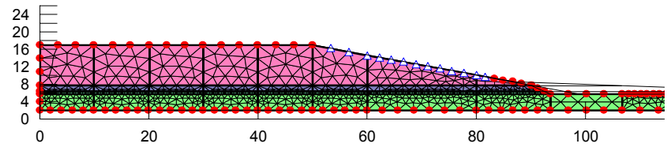

– Specify:

- Type of analysis, steady state
- Node boundary condition, head or flow

– Output:

- Generation of porewater pressures within the soil mass

SIGMA/W

– Define:

- Material properties - linear elastic, effective stress analysis, cohesion, friction angle, modulus of elasticity, poisson's ratio
- Body load - soil unit weight

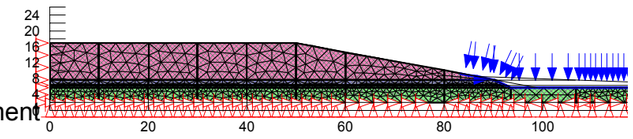

– Specify:

- Type of analysis, steady state
- Node boundary conditions, x and y displacement
- Edge boundary conditions, fluid pressure

– Output:

- Generation of stress distribution within the soil

SLOPE/W

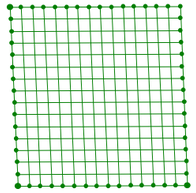

– Define:

- Material properties - strength model (Mohr-Coulomb), cohesion, friction angle, soil unit weight

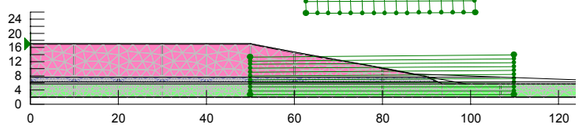

– Specify:

- Type of analysis - FE with SEEP/W porewater pressures and SIGMA/W stresses
- Slip surface grid and radius

– Output:

- Generation of stress distribution within the soil mass

Figure 3.7: Methodology for analyzing aligned cross-sections in FE analysis

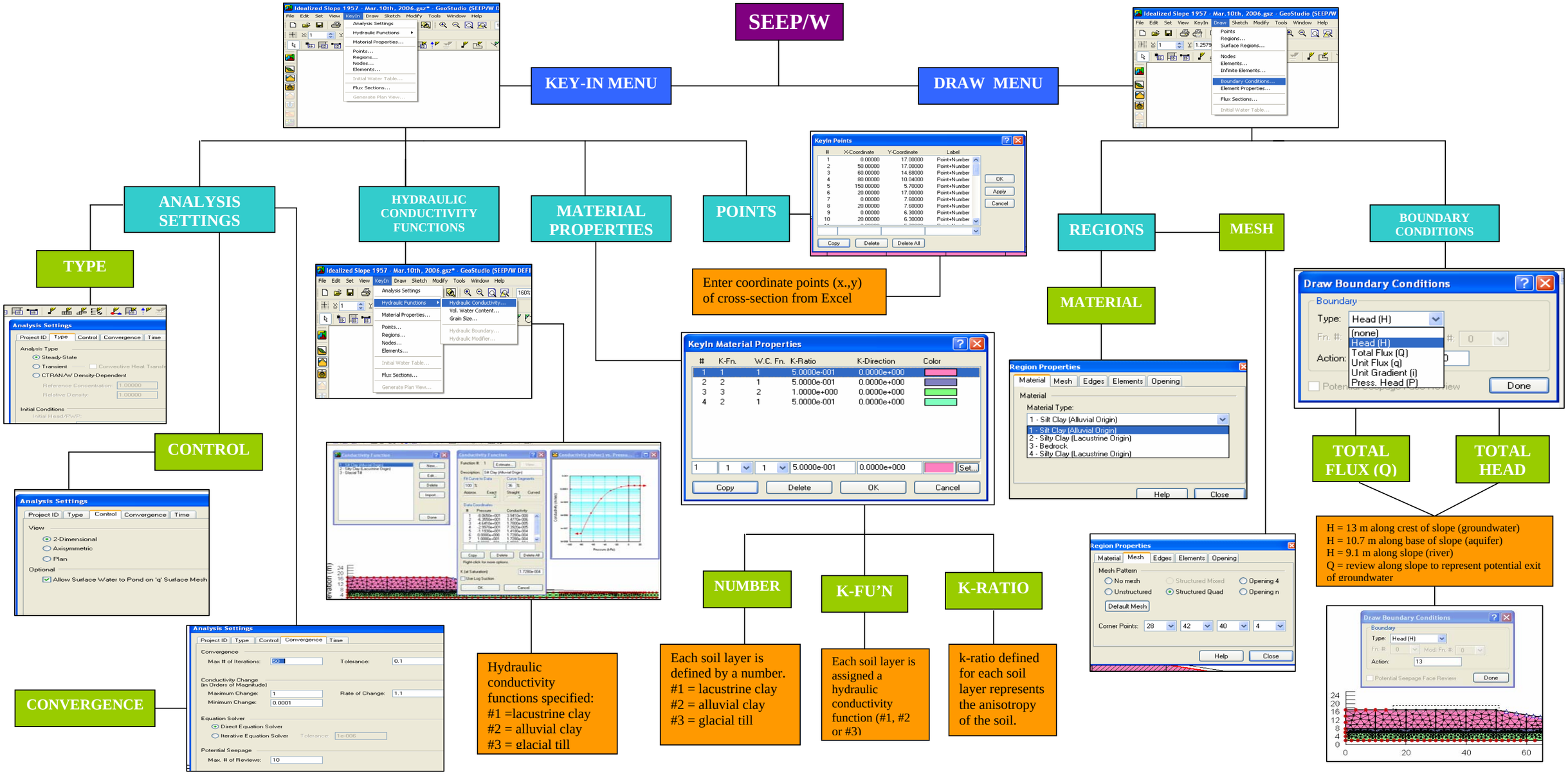

Figure 3.8: Details for setting up SEEP/W model

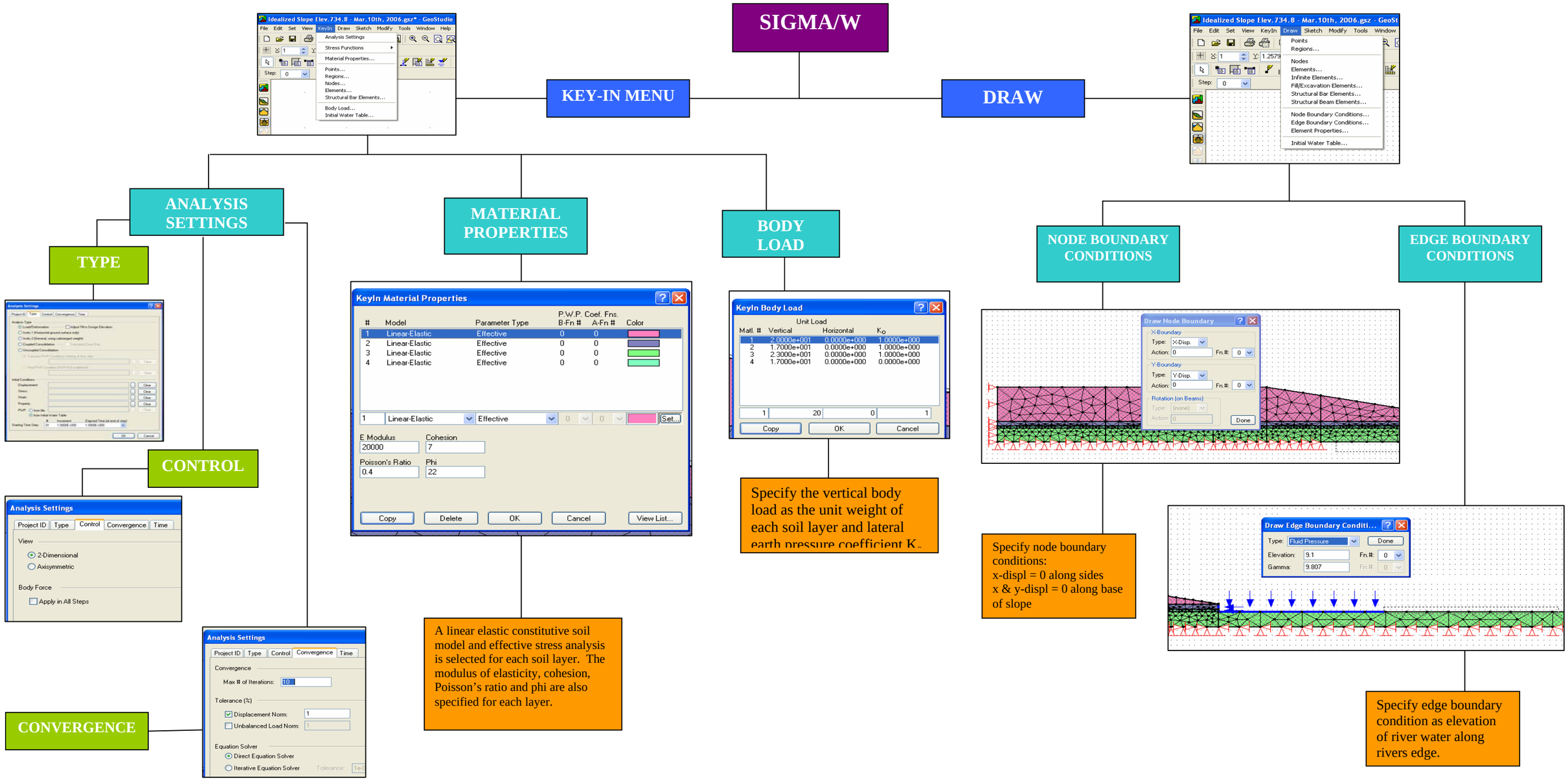

Figure 3.9: Details for setting up SIGMA/W model

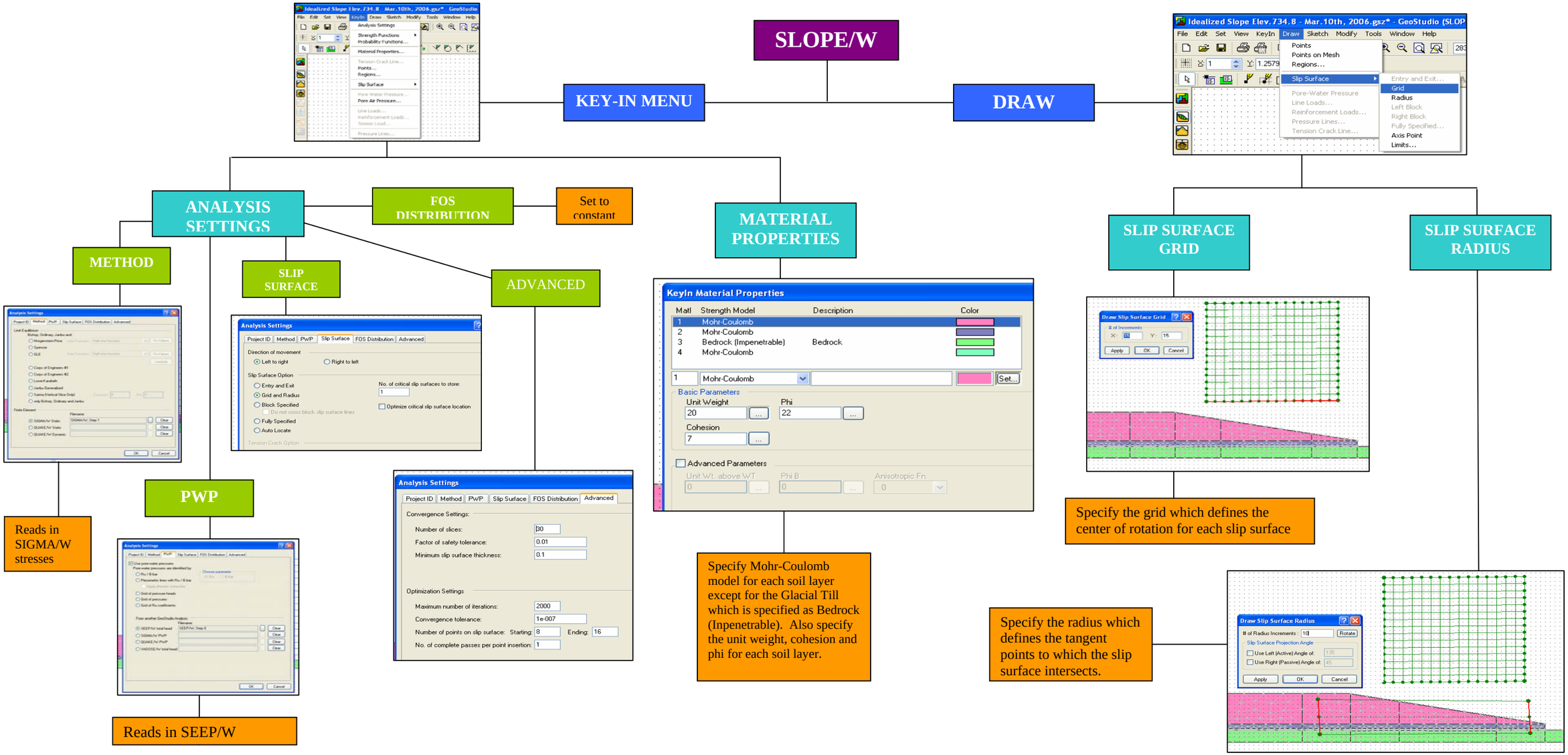

Figure 3.10: Details for setting up SLOPE/W model

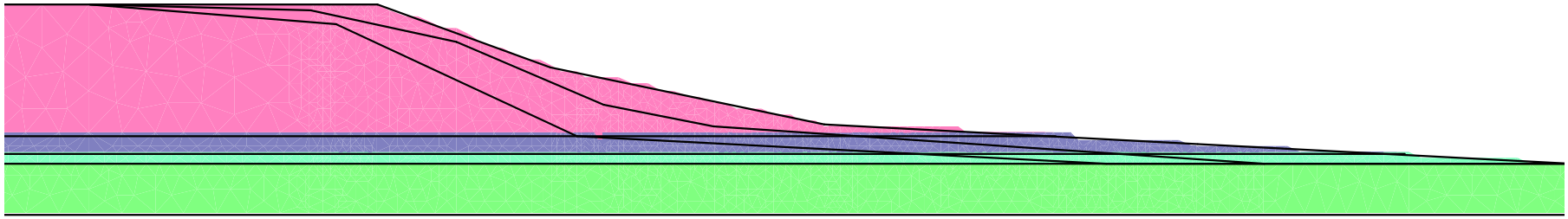

(b) 1912 cross-section

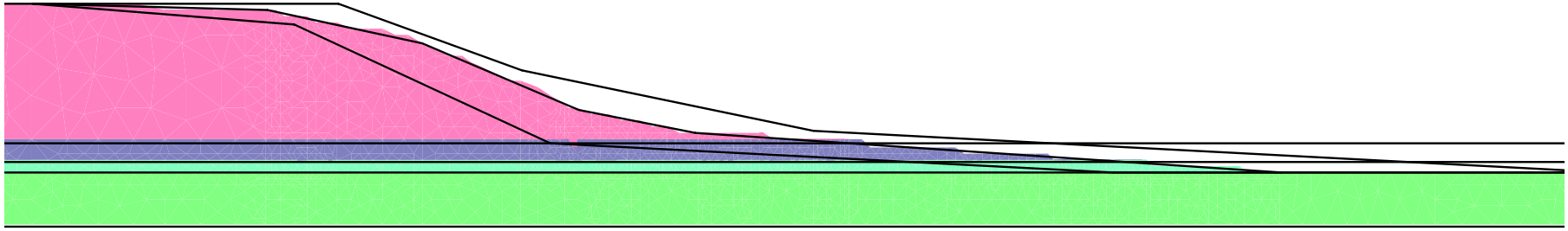

(b) 1951 cross-section

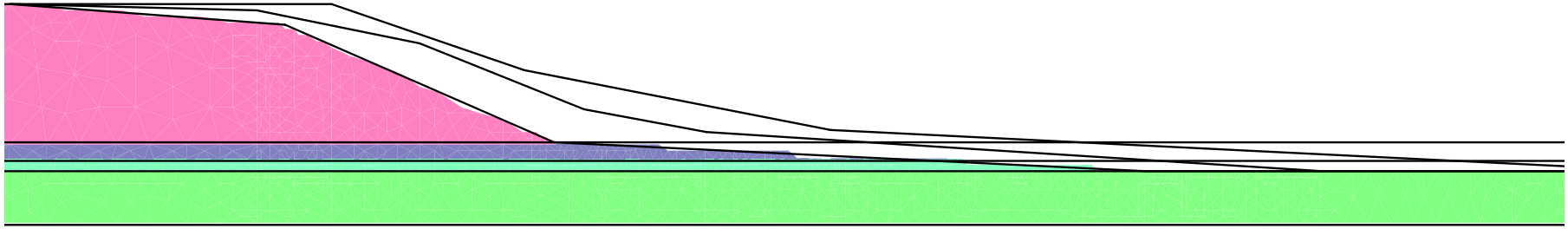

(c) 2001 cross-section

Figure 3.11: Model cross-sections for (a)1912, (b)1951, (c)2001 cross-sections

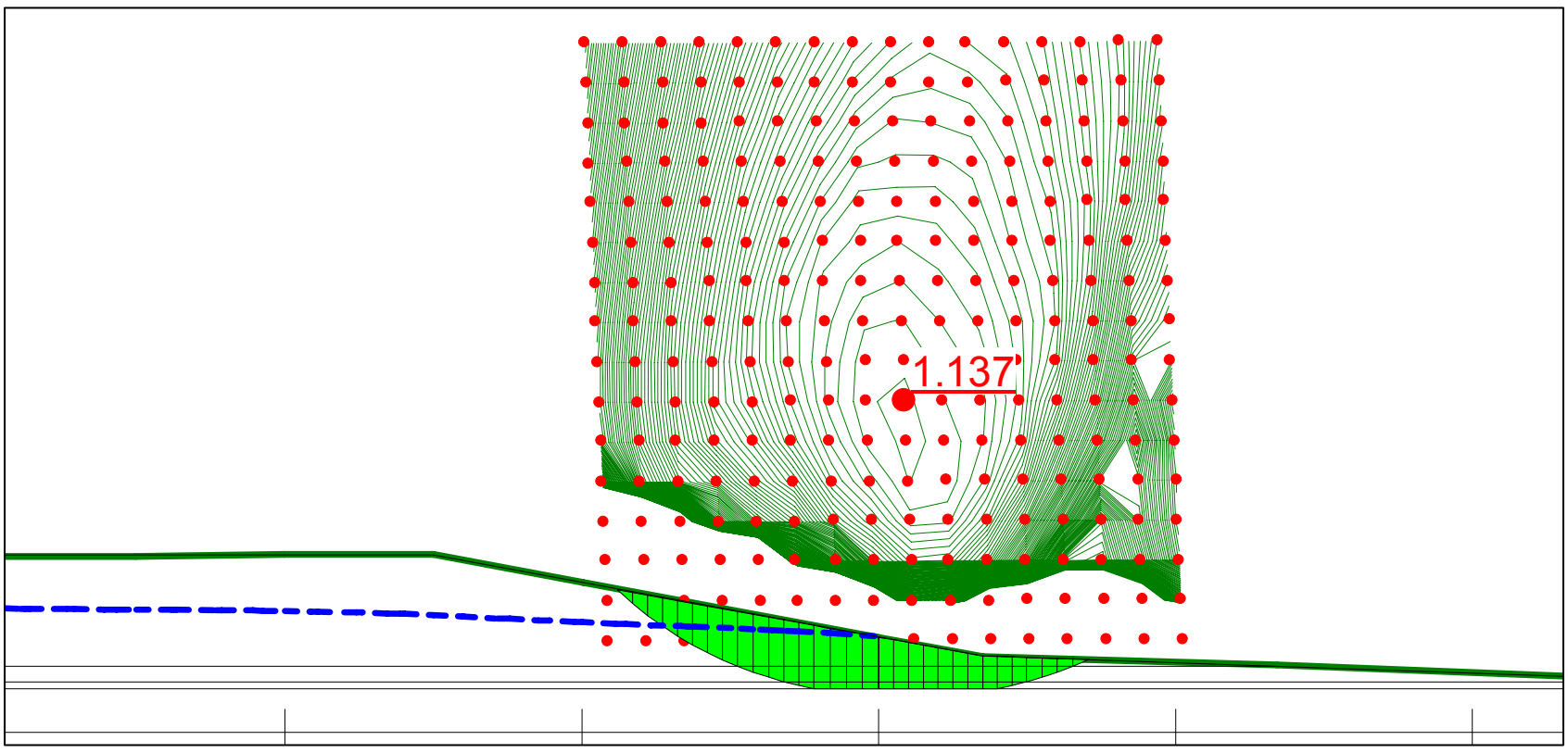

(a)

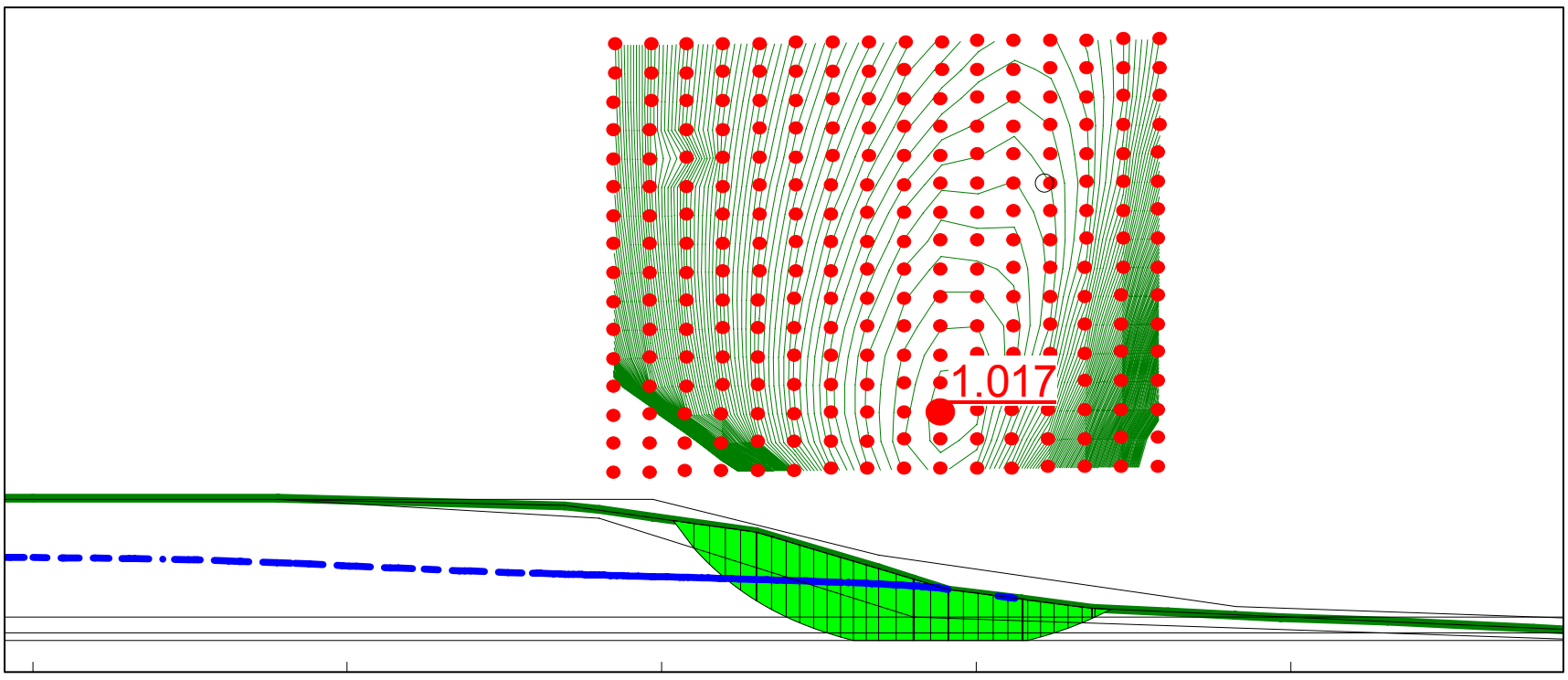

(b)

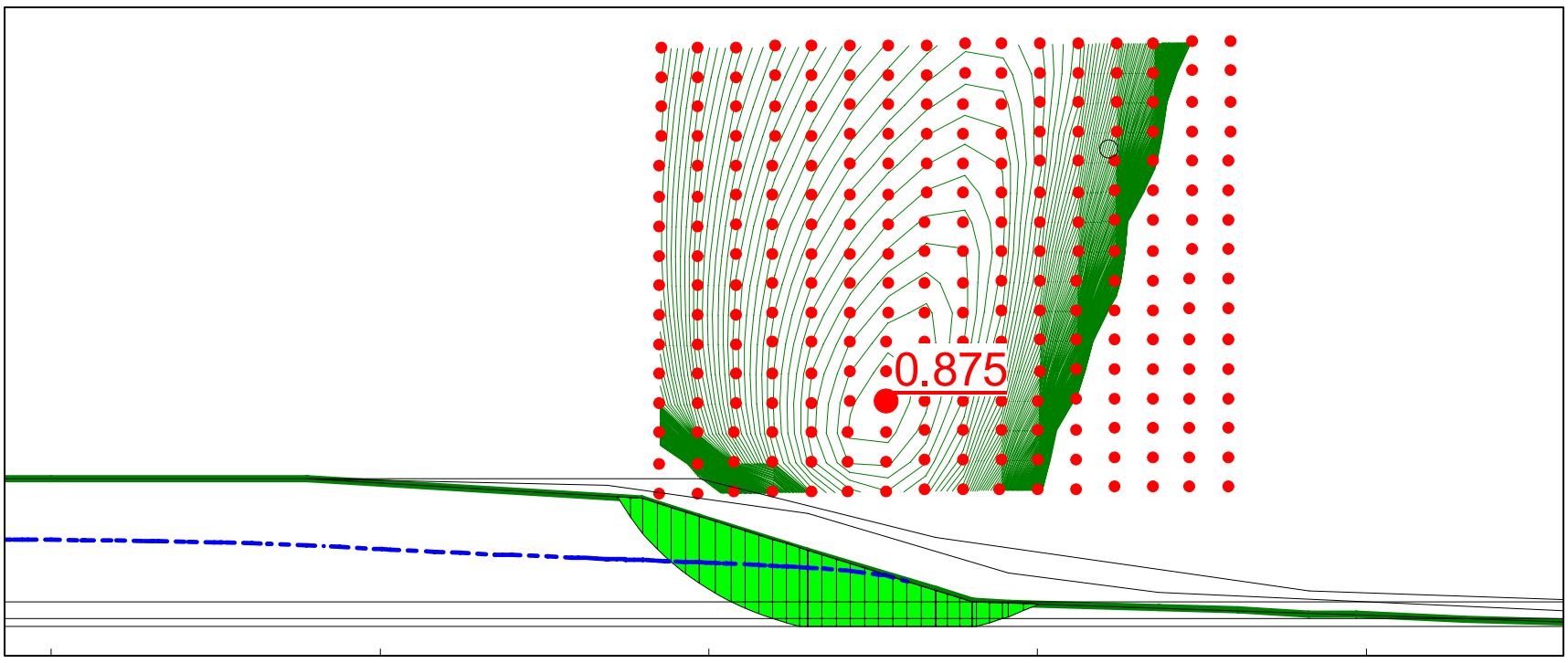

(c)

Figure 3.12: SLOPE/W results for (a)1912, (b)1951, (c)2001 cross-sections

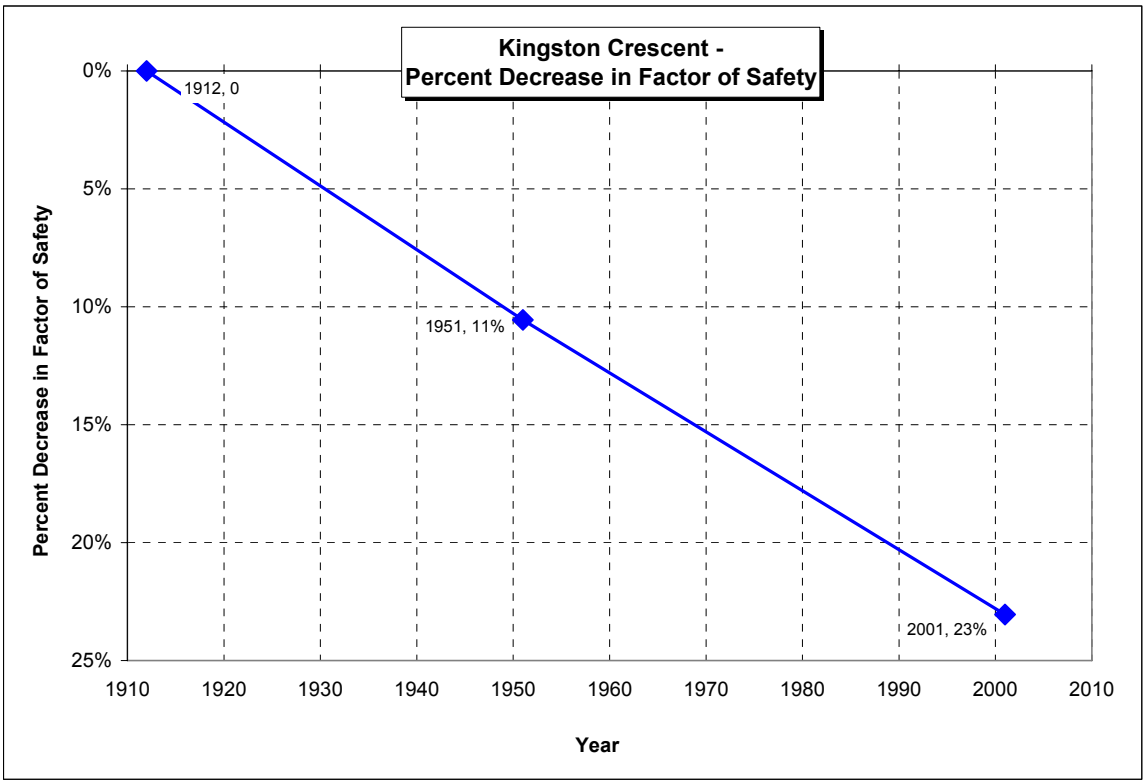

Figure 3.13: Percent decrease in factor of safety between historical surveyed cross-sections

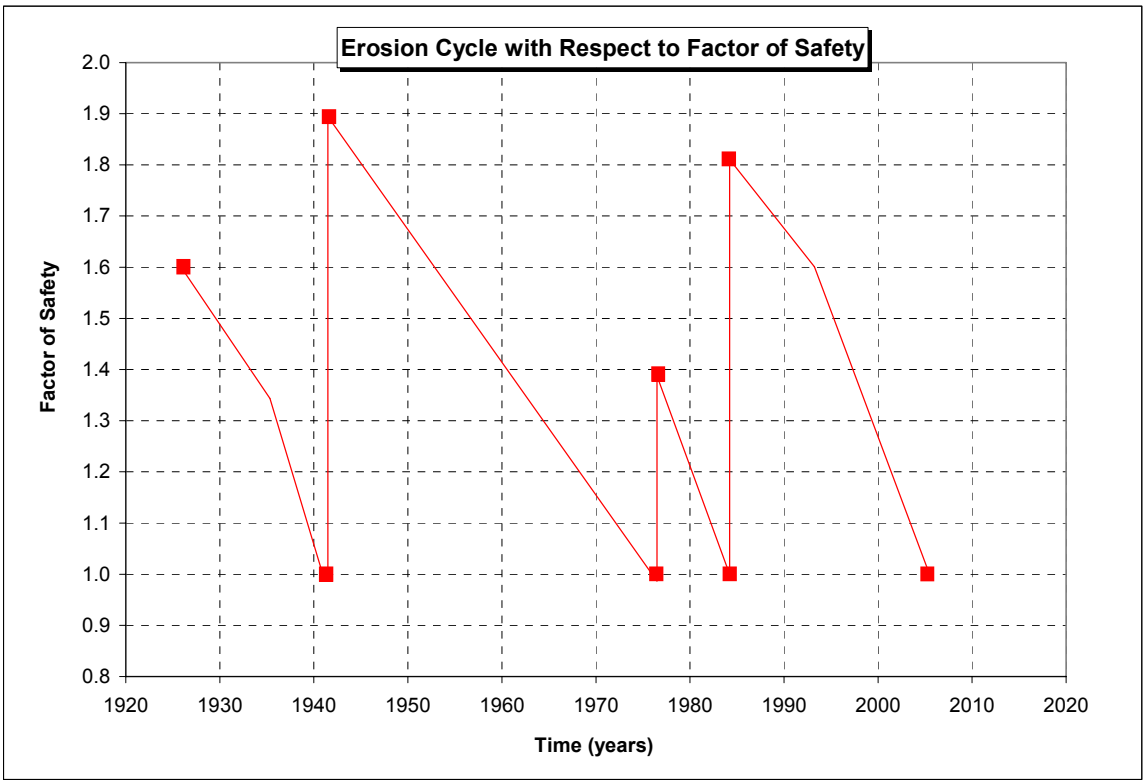

Figure 3.14: Idealized riverbank erosion evolution with respect to factor of safety

Soil Property	Alluvial Clay	Silty Clay	Weak Clay Layer	Glacial Till
Unit Weight (kPa)	20	17	17	23
Friction Angle	22	10	12	30
Cohesion (kPa)	7	4	3	10
k-sat (m/s)	2×10^{-9}	2×10^{-10}	2×10^{-10}	1×10^{-7}
k-ratio	0.5	0.5	0.5	0.5
K_o	1.0	1.0	1.0	1.0
E (kPa)	200,000	200,000	200,000	200,000
Poisson's ratio	0.4	0.4	0.4	0.4

Table 3.1: Soil properties used in finite element analysis

CHAPTER 4: THEORETICAL EROSION

The previous chapter quantified erosion based on measured riverbank cross-sections over a period of 89 years. This chapter details a theoretical method to quantify erosion of riverbanks between successive flow years. Referring back to Chapter 3, three components are required to quantify erosion:

- fluid shear stress
- critical shear stress
- erosion rate

Theoretical equations and numerical methods exist to calculate these quantities. The following sections provide an overview of solution methods selected for analysis.

4.1 Fluid Shear Stress

Chapter 2 presented an equation (Equation 2.3) that requires the input of standard hydraulic parameters for calculating the fluid shear stress based on flow force equilibrium. The method was extended to incorporate the findings of Olsen and Florey (1952) who determined a relationship between shear stress on the riverbed and shear stress on the riverbank. According to their research the distribution of shear stress on the riverbank shows maximum shear stress along the bank-bed interface and minimum shear at the highest point on the riverbank

as shown in Figure 2.8. The maximum shear stress calculated by Equation 4.1 is located approximately one third above the bed.

$$\tau = 1.08(\gamma RS) \qquad \text{Equation 4.1}$$

where,

γ = unit weight of water

R = hydraulic radius

S = slope of riverbed

Based on the graphical distribution of shear stress shown in Figure 2.8 the shear stress at the bank-bed interface appears to be of similar magnitude to the maximum shear stress. Olsen and Florey (1952) give an equation for only the maximum shear stress. Therefore, a relationship to describe the shear stress along the remainder of the riverbank had to be derived. This was done in private discussions with Dr. Shawn Clark at the University of Manitoba during part of this research. The distribution was simplified into a triangular distribution, with the maximum shear stress located at the bed-bank interface and the shear stress along the bank defined by Equation 4.2.

$$\tau = \gamma Sh\left(1 - \frac{y}{h}\right) \qquad \text{Equation 4.2}$$

where,

y = elevation point on the riverbank (m)

h = river stage (m)

S = slope of riverbed

γ = unit weight of water (kN/m^3)

The original coefficient, 1.08, in the equation for the maximum shear stress shown on Figure 2.8, is dropped from the equation for simplicity as its value is close to 1.0 and is not expected to significantly alter the results. Equation 4.2 is used in the analysis to calculate the fluid shear stress at different elevations along the riverbank.

4.2 Critical Shear Stress

Three methods to determine the critical shear stress were presented in Chapter 2. The Shields curve is only applicable for coarse grained soils. As the banks of the Red River are fine grained clay, this method cannot be applied. The second method presented by Alizadeh (1974) and Heinzen (1976) involves the use of Figure 2.10 which shows the critical shear stress as a function of SAR, $\Delta\varepsilon_o$ and CONC. According to personal communications with Alex Man (2005), SAR for the Red River is 4.3 (meq/L)$^{1/2}$, $\Delta\varepsilon_o$ for Winnipeg clay is 60 and the CONC is 0.005 giving a critical shear of 2 dynes/cm^2 or 0.2 Pa. The third method is based on the flume experiments by Briaud *et al*. (2001). To determine the critical shear experimentally, two samples of soil from two different locations along the banks

of the Red River were sent to Briaud's laboratory at the Texas A&M University. The samples were collected in the Fall after the drop of the river elevation and taken from the toe of the bank as close to the river's edge as possible. The toe area of the bank was selected for sampling as it was determined to be the most representative of soils subjected to the erosional forces of the river. A thin-walled Shelby tube was pushed from the surface 0.5 m into a selected riverbank.

Figure 4.1 shows results of the flume experiment for the two locations designated as Winnipeg 1 and Winnipeg 2. The results show shear stress in Pa versus erosion rate in mm/hr. The critical shear stress on the graph is the point at which the erosion rate first shows an increase from zero. In Figure 4.1, Winnipeg 1 shows an initial critical shear stress of 2.7 Pa. The erosion rate marginally increases from this point until a shear stress of 27 Pa is reached, after which the increase in erosion rate is much more dramatic. It is assumed that the true critical shear stress is 27 Pa and the increase in erosion rate prior to this is noise in the data due to experimental error. Also in Figure 4.1, Winnipeg 2 shows an initial critical shear of 9 Pa. Here, however, the increase in erosion rate is insignificant until 19 Pa. The latter is therefore selected as the critical shear stress for Winnipeg 2.

The slopes of the two inclined lines in Figure 4.1 define the relationships between erosion rates and shear stresses. The line for Winnipeg 1 has a slope of 11.5 mm/(hr·Pa) whereas the line for Winnipeg 2 has a much higher rate of 21

mm/(hr·Pa). This large difference cannot be easily explained. The author decided that the results from Winnipeg 1 would be used for the critical shear stress. The results from Winnipeg 1 indicate greater difficulty in initiating erosion and the slope of erosion rate versus shear stress line is not as steep. These two parameters result in a decreased volume of eroded soil

4.3 Erosion Rate

Chapter 2 outlined three methods for calculating erosion rates. The first method was by Partheniades (1965) that required the value of an erodibility coefficient. The coefficient can be calculated using Equation 2.9, which is based on experiments for soils from the southern United States. It is unknown whether the soil conditions are similar to those along the Red River. This method was not selected for analysis because a value for the erodibility coefficient could not be accurately determined for Winnipeg riverbanks due to research budget restrictions. The second method by Briaud *et al*. (2001) is based on experimental results. As shown in Figure 4.1, for every fluid shear stress there is a corresponding erosion rate. The third method, which is described in the following section, is based on Equation 2.11. The equation was proposed by Osmann and Thorne (1988) on the basis of experimental results of Arulanandan *et al*. (1980).

4.4 Theoretically Calculated Erosion

Two methods were selected for analysis, both of which use the same equation to calculate the fluid shear stress distribution. The methods were those proposed by Osmann and Thorne (1980) and by Briaud *et al*. (2001). The major variable in both methods is river elevation: erosion is positively correlated with river elevation. This project used both methods to quantify erosion and determine the new cross-section of the eroded river bank.

4.4.1 Methodology

The initial riverbank cross-section in Figure 3.6 was selected as the 1951 Kingston Crescent cross-section. The cross-section was divided into 11 elevation points for which the erosion was calculated. The erosion was calculated daily for a period of one year using the daily elevation data from James Avenue Pumping Station located in the City of Winnipeg. The data go back to 1948 and have been obtained up to 2005. Maximum yearly elevations recorded at the Station are shown in Figure 4.2. Each bar represents the maximum elevation recorded for each flow year on record, with the flow year shown on the x-axis and the maximum river elevation on the y-axis. In later sections, maximum river elevation and intensity will be used interchangeably. A horizontal line drawn through the data represents the average maximum elevation for all data and has a value of 226.5 m. Flow years are classified into high, medium and low intensity based upon the following elevation ranges attained:

- 221 m to 225 m = low intensity
- 225 m to 227.5 m = moderate intensity
- 227.5 m to 230 m = high intensity

High flow years are representative of flood years while low flow years may represent periods of drought. Figure 4.3 shows durations curves for selected flow years. The x-axis shows the percent of time the flows are less than the corresponding elevation on the y-axis. The flow years all have the same general trend from 0% to approximately 37% (percent of time less than) where the slopes of the lines are relatively flat. A noticeable rise in elevation is observed to approximately 223.6 m from 37% to approximately 45%. From this point, the data flattens again until 60% where the elevations begin to increase again until the maximum elevation for each flow year is reached. The graph shows an increase in elevation at 60% for 1999. All other flow years show an increase after 75%. This indicates that 1999 maintains higher elevations over a longer duration compared to other flow years shown on the graph.

Depending on the flow year selected, different quantities of erosion were expected to be produced. High flow years (or flood years), defined as years where the river elevation is higher than normal (for example 1997), were expected to produce more erosion compared to low flow years such as 1981, which represent drought years. Additionally, erosion is a function of duration,

where very high flows of short duration will produce less erosion than moderate flows of long duration.

The reader is reminded that the actual cause of erosion is due to fluid shear stress, which can be expressed as a function of velocity gradient (Equation 2.1) or as a function of river elevation (Equation 4.2). The latter method has been selected to calculate fluid shear stress for the purpose of this research. The terms river flow and elevation will be used interchangeably because a positive correlation exists between the two variables. High river elevations are directly related to high flows assuming the velocity remains constant.

A moderate flow year of 1951 was selected to test both methods to determine if they produced reasonable quantities of erosion. ('Reasonable' erosion rates were selected by the author based on anecdotal information in press media. They are clearly subject to judgment.) The surveyed cross-section from 1951 (Figure 3.6) was subjected to the daily river elevations of 1951. The program calculated the quantity of erosion at each elevation point on the 1951 cross-section for each day of elevations in 1951. At each elevation point, the fluid shear stress was calculated from both predictor equations. If the elevation of the river was lower than the elevation point, the fluid shear stress was calculated as zero at that elevation point. The fluid shear stress was compared to the respective critical shear stress for the two different methods. If the fluid shear stress surpassed the critical shear, an erosion rate was calculated.

To find the corresponding erosion rate, the Briaud method involved the use of an interpolation function to evaluate the fluid shear stress on the experimental curve The Osmann-Thorne method calculated the erosion rate based on Equation 2.11. The amount of eroded soil was calculated by multiplying the erosion rate by the duration. The Briaud erosion rate was in mm/hr so the rate was multiplied by 24 hours and divided by 1000 to produce the number of meters of erosion per day. Similarly, the Osmann-Thorne erosion rate was in m/min therefore the rate was multiplied by 1440 which represents the number of minutes in one day. The quantity of eroded soil was calculated daily for each river elevation at each of the elevation points along the slope. At the end of the year, the quantity of erosion for each elevation point was summed. The final riverbank cross-section was produced by subtracting the quantity of erosion from the initial x-coordinate associated with the respective elevation point. The final points represent the new cross-section subjected to the erosion of 1951.

4.4.2 Results

The final results of the two methods are shown in Figures 4.4 and 4.5. Figure 4.4 shows pre-erosion and post erosion cross-sections using the Briaud method. Figure 4.5 shows the results of the Osmann-Thorne method. The blue line on both figures represents the pre-erosion or initial cross-section whereas the red line shows the post-erosion cross-section after being subjected to the flows of 1951. It is evident from these figures that the quantity of yearly erosion for a moderate flow year is unrealistic, showing 2200 m of toe erosion for the Osmann-

Thorne method and 400 m for the Briaud method. The critical shear stress for Osmann-Thorne was obtained from Figure 2.10. The resulting shear stress was τ_c = 0.2 Pa. The erosion rate was broken down into an initial rate defined by Equation 2.11 and then an actual rate that was assumed to increase linearly as defined by Equation 2.12. In comparison, the Briaud experimental erosion rate curve based on Winnipeg soils produced a critical shear stress of 27 Pa and a linear rate of change of erosion rate defined as ε of 4.7 mm/hr·Pa. Values of corresponding critical shear stresses and erosion rates differ substantially between the two methods. A critical shear stress of 0.2 Pa from the Osmann-Thorne method corresponds to a river elevation of 219.02 m. This indicates the riverbanks are continuously eroding since the bed elevation is 219 m and the lowest elevation recorded on the Red River since 1948 is 220.85 m. In comparison, the critical shear stress of 27 Pa from the Briaud method is more reasonable as it corresponds to an elevation of 221.76 m.

An explanation is not provided to describe how the erosion rate equation is derived by Osmann and Thorne (1980). This gives little confidence in the method. The erosion rate by the Briaud method is based on experimental results which show a linear increasing erosion rate of slope 5:1 which is a rate that is still unacceptably high. However the Briaud results may be explained by the fact that tap water instead of river water was used as the eroding fluid in the experiment. According to the observations from Briaud *et al*. (2001) and Arulanandan *et al*. (1980), both researchers suggest that the concentration of

eroding fluid has a direct impact on erosion rate and critical shear stress. The critical shear stress decreases and the erosion rate increases as the concentration of eroding fluid approaches that of distilled water. Briaud *et al.* (2001) recommends the use of river water as the eroding fluid in order to replicate actual erosion conditions. Of the two methods, since the Briaud method is based on simple experiments on Winnipeg soils and uses equations that are comprehensible and replicable, it is selected for further study.

4.5 Extended Analysis

The second part of the study examined the 2001 erosion cross-section using the 1951 surveyed cross-section as the starting point for erosion. The envisioned approach incorporated a modified version of the Briaud erosion rate curve because the original curve produced unreasonable amounts of erosion. The proposed study subjected the 1951 cross-section to annual historical flows between 1952 and 2001, with a new erosion cross-section generated for each flow year. For example, the 1951 cross-section was subjected to the 1952 annual flows to produce the 1952 erosion cross-section. This new cross-section would then be subjected to the 1953 annual flows to generate the 1953 cross-section and so on. The method was continued for consecutive yearly flows until the 2001 cross-section was produced. This cross-section was then be matched to the surveyed 2001 cross-section to determine how closely the surveyed and measured cross-sections compared. Agreement between the surveryed and measured cross-sections would indicate the accuracy of the modified erosion

rate curve. Subsequently, the stability of the cross-section for each year would be assessed using Geostudio. The percent decrease in factor of safety between eroded cross-sections (impact), could then be correlated to the yearly flows. The results ultimately indicate which flow events have a greater contribution towards riverbank failure.

While this study was being undertaken, it became evident that there was a major limitation in the analysis. The limitation was that the new geometry of the riverbank after a failure was unknown – limit equilibrium analysis does not provide information about post-failure geometry. It was therefore impossible to calculate the factor of safety without making assumptions about the post-failure geometry.

Due to this limitation, it was not possible to replicate the 2001 cross-section accurately. Instead, and alternative approach was applied. The 1951 cross-section was used as a base case that was subjected to erosion from selected flow events of low, medium and high intensity and duration. Each cross-section that was generated was modeled in Geostudio to determine the factor of safety. Finally, a comparison between factors of safety of the eroded cross-sections showed how flow events affect riverbank stability.

4.5.1 Modified Erosion Rate Curve

To apply Briaud's method for this purpose, the parameters of the original erosion rate curve had to be modified in order to produce 'reasonable quantities' of erosion (Section 4.4.1). The critical shear stress was adjusted to 45 Pa which corresponds to a river elevation of 223.7 m as calculated from Equation 4.2. Based on the duration curve in Figure 4.3, elevations on the Red River are less than 223.7 m 65% of the time. This means that under a critical shear stress of 45 Pa, 35% of the time the riverbanks will be subjected to erosion. This elevation represents the level at which the river is maintained during the summer once the spring flows subside. It is also the inflection point on the duration curve (Figure 4.3) where the data begin to plateau at the transition from low to average elevation.

The erosion rate of the original curve was approximated by a straight line crossing the x-axis at the modified critical shear stress. In order to determine the slope of the line, erosion rate curves with different slopes were tested to compare the amount of erosion produced under the moderate flow conditions of 1951. Figure 4.6 and Figure 4.7 show different erosion rate curves and cross-sections generated by the various lines. Each erosion rate curve is labeled by the slope $\acute{\epsilon}$ with units mm/hr·Pa. The blue lines in Figure 4.7, indicate the initial configuration of the riverbank and the red lines, give the final cross-section after erosion. The erosion rate curve selected for the study was the curve that generated the most realistic cross-section for the average flow event. Based on Figure 4.7, a slope $\acute{\epsilon}$

of 0.1 to 0.2 mm/hr·Pa produced marginal amounts of erosion whereas slope ἐ of 1.0 to 3.0 mm/hr·Pa produced excessive erosion. Finally, a slope ἐ of 0.3 mm/hr·Pa was selected for the study as it produced the most 'reasonable' quantity of toe and mid-bank erosion.

The selected erosion rate curve for ἐ = 0.3 mm/hr·Pa with τ_c = 45 Pa was applied to the 1951 riverbank cross-section. This was tested using a spreadsheet developed by the author for the flow years shown on the duration curve in Figure 4.3, which span different intensities and durations from 1951 to 2004. The methodology described in the previous section to quantify erosion, was again used to produce the new riverbank cross-sections. The spreadsheet was modified to include the revised erosion rate curve. Each erosion cross-section generated from the various flow events, was exported into GeoStudio to calculate the factor of safety. The analysis used the same soil properties and boundary conditions as the analysis described in the previous section.

4.5.2 Effect of Erosion on Factor of Safety

Figure 4.8 summarizes the results of the study, which show the percent change in factor of safety versus maximum elevation for each of the tested flow years. As expected, the factor of safety decreased with increased river elevation above 227 m. The decreasing factors of safety correspond to increased erosion that causes the riverbank to be less stable.

Areas of the graph (Figure 4.8) where the calculated results show a negative percent change in factor of safety appear to suggest increasing riverbank stability. The modeling does not include physical mechanisms that would produce this result. They are assumed to be produced by assumptions made in the SLOPE/W analysis.

The analysis shows that rates of decrease of factor of safety, increase with (1) increasing river elevation and with (2) increasing durations of a given river elevation. Largest rates of decrease are associated with lengthy periods of high water level. It seems reasonable, therefore, to examine the relationship between percent decrease in factor of safety and the area under duration curves such as those shown in Figure 4.3, using an elevation of 223.7 m as the elevation at which the flow begins to erode the riverbank.

A plot was also generated for duration of flow versus percent change in factor of safety (Figure 4.9). A quantity to represent duration was calculated by taking the area of the duration curve above the critical shear stress corresponding to a river elevation of 223.7 m. This quantity was termed the erosion potential with units of m/%

The scatter in the results in Figures 4.8 and 4.9 can be attributed to several factors. In Figure 4.8, the scatter between elevations 226 m to 229 m is due to the different durations of the periods of high flow. Long durations produce more

erosion, whereas short durations cause less erosion. These result in higher and lower percent changes in factors of safety respectively. Similarly, in Figure 4.9 the point with the highest erosion potential of 0.71 m/% has a lower percent change in factor of safety compared to the percent changes for lower erosion potentials. There is some evidence in the records (not included) that the lower percent change in factor of safety at erosion potential of 0.71 m/% may be due to erosion that resulted in a more stable riverbank cross-section. It is important to recognize that some of the data on Figures 4.8 and 4.9 are outliers. However the trends of decreasing percent change in factor of safety with increasing maximum elevation and erosion potential are evident. 'Erosion potential' includes both the magnitude and the duration of different flow events.

4.6 Evolutionary Stability

The analysis was taken one step further by returning to the project's original idea of recreating the riverbank's evolutionary stability from 1951 to 2004. The goal was to show how the factor of safety decreases over time due to erosion, until the riverbank eventually fails. The following analysis applies to a generic riverbank that is a simplification of the Kingston Crescent riverbank studied in earlier sections. The riverbank was assumed to erode over time, with resulting annual decreases in factor of safety. Failure was assumed when the factor of safety dropped to 1.0. Subsequently, the post-failure geometry was assumed to have a factor of safety of 1.5, after which the erosion cycle resumed.

4.6.1 Methodology

The procedure produced erosion cross-sections due to flows of constant river elevations in 1 m intervals from 225 to 230 m, maintained over one month. The erosion cross-sections were generated using the modified Briaud erosion rate curve used in the previous analysis. The Kingston Crescent geometry was simplified to have a slope of 4H:1V from crest to toe. Erosion cross-sections were produced for different river elevations, with each cross-section modeled in Geostudio to determine its factor of safety. In the previous section, a series of grid and radius points were specified to allow the SLOPE/W application to seek the most critical slip surface. In this section, only one grid and radius point were specified so that the same slip surface would be generated for each cross-section. This allowed a common comparison between factors of safety. The selected slip surface corresponded to a deep-seated non-circular surface that extended from the crest to the clay-till interface and then to the toe. Crest loss over the studied time period of one month was approximately 3.5 m.

Figure 4.10 shows results from the SLOPE/W analysis for the different river elevations maintained over one month. The factor of safety for each river elevation was subtracted from the initial factor of safety and the result divided by the number of days over which the elevation was maintained, namely 31 days. The result was the decrease in factor of safety per day for a given river elevation. Results are shown in Table 4.1.

Given daily river elevations in real flow events, Table 4.1 can be applied to determine the decrease in factor of safety due to erosion. In order to apply Table 4.1, an interpolation function was used to look up the daily river elevation in the table and select the corresponding value for daily decrease in factor of safety.

The final output was the chart shown in Figure 4.11 of time in years versus factor of safety. The chart shows calculated monthly decreases in factor of safety from 1951 to 2005. Erosion begins in 1951 with the idealized riverbank cross-section assumed to be initially stable at a factor of safety of 1.5. Over the course of the year, the factor of safety decreases due to the 1951 flows and at the end of the year, the factor of safety is 1.48. This factor of safety is used as the starting condition at the beginning of 1952. The decrease in factor of safety is again calculated based on the flows record for 1952. The initial value of 1.48 minus the sum of the daily decreases during 1952 produces a factor of safety of 1.47 at the end of 1952.

The process is repeated for consecutive years until a factor of safety of 1.0 is reached, which implies failure at the end of 1968. After failure, the riverbank is assumed to deform to a stable configuration with a factor of safety of 1.5 for the subsequent year. Some flow years such as 1997, had an incomplete record of flows. In this situation, the last known elevation was assumed for the missing data.

4.6.2 Results

Figure 4.11 shows the evolutionary factor of safety in red, with yearly hydrographs shown on the graph in blue. In addition, Figure 4.12 shows the percent decrease in factor of safety for each flow year. The analysis shows that failure first occurs at the end of 1968, with the slope returning to a stable position with a factor of safety of 1.5 in 1969. Following further erosion, failures are also noted in 1987 and 2003. Of interest is how the factor of safety reacts to high and low intensity flows and to the duration of these flows, earlier called 'erosion potential'.

The first significant drop in factor of safety is in 1956, where a 4.5% decrease from 1.43 to 1.37 is observed in response to elevated flows that reached 228.3 m. Similar drops are observed in 1960, 1965 and a noticeable drop in 1966. The years with the highest elevations of long duration such as 1966, 1979 and 1997 showed the greatest decreases in factor of safety by as much as 10% compared to the lowest flow years of 1954, 1957 and 1981, which showed a 1% or less decrease in yearly factor of safety. Medium flow years of similar elevation with different erosion potentials, such as 1955 and 1999, show considerably different factors of safety. The year 1999 had a maximum elevation of 227.0 m and 1955 had 227.3 m. However, 1999 had a much longer duration of peak flows and hence it produced a 4% decrease in factor of safety compared with 1.4% for 1955.

Overall, the analysis achieves the goal of recreating the evolutionary stability of the riverbank and showing the combined effects of elevation and duration (erosion potential) on the factor of safety. Although theoretical in nature, the modeling demonstrates the cyclic nature of river morphology.

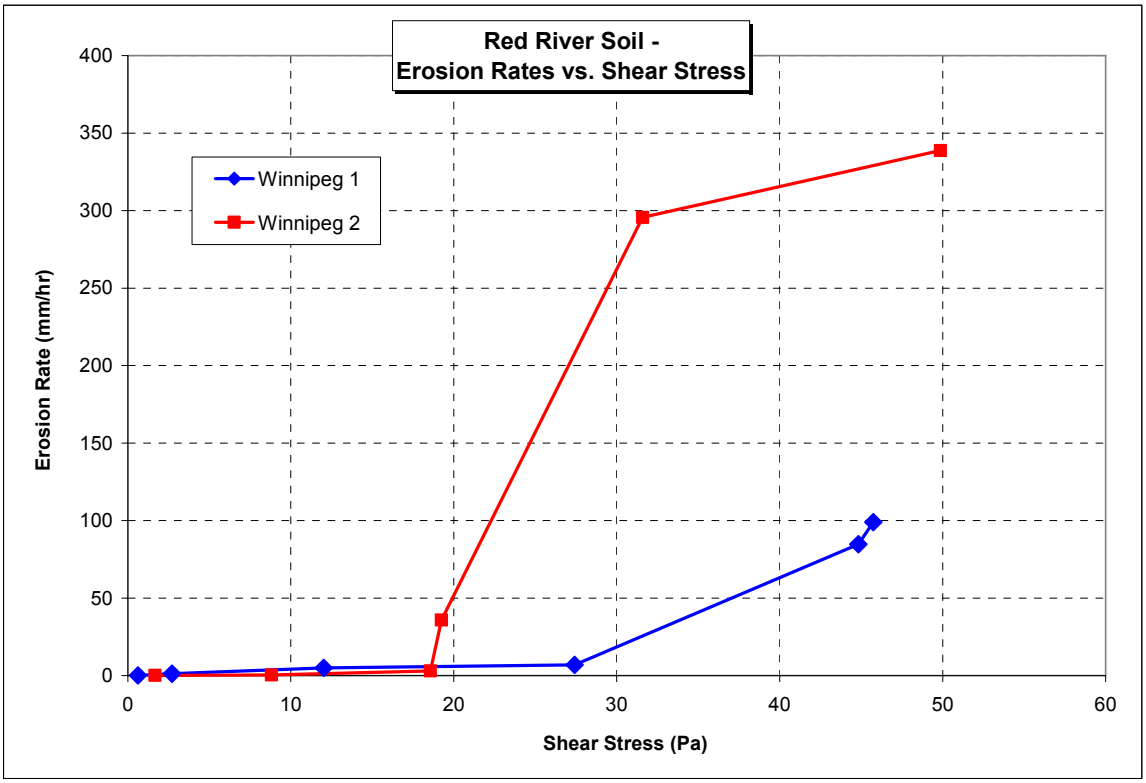

Figure 4.1 - Results from EFA test from Texas A&M University
(data from Texas A&M University, 2006)

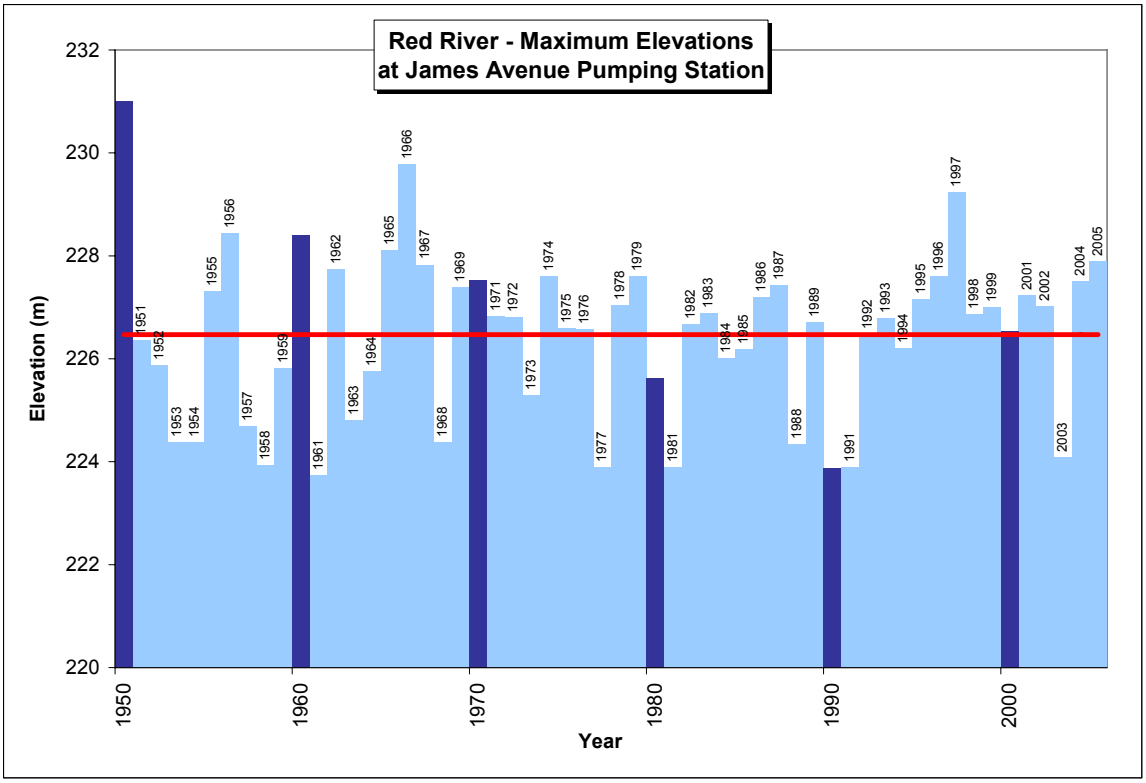

Figure 4.2: Maximum Yearly Elevations for the Red River at James Avenue Pumping Station (data from Manitoba Water Resources, 2005)

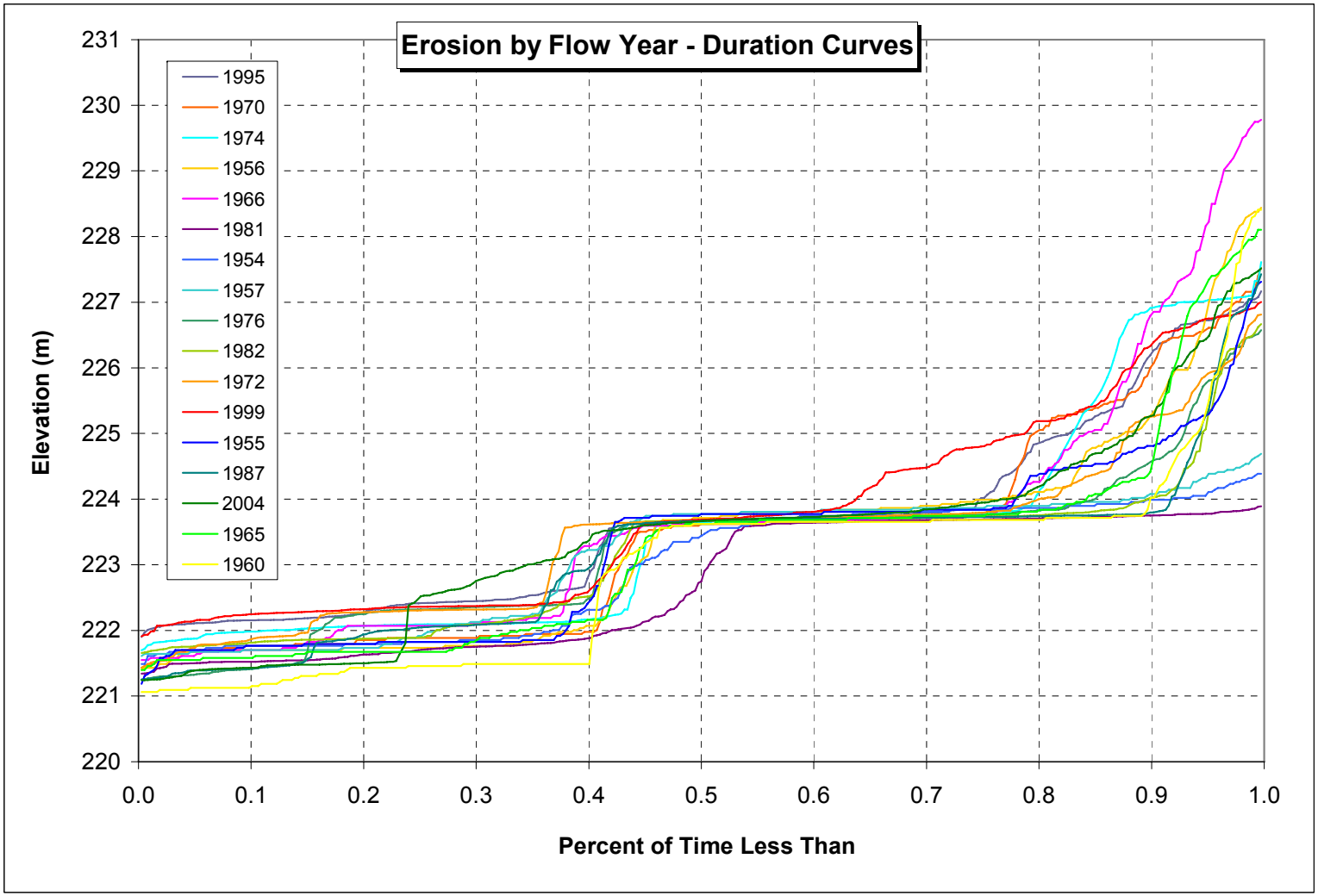

Figure 4.3: Duration Curves for Various Flow Years (data from Manitoba Water Resources, 2005)

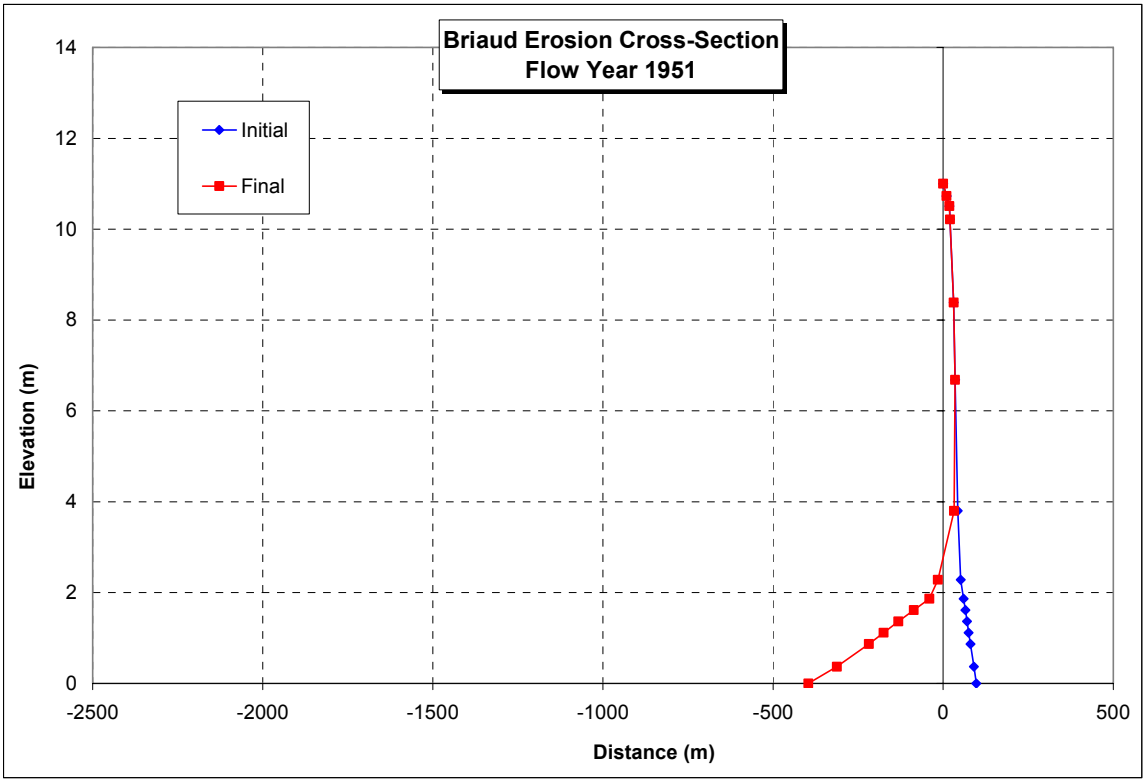

Figure 4.4: Erosion cross-section using the Briaud method

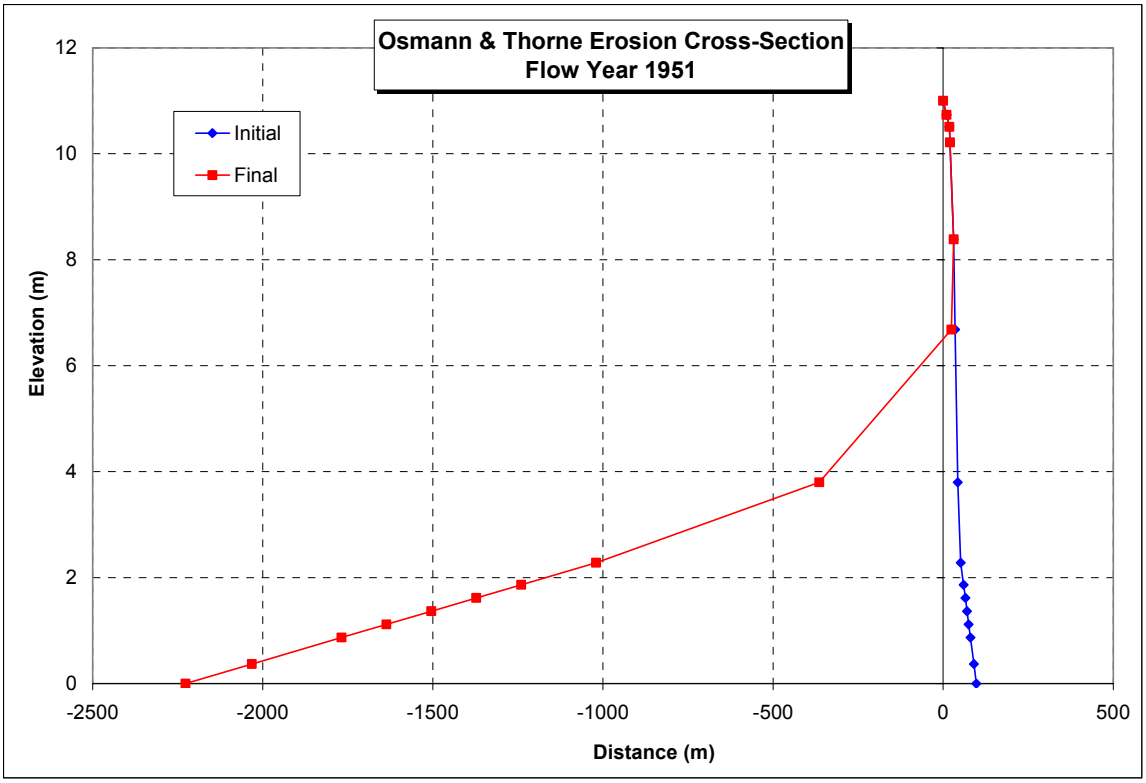

Figure 4.5: Erosion cross-section using the Osmann-Thorne method

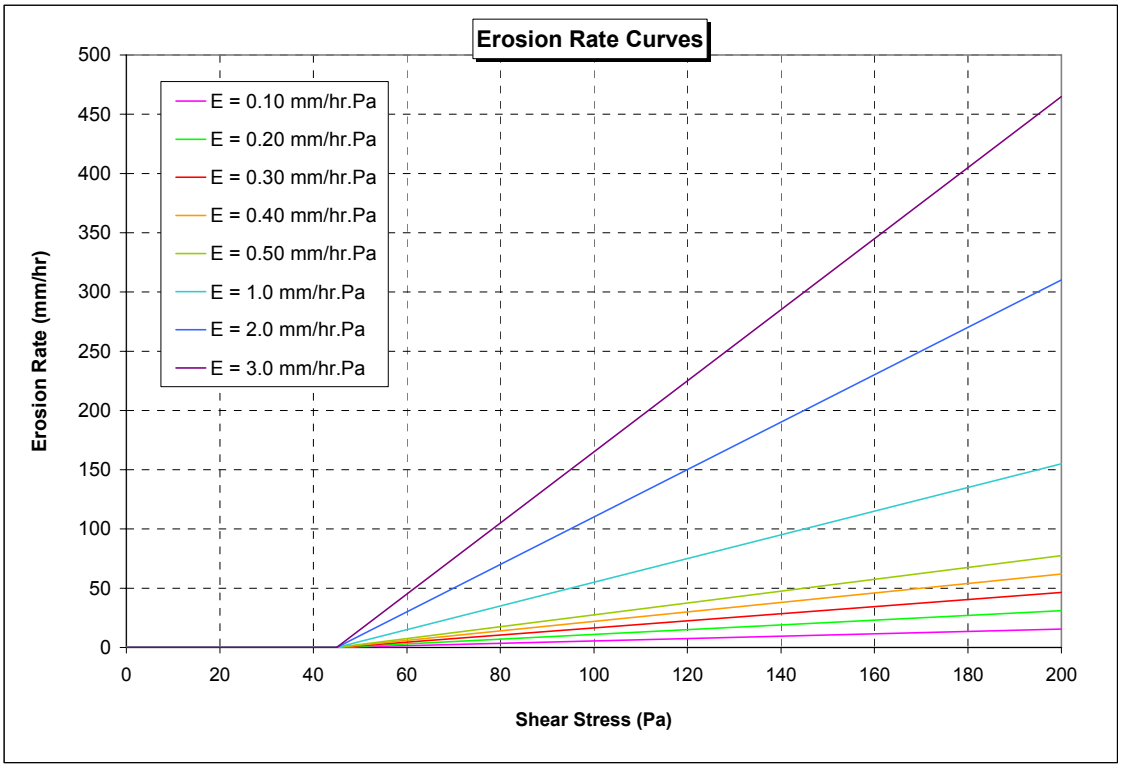

Figure 4.6: Erosion rate curves using τ_c = 45 Pa

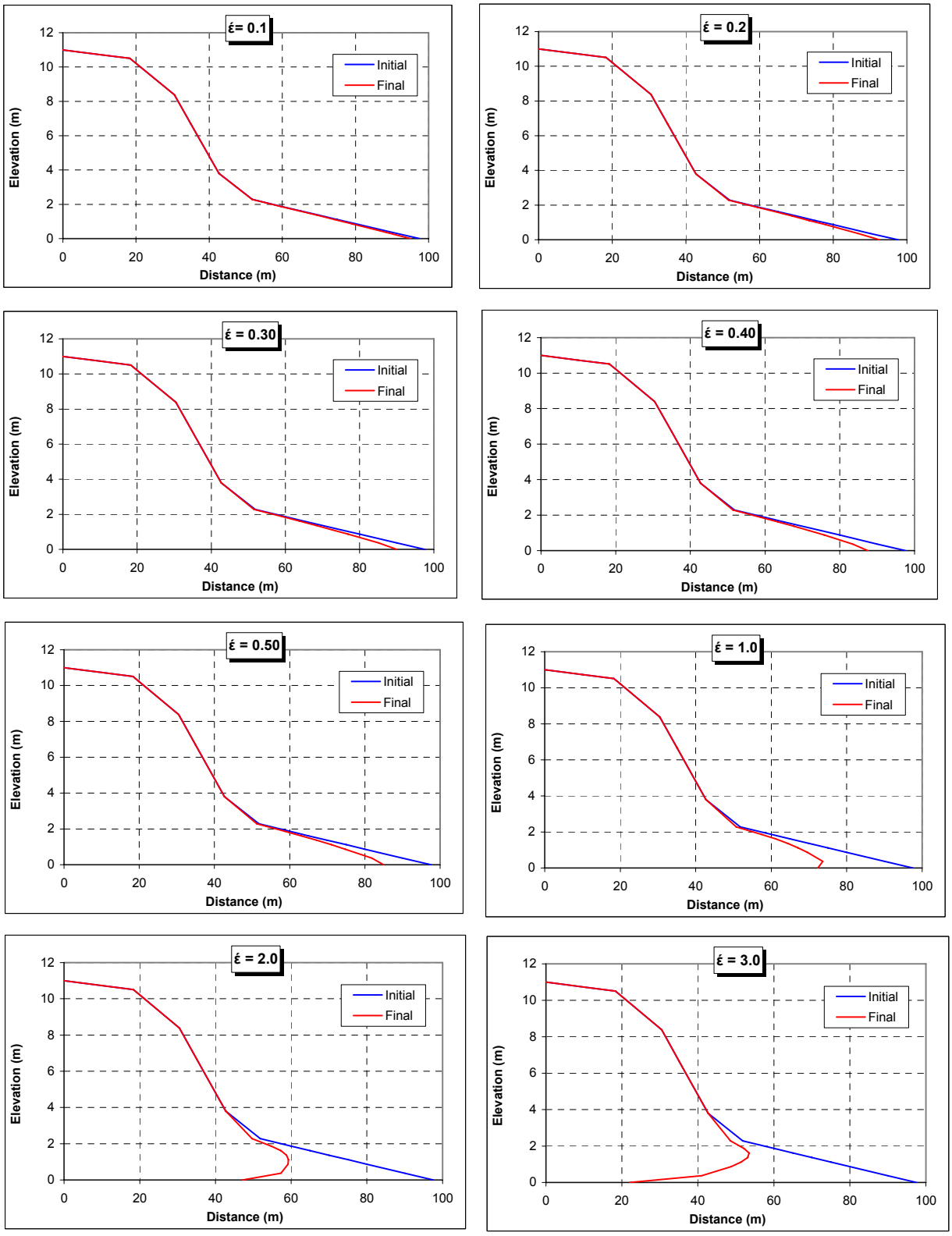

Figure 4.7: Riverbank erosion profiles with respect to different erosion rate curves

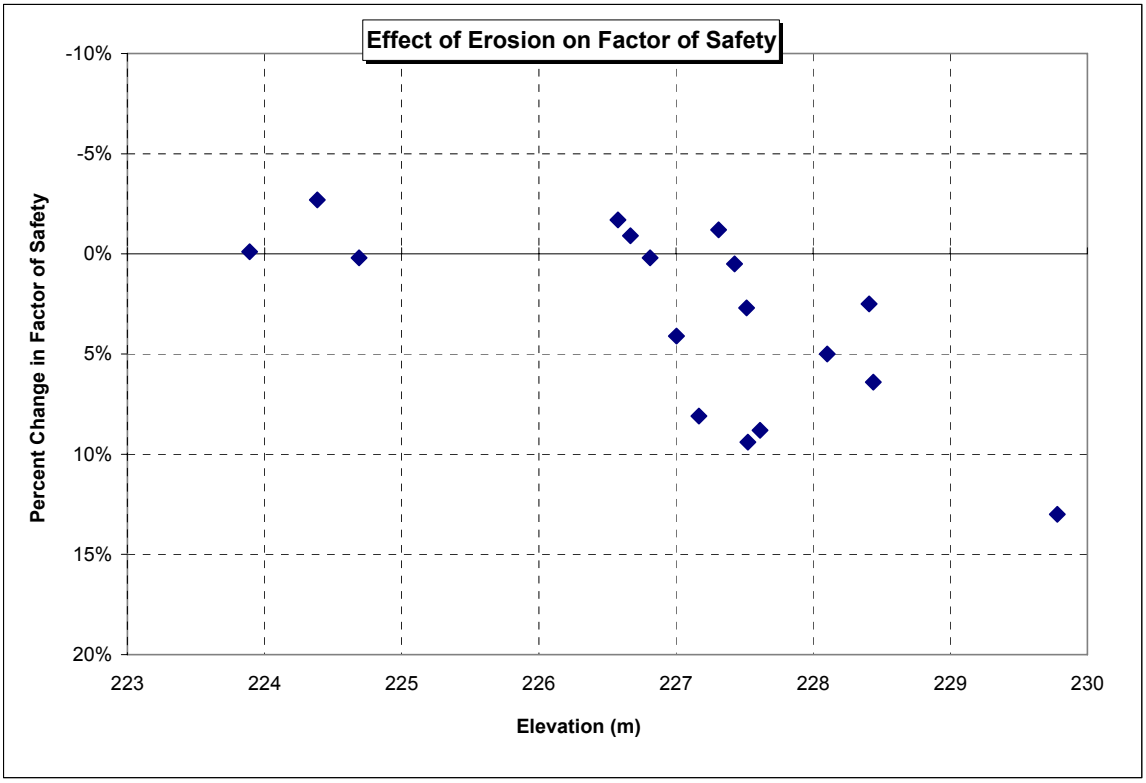

Figure 4.8: Effect of river elevation on factor of safety using modified erosion rate curve

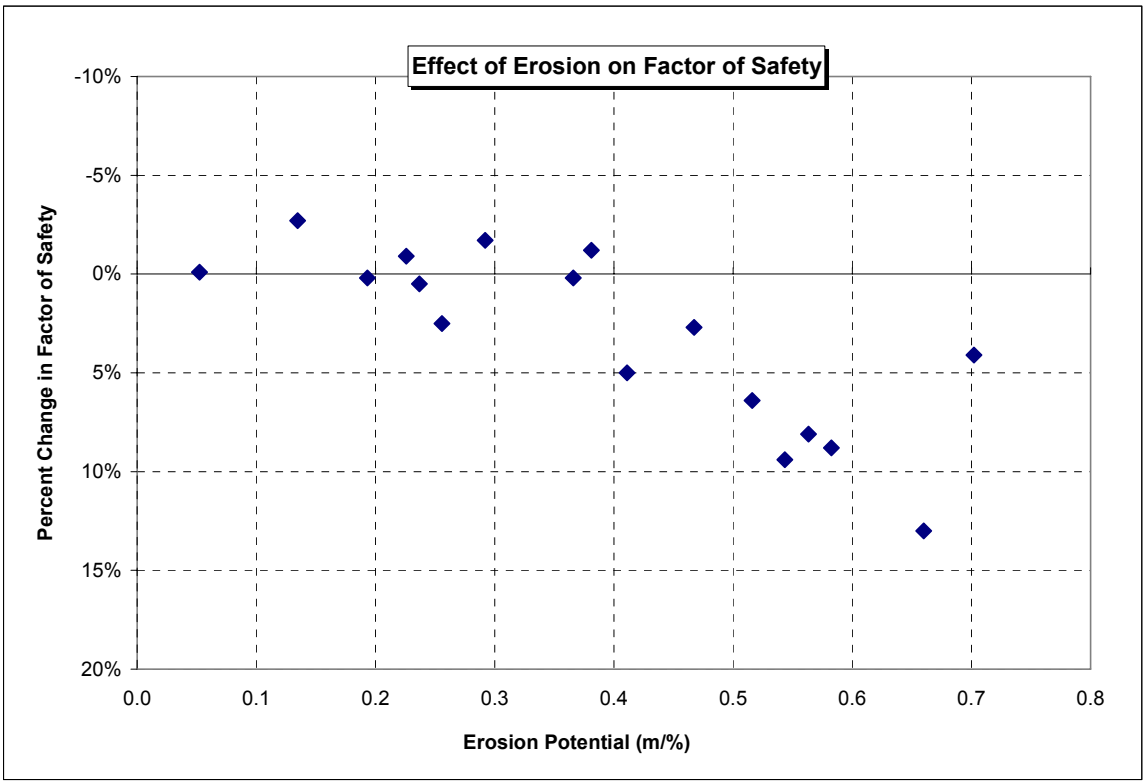

Figure 4.9: Effect of erosion potential on factor of safety using modified erosion rate curve

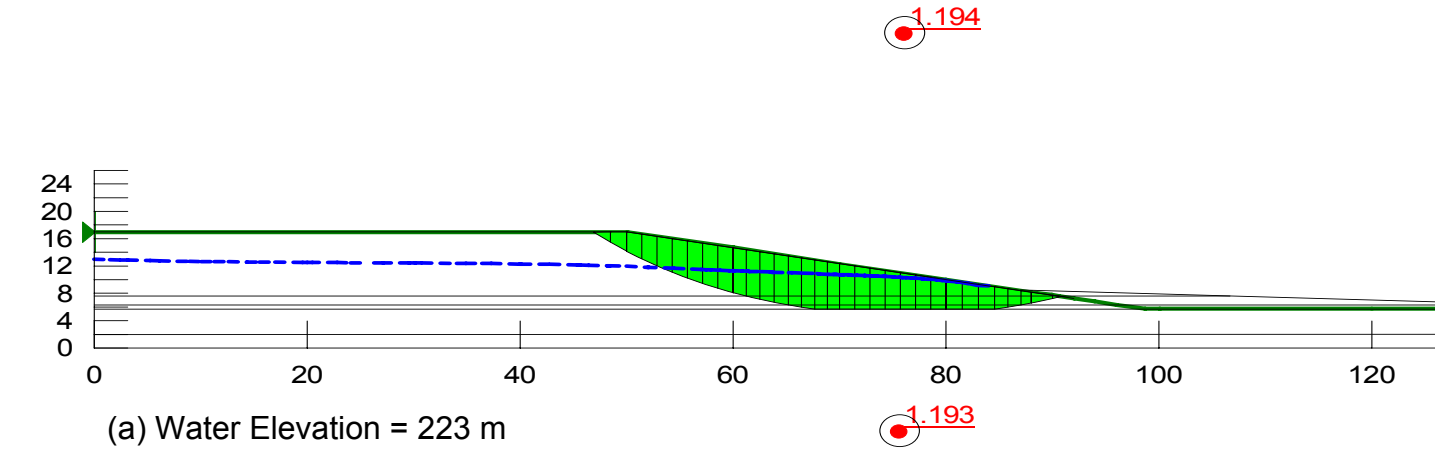

(a) Water Elevation = 223 m

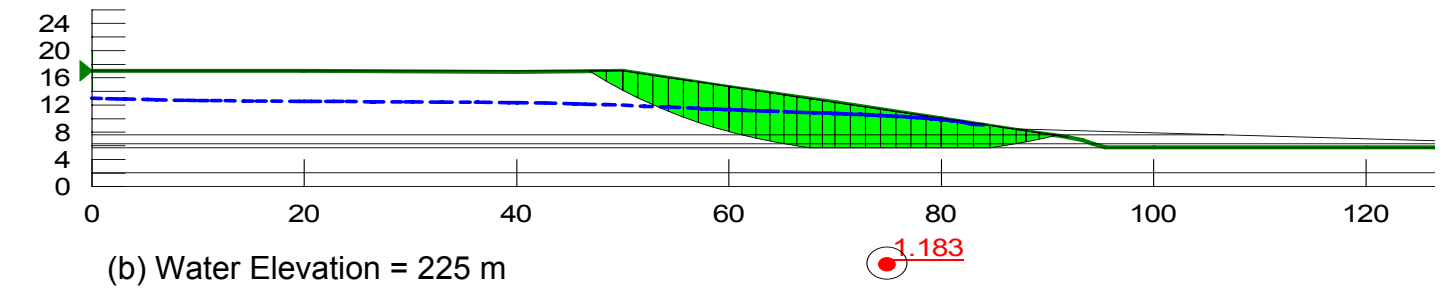

(b) Water Elevation = 225 m

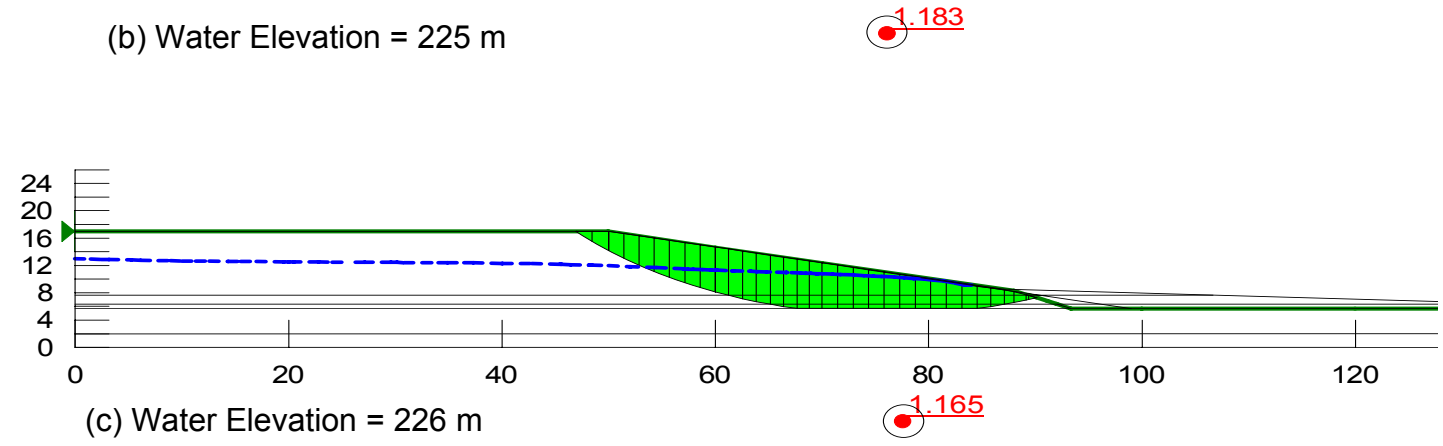

(c) Water Elevation = 226 m

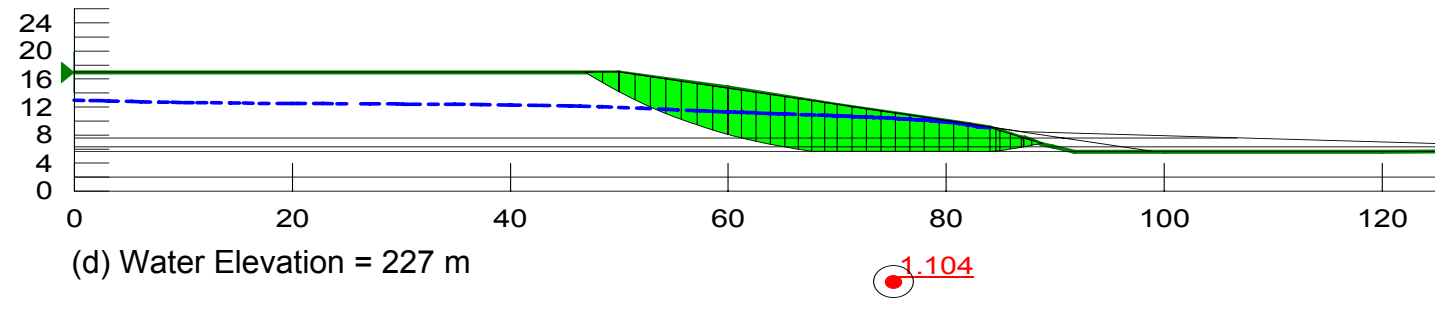

(d) Water Elevation = 227 m

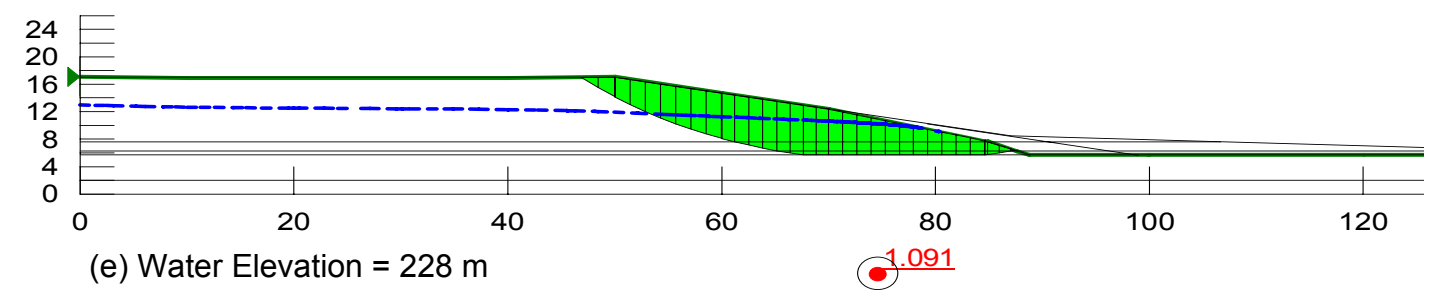

(e) Water Elevation = 228 m

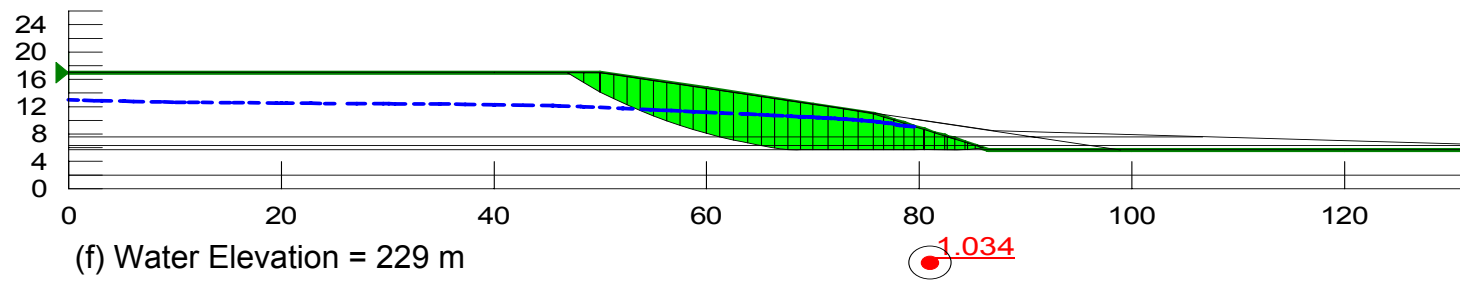

(f) Water Elevation = 229 m

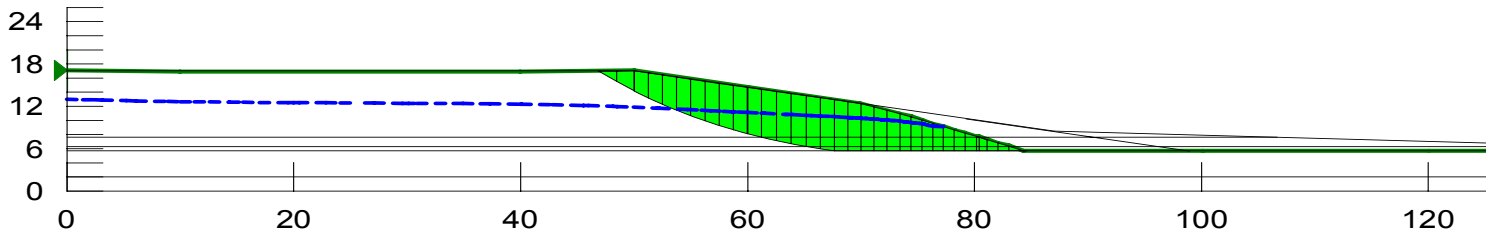

(g) Water Elevation = 230 m

Figure 4.10: Factors of safety determined over a 31 day period of erosion for different river elevations

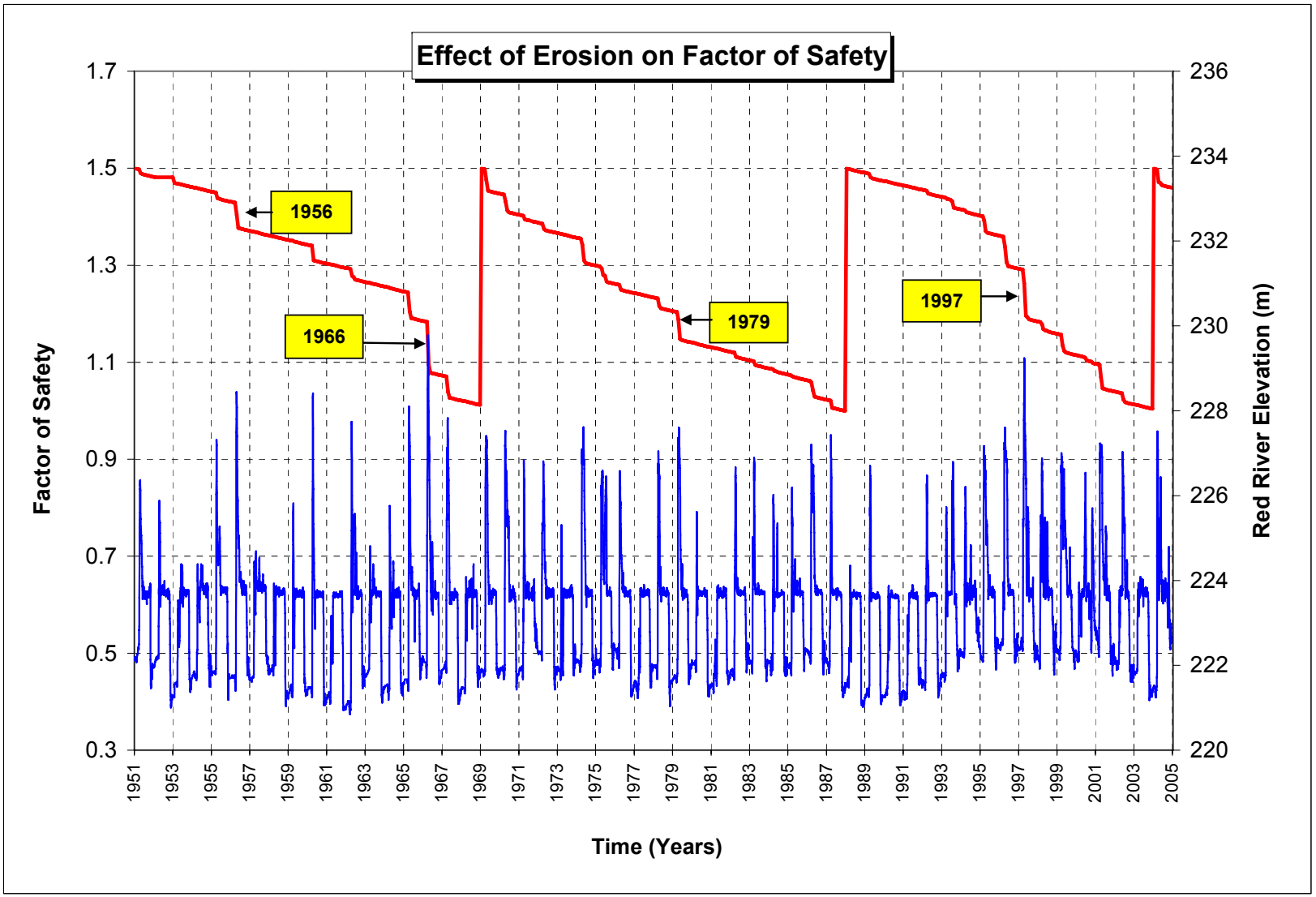

Figure 4.11: Evolutionary stability of a riverbank from 1951 to 2004

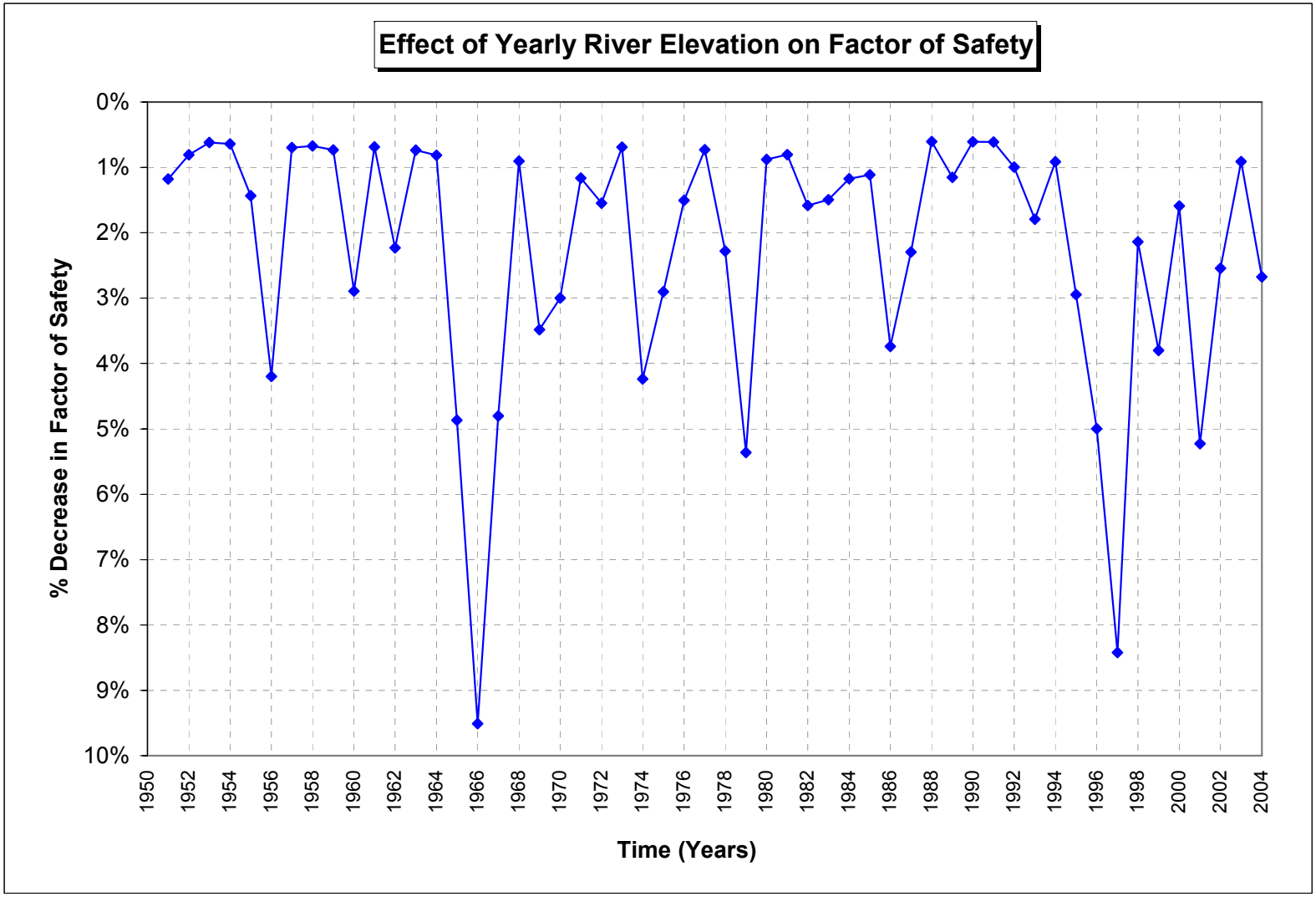

Figure 4.12: Annual percent decrease in factor of safety from 1951 to 2004

River Elevation (m)	Daily Decrease in Factor of Safety
215	0
225	0.00003226
226	0.00035484
227	0.00093548
228	0.00290323
229	0.00332258
230	0.00516129

Table 4.1: Daily decrease in factor of safety as a function of river elevation

CHAPTER 5 - DISCUSSION AND RECOMMENDATIONS

5.1 Introduction

The preceding chapters presented methods for quantifying flow induced erosion and the related effect on factor of safety. This research is among the first specific to the Red River and since it is a first attempt to quantify erosion the methods presented still require further improvement. The following sections outline limitations of the analysis methods and recommendations for improvement.

5.2 Erosion Based on Historically Surveyed Cross-Sections

The first method to quantify annual erosion involved obtaining historical to present day surveyed cross-sections at a given location along the Red River. The cross-sections were aligned to a common reference point. Then the annual retreat in riverbank crest and toe was measured directly from the graph and related to the respective annual flow event. The limitation of this method was that there are no locations along the Red River where annual surveys of the riverbank have been recorded. The availability of surveyed cross-sections was limited to surveys from 1912, 1951 and more recent surveys which date back to the late 1980's at various locations along the Red River. The location selected for analysis with overlapping cross-sections from each set of surveys was Kingston Crescent. The study showed that 40 m of riverbank eroded between 1912 and 2001 which translates into an average 0.44 m of erosion per year or a

0.26% decrease in factor of safety each year. However several assumptions and simplifications were required in order to perform the analysis.

Aligning the cross-sections to their common datum required some judgment and manipulation to ensure the cross-section retreated from past to present. The reference point was selected as the edge of the road that runs adjacent to the river. However it was unknown whether the location of the road was actually surveyed onto the 1912 and 1951 maps or arbitrarily drawn onto the maps. It was also questionable as to how accurately the historical cross-sections were surveyed. Equipment used today to survey riverbank cross-sections offer greater accuracy over older methods. Sonar equipment is used to survey below the river elevation whereas in 1912 and 1951 the bed elevation was measured by lowering a rod to the bottom of the river. Further simplifications were involved in defining the soil stratigraphy, soil properties and porewater pressure conditions for the study site. The parameters were obtained from secondary sources which were a combination of previous research, published reports and local Winnipeg practice. Therefore the conditions used to define the site in the FE model were not entirely specific to that site. The river elevation applied to the site was not specific to the location. The river elevation was based on historical data collected at James Avenue Pumping Station which was directly used in the analysis. This elevation data is specific to the river cross-section at James Avenue Pumping Station and should be modified to account for the study cross-section using the appropriate backwater rating curve. Typically a rating

curve is applied to modify the data from one cross-section to another however a rating curve was not available for this study site.

This research attempted to recreate the evolutionary stability of a riverbank by reproducing the erosion-failure cycle with historical riverbank cross-sections. However, the limitation of the method was that the stage at which each cross-section was at in the evolution was unknown. According to anecdotal records, it is unlikely the riverbank has not experienced failures between these years even though the factors of safety follow a decreasing order. Therefore a decrease of 0.26% per year in factor of safety may not entirely be an accurate statement but rather an overall average value.

5.3 Erosion Based on Theoretical Equations

The second part of the research involved theoretical equations to quantify erosion. One method was selected for the fluid shear stress. Two methods were selected for the critical shear stress and erosion rate, namely the Osmann-Thorne and Briaud methods. Neither method produced erosion cross-sections that matched observed average yearly erosion. The methods showed 2200 meters of toe erosion from Osmann-Thorne and 400 meters from Briaud. The Osmann-Thorne method produced a very low critical shear stress that resulted in the river bank continuously eroding under even the lowest flows on record. In comparison, the Briaud method had a reasonable critical shear stress however the erosion rate was excessive. Between the two methods, the

high volume of erosion produced by Briaud's method could be explained with supporting arguments whereas the Osmann-Thorne method could not be similarly defended. The author suggests that the erosion rate curves produced by Briaud's method were not entirely representative of erosion rates along the Red River since tap water instead of river water was used as the eroding fluid in the experiment. Several researchers including Briaud have stated that tap or distilled water produce greater quantities of erosion due to the greater affinity of the water for soil particles as compared to river water which contains an existing sediment load. This is similar to the effect of osmosis where greater diffusion of particles occur from high concentration to low concentration. It was assumed that if river water had been used in the study, the erosion rate would have been much lower. On this basis the Briaud method was pursued for further study by modifying the parameters of the graph.

5.3.1 Erosion Rate Curve

The parameters of the Briaud curve were put through a sensitivity analysis to determine the best combination that produced the most reasonable quantity of erosion based on anecdotal records. The modified curve was used in two separate analyses to quantify the effect of flow induced erosion on factor of safety. The first analysis incorporated the use of the 1951 surveyed cross-section, which was used as a base case cross-section subjected to different yearly flow events ranging from low flow years such as 1981 to high flow years like 1966. The different erosion cross-sections were modeled in Geostudio with

the factors of safety compared between the different cross-sections. The 1951 cross-section allowed for a baseline comparison to assess how flows of different intensity and duration affect the factor of safety. The study showed that low flow years have the least effect on factor of safety of about 1% per year since these flows produce the least amount of erosion. Moderate flow years showed an average 4% decrease in factor of safety with flows maintained over longer durations showing decreases as high as 10%. High flow years showed the greatest percent decrease in factor of safety averaging an 8% decrease and as high as 14.5% for flows of high intensity and long duration. The decreasing trend in the data is apparent although it is not dramatic over the entire range of elevations. The decrease in factor of safety is most noticeable above river elevations of 227 m. Between the elevations of 227 m to 229 m, the decrease in factor of safety is not linear due to the fact that duration of the high intensity flows also impacts the factor of safety. The points with lower factors of safety within this region maintain longer durations of high intensity producing more erosion and thus a greater decrease in factor of safety.

5.3.2 Modeling Process

It is important to recognize that the results of the study depend strongly on parameters selected for the erosion rate curve, especially the critical shear stress. The critical shear stress was selected as 223.7 m therefore erosion will only initiate once this elevation is surpassed. To validate this elevation, soil samples from the study site need to be obtained and tested through the EFA

(Briaud *et al*. 2001) to more accurately determine the critical shear and slope of the erosion rate curve. In addition, samples of river water need to be used as the eroding fluid in the experiment to truly replicate river conditions. The EFA can be subject to much criticism in terms of how closely it replicates actual riverbank erosion conditions. One criticism is that the samples are inserted at the base of the erosion flume and therefore the experiment represents erosion of the riverbed and not the riverbank. The experiment was originally designed for quantifying riverbed erosion however this research has attempted to apply it to riverbank conditions. It is suggested that the EFA (Briaud *et al*. 2001) be re-designed so that the soil sample is held in an angled position on the side of the erosion flume to more closely replicate riverbank conditions.

Another limitation of the method was that the modeling process for the different erosion cross-sections was time consuming due to the complex geometry of the slope. Ideally the regions function of the SEEP/W program should allow one region to be defined for each soil layer. However, due to the composite geometry of the slope, if only one region was defined for each soil layer the stress distribution results from SIGMA/W were not plausible. In order to generate acceptable results, the cross-sections had to be discretized into several regions. Due to the complexity of discretizing the cross-sections, only select flow years between 1951 to 2004 were modeled. Ideally, it is recommended that factors of safety be generated for each flow year between 1951 and 2004. The results would be added to the graphs of elevation and duration versus percent decrease

in factor of safety (Figure 4.8 and Figure 4.9) to more clearly show the trends in the data. Similar modeling limitations from the initial analysis also applied to this analysis in terms of limited knowledge of site specific soil and boundary conditions.

5.3.3 Fluid Shear Stress

The fluid shear stress equation applied was a simplification of the shear stress distribution proposed by Olsen and Florey (1952) and specific to a riverbank with side slopes of 3:1. To have more accuracy in the fluid shear stress calculation, the relationships derived by the Highways Research Board (1970) from Figure 2.8 should be applied to the analysis. The use of this graph will permit different coefficients for the maximum shear stress to be applied for different elevations of the river and slopes of the riverbank. Depending on the angle of the riverbank slope, the fluid shear stress results could increase by a maximum of 40% for slopes of 2:1 to 80% for slopes of 6:1 under peak river elevations.

5.4 Evolutionary Stability

The corresponding analysis to the use of theoretical equations to quantify erosion was the evolutionary stability analysis of the riverbank from 1951 to 2004. The end result was a plot showing the initial factor of safety in 1951 assumed to be 1.5 and the yearly decrease as a result of river flows. A number of assumptions were required to generate this plot as follows:

- Analysis was performed on an idealized riverbank slope of 4:1 for ease of discretizing the domain in SEEP/W and SIGMA/W
- Upon failure, the riverbank regained a stable configuration with a factor of safety of 1.5
- Center of rotation for all slip surfaces generated was the same for all failures

The plot generated (Figure 4.11) showed the effect of river intensity and duration on factor of safety. The annual factor of safety was superimposed on the same graph as the yearly hydrographs to show the correlation between river intensity and duration on decrease in factor of safety. Noticeably, the decrease for low flow years is not as large as for high flow years such as 1966. A second chart (Figure 4.12) showing the percent decrease in factor of safety as a function of flow year was also generated. The minimum decrease was 1% for low flow years with a maximum of 10% for high flow years. These results compare to the preceding analysis (Figure 4.8 and 4.9) although a smaller decrease in factor of safety is observed for higher flow years in this analysis. Overall the effect of river intensity and duration is much more evident in these plots compared to the previous analysis.

In general, under maximum river elevations of long duration the average decrease in annual factor of safety is 10 to 15% as shown from the two analyses, which compare closely to current assumptions in local pratice. However,

assuming this kind of decrease every year is overly conservative and can lead to expensive remedial measures. A more cost-effective quantity for design is the average of all results between both analyses which ranges from 2.3% to 5.4%.

5.5 Recommendations for Future Research

It is important to recognize that riverbank failures are not solely due to flow induced erosion. Several factors that were not considered in this study also impact riverbank stability. These include ice scour, flow concentrations in river bends and deposition of sediment. To more accurately assess each of these factors and eliminate many of the uncertainties in this research it is recommended that a full-scale experimental study of a riverbank be undertaken over a period of 5 to 10 years. A survey of the riverbank would be reported twice a year, once in the spring after the ice breakup and once in the fall just before the river freezes. The cross-sections from fall to spring would show how much erosion is due to ice scour and from spring to fall would be due to spring and summer flows. During each survey, the amount of sediment deposited on the bank would also be measured to gain a better understanding of how much the sediment contributes towards destabilizing the banks. In addition, the bank would be instrumented with piezometers to monitor porewater pressures for modeling and for seepage calibration purposes.

Further to this, it is recommended that a routine soils investigation and laboratory testing be undertaken to accurately define the soil stratigraphy and soil properties

of the site. It is also clear from this research that the erosion rate curve needs more refinement to determine the exact value for critical shear stress and slope of the erosion rate line. It is recommended that samples directly from the study site be run through the EFA to produce a number of erosion rate curves. From the curves, it is expected that an overall range for the critical shear and erosion rate would be evident. Also it is imperative that river water be used as the eroding fluid as this affects both quantities for critical shear and erosion rate.

CHAPTER 6 - CONCLUSION

The study of flow-induced erosion along the Red River in Winnipeg is important as it is a significant contributor towards riverbank failures. Riverbank failures result in the loss of property to the City and private landowners. Loss of property can undermine near-by-structures making them uninhabitable and decrease overall property value. The cost to remediate slope failures is extremely high and for private landowners there is little financial assistance from the City to cover the cost of repairs. Based on observations, it is clear that several factors lead to slope failure one of them being flow induced erosion. Researchers have linked erosion to river flows through observations. However no researchers have quantified the volume of erosion associated with flows of different intensity and duration and the subsequent effect on factor of safety. Local Winnipeg practice assumes erosion induced by river flows decreases the factor of safety by 10% each year however this quantity has never been validated. The purpose of this research program was to shed light on how much the factor of safety decreases as a result of flow induced erosion of different intensities and durations. The answer to this question will assist engineers identify slopes at greatest risk for failure if subject to flows of a given intensity and duration. The hypothesis tested was as follows:

“Evolutionary stability of natural riverbanks is linked to both intensity and duration of river flows that cause erosion of the lower toe and mid bank regions”

Three different methods of analysis were undertaken to test this hypothesis. The first method involved the use of historical riverbank surveys with the discovery that no sites along the Red River have been surveyed on a regular basis which made it difficult to correlate erosion of surveyed cross-sections to flow events. The findings of the analysis with the limited surveys available showed that approximately 0.44 m of soil is eroded from the toe of the riverbank each year which amounts to a 0.26% decrease in factor of safety each year. The subsequent analysis involved using the 1951 surveyed cross-section as a baseline subjected to the erosion from various flow years as calculated by theoretical equations. The results indicated that the factor of safety depended on the intensity and duration of the selected flow year. A 1% decrease in factor of safety was observed for low flow years with an average 4% decrease up to a maximum of 10% for medium flow years. High flow years showed an average decrease of 8% with a maximum of 14.5%. The range in results under moderate and high flow conditions reflects the duration over which the flows are maintained. The final analysis involved recreating the evolutionary stability of the riverbank from 1951 to 2004 using the same theoretical equations as the previous analysis. The results for the different flow ranges were similar to those from the previous analysis however the relationship of decreasing factor of safety due to increased flow intensity and duration was more pronounced. A 1% decrease in factor of safety was observed for low flow years, an average 2% to a maximum of 5% decrease for moderate flows and an average 5% to 10% for high flows.

Current Winnipeg practice assumes a 10% decrease each year in factor of safety due to erosion. This matches closely with the results from this research under high flow conditions. It is highly conservative to assume this percent decrease each year since high flow conditions do not occur every year. Assuming such a quantity will result in remedial designs of greater cost that may potentially limit the number of sites to be remediated in a given year. A more suitable quantity suggested is the average percent decrease of all moderate to high flow results as calculated from the evolutionary stability analysis. This quantity is 3% and represents a more realistic average yearly percent decrease for which economical remedial measures can be designed.

REFERENCES

Alizadeh, A., 1974. "Amount and Type of Clay and Pore Fluid Influences on the Critical Shear Stress and Swelling of Cohesive Soils", Ph.D. Dissertation, University of California, Davis.

Arulanandan, K., Lganathan, P., and Krone, R.B., 1975. "Pore and Eroding Fluid Influences on Surface Erosoin of Soil." Proceedings of the American Society of Civil Engineering - Journal of the Geotechnical Engineering Division, January, pp.51-66.

Arulanandan, K., Gillogley, E., and Tully, R., (1980). "Development of a Quantitative Method to Predict Critical Shear Stress and Rate of Erosion of Natural Undisturbed Cohesive Soils." Report GL-80-5, U.S. Army Corps of Engineers, Waterways Experiment Station, Vicksburg, MS.

ASCE (1998). "River Width Adjustment. I: Processes and Mechanisms." Journal of Hydraulic Engineering, 124(9), 881-902

Baracos, A., 1960: "The Stability of Riverbanks in the Metropolitan Winnipeg Area". Preceedings of the 14th Canadian Soil Mechanics Conference, Niagara Falls, Ontario.

Baracos, A., 1971. "River Bank Investigation Tache Avenue St.Boniface, Manitoba". Letter report to Mr. R.Todd, Distric Director, Canada Public Works, Winnipeg, Manitoba, December 21, 1971. University of Manitoba, Department of Civil Engineering, Winnipeg, Canada.

Baracos, A., 1977. "Compositional and Structural Anisotropy of Winnipeg Soils - A Study Based on Scanning Electron Microscopy and X-Ray Diffraction Analysis." Canadian Geotechnical Journal, 14, 125-137.

Baracos, A., 1978: "The Effects of River Levels, Ground Water and Other Seasonal Changes on Riverbanks in Winnipeg". 31st Canadian Geotechnical Conference, Proceedings, p.7.2.2 - 7.2.19.

Baracos, A., and Graham, J., 1981: "Landslide problems in Winnipeg". Canadian Geotechnical Journal, vol.18, p.390-401.

Baracos, A., Graham, J., Kjartanson, B.H., and Shields, D.H. 1983. "Geology and soil properties of Winnipeg." Geological Environment and Soil Properties. ASCE Convention, Houston, TX, October 1983, 39-56.

Baracos, A., Kingerski, D. and Leung, K., 1988: "Riverbank Stability Analyses with Uncertain Soil Properties". 41st Canadian Geotechnical Conference, Proceedings, Winnipeg, Manitoba.

Baracos, A., and Kingerski, D., 1998. "Geological and Geotechnical Engineering for Urban Development of Winnipeg, Manitoba in Urban Geology of Canadian Cities". Edited by P.F. Karrow and O.L. White, GAC Special Paper 42, p. 171-190.

Baracos, A., Lew, K.V., 2003. "Riverbank Slides, Erosion and Deposition at 758 Crescent Drive, Winnipeg, Manitoba - Volume 1 Report", prepared for Department of Justice Canada, Winnipeg, Manitoba.

Barbour, S.L., Fredlund, D.G. 1989. "Physico-Chemical State Variable of Clay Soils", In Proceedings, 12th International Conference of Soil Mechanics and Foundation Engineering, Rio de Janeiro, Brazil, vol.3, pp.1839-1843.

Barbour, L.S., Krahn, J., 2004. "*Numerical Modelling – Prediction or Process?"*, Geotechnical News.

Briaud, J.L., Ting, F.C.K., Chen, H.C., Cao, Y., Han, S.W., Kwak, K.W., 2001. "Erosion Function Apparatus for Scour Rate Predictions". ASCE Journal of Geotechnical and Geoenvironmental Engineering, Vol. 127, No. 2, February.

Brooks, G.R., and Nielsen, E., 2000. "Red River, Red River Valley, Manitoba". The Canadian Geographer, 44, no.3, pp.304-309.

Brooks, G.R., 2002. "Floodplain Chronology and Vertical Sedimentation Rates Along the Red River, Southern Manitoba". Geographie Physique et Quaternaire, vol. 56, no. 2-3, p.171-180.

Brooks, G. R., 2003. "Holocene Lateral Channel Migration and Incision of the Red River, Manitoba, Canada". Geomorphology, 54, pp.197-215.

Brooks, G.R., 2003. "Alluvial Deposits of a Mud-Dominated Stream; the Red River, Manitoba, Canada". Sedimentology, 50: 441-458.

Brooks, G.R., St.George, S., Lewis, C.F.M., Medioli, B.E., Nielsen, E, Simpson, S. and Thorliefson, L.H., 2003. "Geoscientific Insights Into Red River Flood Hazards In Manitoba". Geological Survey of Canada Open File Report 4473, 35 p.

Brooks, G.R., 2005. "Overbank Deposition Along the Concave Side of the Red River Meanders, Manitoba, and Its Geomorphic Significance". Earth Surface and Processes and Landforms (in press).
Brooks, G.R., 2007. Personal communication.

Chang, H, 1988. "Fluvial Processes in River Engineering", John Wiley & Sons, Inc., New York.

City of Winnipeg, 2000. "Riverbank Stability Characterization Study". Planning, Property and Development Department, Waterways Section.

Clark, S., 2006. Personal communication.

Darby, S.E., 1998. "Modeling Width Adjustment in Straight Alluvial Channels". Hydrological Processes, 12, pp.1299-1321.

Department of the Interior Canada, Water Power Branch, 1912. "Manitoba Hydrographic Survey Red River Topographic Sheet No.5".

Department of Resources and Development Canada, 1951. "Red River Hydrographic Survey Mile 50.8 to 54.4", Sheet 15 of 41.

Department of Resources and Development - Water Resources Division, 1953. "Red River Basin Investigation - Report on Investigations into Measures for the Reduction of the Flood Hazard in the Greater Winnipeg Area", Manitoba.

Duncan, J.M., 1996. "State-of-the-Art: Limit Equilibrium and Finite-Element Analysis of Slopes", ASCE Journal of Geotechnical Engineering, Vol. 122, No. 7, July, pp.577-596.

Fredlund, D.G., Scoular, R.E.G and Zakerzadeh, N., 2004. "Using A Finite Element Stress Analysis to Compute the Factor of Safety", 52nd Canadian Geotechnical Conference, pp.73-78.

Friedkin, J.F. (1945) A laboratory study of the meandering of alluvial rivers: U.S. Waterways Experiment Station.

Graham, J. and Shields, D.H., 1985. "Influence of Geology and Geologic Processes on the Geotechnical Properties of a Plastic Clay." Engineering Geology, 22, 109-126.

Griffiths, D.V. and Lane, P.A., 1999. "Slope Stability Analysis by Finite Elements", Géotechnique, 49, No.3, pp.387-403.

Hanson, G.J. and Simon, A., 2001. "Erodibility of Cohesive Streambeds in the Loess Area of the Midwestern USA". Hydrological Processes 15(1): 23-38.

Heinzen, R.T., 1976. "Erodibility Criteria for Soils", MS Thesis, University of California, Davis.

Highway Research Board, 1970. “Tentative Design Procedure for Riprap-Lined Channels”, National Academy of Sciences, National Cooperative Highway Research Program, Report 108.

Julien, P.Y., (1998), "Erosion and Sedimentation", Cambridge University Press, NY, USA

Krahn, John, 2003. “The 2001 R.M. Hardy Lecture: The Limits of Limit Equilibrium Analyses”. Canadian Geotechnical Journal, 40: 643-660.

Krahn, John, 2004. “Seepage Modeling with SEEP/W: An Engineering Methodology”, GEO-SLOPE International Ltd, Calgary.

Krahn, John, 2004. “Stress and Deformation Modeling with SIGMA/W: An Engineering Methodology”, GEO-SLOPE International Ltd, Calgary.

Krahn, John, 2004. “Stability Modeling with SLOPE/W: An Engineering Methodology”, GEO-SLOPE International Ltd, Calgary.

Lane, E.W., 1953. “Progress Report on Studies on the Design of Stable Channels by the Bureau of Reclamation”, American Society of Civil Engineers - Proceedings, v79, separate n 280, Sept., 31p.

Langendoen, E.J., 2000. “CONCEPTS - Conservational Channel Evolution and Pollutant Transport System”, USDA-ARS National Sedimentation Laboratory, Oxford, MS.

Macdonald, A.E., Report of the Winnipeg Branch of the Engineering Institute of Canada Committee on Foundations, The Engineering Journal, November 1937.

Manitoba Geological Survey, 2002. “Environmental Geoscience in the Red River Valley”, 2002 Energy and Mines Ministers’ Conference, Winnipeg, Manitoba, CPG/NGSC Field Trip Guide Book.

Man, A., 2005. Personal communication.

Mishtak, J., 1964. “Soil Mechanics Aspects of the Red River Floodway”. Canadian Geotechnical Journal.

Mitchell, J.K. and Soga, K., 2005. “Fundamentals of Soil Behavior 3rd Edition”, John Wiley and Sons Inc., New Jersey.

Morisawa, M., 1968. “Streams: Their Dynamics and Morphology”, McGraw-Hill Book Company, New York.

Morisawa, M.,1985. “Rivers”, Longman Group Limited, New York.

Nielsen, Eric, Brian, W., McKillop, B. and Conley, G.G., 1993. “Fluvial Sedimentology and Peleocology of Holocene Alluvial Deposits, Red River, Manitoba”. Geographie physique et Quaternaie, 1993, Vol. 47 no. 2, p.193-210, 17 fig., 3 tabl.

Olsen, O. J., Florey, Q.L., 1952. "Sedimentation Studies in Open Channels Boundary Shear and Velocity Distribution by Membrane Analogy, Analytical and Finite-Difference Methods," U.S. Bureau of Reclamation, Laboratory Report N. SP-34, August 5.

Osman, A. M., and Thorne, C.R., 1988. “Riverbank Stability Analysis. I: Theory.” Journal of Hydraulic Engineering., 114(2), 134-150.

Partheniades, E., 1965. “Erosion and Deposition of Cohesive Soils”. Journal of Hydraulics Division of the American Society of Agricultural Engineers, 91: 105-139.

Preston, J.H., 1954. “Determination of Turbulent Skin Friction by Means of Pitot Tubes”, Jour. Royal Aeronautical Society, Vol. 8.

Quigley, R.M., 1980. “Geology, Minerology and Geochemistry of Canadian Soft Soils: A Geotechnical Perspective.” Canadian Geotechnical Journal, 17, 261-285.

Raudkivi, A.J., 1976. "Loose Boundary Hydraulics”, Pergamon Press, New York.

Render, F.W., 1970. “Geohydrology of the Metropolitan Winnipeg Area as Related to Ground Water Supply and Construction.” Canadian Geotechnical Journal, 7(3), 243-274.

Richards, K., 1985. “Rivers: Form and Process in Alluvial Channels”, Methuen & Co. Ltd, New York.

Rutherford, D.H., and Baracos, A., 1953. “Damage to Houses - Red River Valley Flood 1950”. Technical Report No.9 of the Division of Building Research, Ottawa, NRC No. 2976, DBR No. 23.

Schumm, S.A., 1960. “The shape of alluvial channels in relation to sediment type”, U.S. Geol. Surv. Prof. Paper 352B.

Shulits, S., 1941. “Rational equation of riverbed profiles”, Trans. Am. Geophys. Union, Vol. 22, pp.622-629.

Simon, A., Curini, A., Darby, S.E., and Langendoen, E.J., 1999. “Streambank Mechanics and the Role of Bank and Near-Bank Processes in Incised Channels.”

Incised River Channels, S.E. Darby and A. Simon, eds., John Wiley and Sons, New York, NY, 123-152.

Simon, A., Langendoen, E.J., Collison, A., Layzell, A., 2003. "Incorporating Bank-Toe Erosion by Hydraulic Shear into a Bank Stability Model: Missouri River, Eastern Montana", American Society of Civil Engineers Water Resources Conference Proceedings, World Water and Environmental Resources Congress.

Simons, D.B., Senturk, F., 1992. "Sediment Transport Technology - Water Sediment Dynamics", Water Resources Publications, Colorado.

Sutherland, H.B., 1966. "The Stability of the River Banks in the Winnipeg Area." Unpublished report to the Rivers and Streams Authority, No.1, Winnipeg, MB.

Teller, J.T. and Fenton, M.M., 1980. "Late Wisconsinan Glacial Stratigraphy and History of Southeastern Manitoba." Canadian Journal of Earth Sciences, 17, 19-35.

Teller, J.T. and Clayton, L., 1983. "Glacial Lake Agassize" Special Paper 26, Geological Association of Canada, 3-5.

Thorleifson, H., Brooks, G., Hanuta, I., Kroker, S., Matile, G., Nielson, E., Prevost, C., and Rannie, W. 1998. "Red River Flooding: Evolutionary Geomorphic Trends and Evidence for Major Floods in Recent Centuries (NTS 62H/W)". In Manitoba Energy and Mines, Geological Services, report of Activities, 1998, p.186-195.

Thorne, C.R., 1982. "Processes and Mechanisms of River Bank Erosion", Gravel-Bed Rivers, edited by R.D. Hey, J.C. Bathurst and C.R. Thorne. John Wiley and Sons Ltd.

Tutkaluk, J., 2000. "The Effect of Seasonal Variations in the Red River and Upper Carbonate Aquifer on Riverbank Stability in Winnipeg", M.Sc. Thesis, University of Manitoba.

Tutkaluk, J., Blatz, J., Graham, J., and Wingrove, T., 2002. "A Generic Study of the Influence of a Confined Aquifer on Slope Stability in Lacustrine Clay Slopes". Proceedings from the 2002 Canadian Geotechnical Conference.

APPENDIX A

Winnipeg Free Press Article:
"The River's Toll" - Sunday, August 28th, 2005

(used with permission from
Steve Pona of the Winnipeg Free Press, obtained July 17th, 2007)

Winnipeg Free Press
SUNDAY, AUGUST 28, 2005

PERSPECTIVE

Editor, Boris Hrybinsky 697-7430
boris.hrybinsky@freepress.mb.ca
B1

winnipegfreepress.com

Brian Turnbull looks out over his property, which is rapidly crumbling into the river.

BORIS MINKEVICH / WINNIPEG FREE PRESS

High river levels have caused unprecedented damage and loss of land to private property and parks along the Red

THE RIVER'S TOLL

By Patti Edgar

BERYL and Brian Turnbull recall summer nights when they would eat dinner in a glassed-in gazebo in their riverfront backyard, reluctantly walking back to their home at midnight.

This month, six metres of their yard tumbled into the Red River, on top of the seven metres they lost in the 1997 flood. Now buried in the silt below their home are a bird bath, a flagpole, an elm, a spruce and a rock garden.

The gazebo survived thanks to a taut rope and pilings, but it's now dangling precariously over the newly created cliff. The Turnbulls plan to take it apart and rebuild it closer to the house.

"It's just devastating. We lost quite a lot of property in '97 but it didn't really affect our lifestyle," said Beryl. "I've accepted it now, but I was too upset to go down there for awhile."

Four months of higher-than-normal river levels this spring and summer caused riverbank damage within the city limits as bad — if not worse — than the 1997 flood, says the city's expert on the topic.

"This is something that was unprecedented," said riverbank engineer Don Kingerski.

"The '97 flood was very, very tough on our riverbanks, but we didn't have as long of a sustained flooding as we did this time around and maybe that's entered into it. From my observation, it's not unlike the '97 flood event in terms of damage."

The water started rising in early April this year, peaked on July 5 at 6.4 metres above normal summer levels, then dropped back to a normal height (two metres above winter freezing levels) on Aug. 9.

Kingerski can't estimate the damage from this year's flood yet, but hopes to hire an engineering student this fall to help him survey the destruction. On an average year, tumbling riverbanks eat up an estimated $1 million of real estate and hundred of elms.

The riverbank expert has received more phone calls this summer about damage to private property than he has during his 20 years with the city.

Documenting the damage

Earlier this week, *Free Press* photographer Boris Minkevich and reporter Patti Edgar boated up the Red River from the floodgates near the Perimeter Highway to North Perimeter Park to document the damage, especially in the hard-hit southwest of the city.

The Assiniboine River also flooded, with land slipping away upstream near Headingley, where Kingerski never expected to see drops.

Along the banks of the Red River, backyards have washed down the river, while gazebos and sun porches are just a few steps away from the edge.

Parkland slumped into the rivers, taking along trees and leaving benches precariously close to steep cliffs.

An untold number of riverbank trees have vanished, while others are threatening to tumble because fast water has carved their roots out of the soil.

Tree experts fear the unusually long flood could be felt for years to come on the elms left standing. Submerged roots don't get the oxygen they need during the summer, putting stress on the trees that could eventually kill them.

Some of the worst damage to private property is through Fort Garry and St. Vital, where the river narrows and bends, undercutting the soft riverbanks. North of The Forks, the damage is less severe, but if it hadn't been for last winter's $1.2 million of work along the shoreline of the Elmwood Cemetery, Kingerski said gravestones could have washed away.

Too much water, too long

Like a heavy, wet sponge, the banks of Winnipeg's rivers were saturated by rain this spring.

High, fast-running water scraped away at soft, unsupported banks like those in Crescent Park. When the river levels dropped, the support on those heavy wet banks disappeared, sending soil tumbling.

Homeowners are responsible for tackling their own riverbank problems, ranging in cost from $500 per metre of waterfront to $5,000.

St. Norbert Coun. Justin Swandel, who lives on the Red River, says the huge price tag is keeping homeowners from doing the needed work, even though they can lose metres of property in one flood. At city hall this spring, he proposed offering a tax credit as encouragement.

"We are losing land all the time — a one-acre lot is all of a sudden a three-quarter lot. That could affect the assessment base."

Others argue city hall can't afford to help. The city owns riverbank that collectively needs $80 million worth of stabilization work and staff have drafted a list of 11 critical stabilization projects in city parks worth $1 million each.

However, once again there's only $200,000 in the budget this year for slumping riverbanks. Longtime riverbank champion Coun. Harry Lazarenko had to fight his fellow councillors to get any money at all.

With no tax incentives on the horizon, Riverside Drive homeowner Jim Flood will have to share with his neighbour the estimated $50,000 cost of repairing their backyards from a massive slide earlier this month that was triggered by flooding.

But the boating enthusiast tries to focus on the bigger loss to the city.

Trees and parkland slip into the rivers, while fluctuating water levels make this city's natural asset less accessible for businesses and residents.

"It's a nice gift for the city to have that we aren't even using," said Flood. "Stabilize it, reduce erosion and make the river more economically viable for tourism, recreation and sightseeing."

Riverside Drive resident Jim Flood now has to use a ladder to get down to the waterfront after riverbank erosion ate away part of his property.

BORIS MINKEVICH / WINNIPEG FREE PRESS

The damage, in photographs / B4,5

patti.edgar@freepress.mb.ca

SUNDAY
AUGUST 28, 2005

Winnipeg Free Press

SUNDAYSPECIAL: Abnormally high water levels on the Red River this summer have caused as much property damage in the city as the Flood of '97

Top, Brian Turnbull of Jubilee Avenue surveys damage to his riverside gazebo. Above, the structure crumbles on the bank of the Red River.

GAZEBOS hanging on by a thread over a crumbled riverbank... hundreds of elms washed up in huge logjams near city bridges... acres of prime real estate reduced to river sludge. Flooding on the Red River has taken a huge toll this summer — perhaps the worst in decades. Millions of dollars are needed to shore up the riverbanks and stop the staggering losses. But the city has only $200,000 in its budget for the task. We've got the story, plus a map and two pages of photos, in Perspective.

THE RIVER'S TOLL / B1,4,5

‘This is something that was unprecedented’

— Riverbank engineer Don Kingerski.

Bunn’s Creek
Noticeable riverbank erosion is occurring to the north of the creek.

Shooters Family Golf Centre
From the river, golfers at Shooters Family Golf Centre appear to be swinging out of a sand trap, but owner Guido Cersani laid the sand on four riverside holes that had been submerged in the flood to cover the mud. For a month, the back nine was closed and the water caused $150,000 in damage not covered by insurance. The entire course is open now and Cersani bills it as more challenging thanks to the sand.

Scotia Street
A homeowner takes a break as more and more of the property disappears.

Crescent Drive home
The flood waters sliced under a modest rental home on Crescent Drive, buckling a massive balcony this month. “This house is in danger of going in. This isn’t a gradual drop, it’s like a cliff,” said Eric Matthies, a longtime next-door neighbour. His home isn’t threatened by the slump - yet. “I’m concerned the cliff will do a right turn.”

Scotia Street
Hopefully, no one was in the dog-house when it tumbled toward the river.

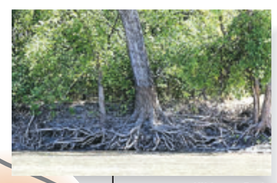

Kildonan Park
If you’ve ever wondered what a tree’s roots look like exposed, now you know.

North of St. John’s Park
While St. John’s Park is on the priority list for shoreline stabilization, a nearby homeowner says properties further north rarely experience erosion. But this summer a swirling undercurrent collapsed at least a metre of yard.

Mager Drive
Riverbank erosion threatens a home just south of St. Mary’s and St. Anne’s roads.

St. Mary’s Road
An apartment block near the intersection with St. Anne’s Road edges closer to the river.

Kildonan Drive
A faded wood fence dangles over the Red River at the south end of Kildonan Drive, revealing how much land has slipped into the Red River.

Kildonan Park
The park is a little bit smaller now, thanks to riverbank erosion.

Norwood Bridge
A large log-jam gathers on the southwest side of the bridge.

St. Cross Street
A glassed-in gazebo belonging to a house near St. John’s Park is dangerously close to the banks.

Lyndale Drive
The banks along here have fallen in the river.

Jubilee Avenue
Six metres of Beryl and Brian Turnbull’s yard tumbled into the Red River this summer, on top of the seven metres they lost in 1997. A bird bath, a flagpole, an elm, a spruce and a rock garden are buried in the silt below. The gazebo survived thanks to a taut rope and pilings, but it’s now dangling precariously over a cliff. The Turnbulls plan to take it apart and rebuild it closer to the house.

Jubilee Avenue
This gazebo, at home near the Bridge Drive-In, is holding on.

Riverside Drive
Jim Flood’s backyard suffered massive erosion.

Riverside Drive
A ladder is propped up against a slumped riverbank so Barry McMillian can reach his boat. McMillan and neighbour Jim Flood spent $14,000 two years ago shoring up the bank in front of both homes with limestone. This August, four metres of their backyards tumbled into the Red River, burying the project and yanking out trees and lawn along four properties. A heartbroken Flood points to ominous cracks along the soil that show where the grass will slump next, taking along at least one more tree. He estimates repairs could cost $50,000 for both properties. “My story isn’t unique. Perhaps the money we put in reduced the amount of land we lost.”

St. Vital Park
Free Press reporter Patti Edgar surveys the massive loss of riverbank.

University of Manitoba
Erosion is visible around the first bend on the south side of the university.

McNulty Crescent
Contractor Walter Goshulak prepares to make repairs from unusually high river levels that tore away a deck and stairs, tossed over a picnic table and swamped a garden.

Crescent Drive Park
There’s not much room left for visitors to sit and enjoy the view on this wooden bench along the river.

Crescent Drive Park
This tree appears to be sliding toward the river, roots and all.

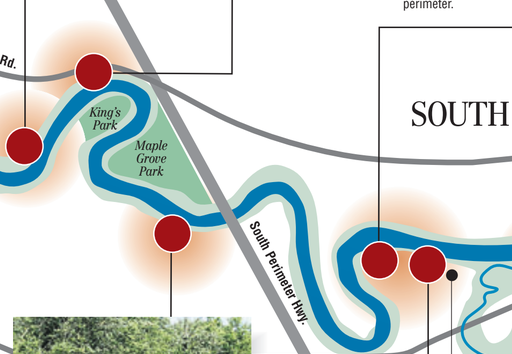

Kilkenny Drive
Trees along the encroaching banks have fallen into the river.

St. Norbert Heritage Park
Signs in the park are now dangerously close to the banks.

Off a private road in St. Norbert
A curve in the Red River creeps closer each year to this rural rental home. The water is now just a few steps away from the sunroom. The bulk of the damage happened in 1997, but this summer two more trees were swept away.

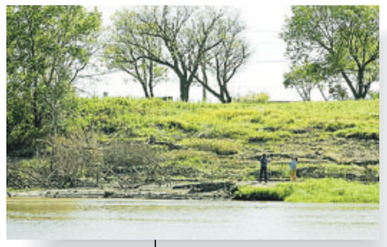

St. Mary’s Road
People check out the damage along the riverbank that collapsed near the south perimeter.

Lord Avenue
Homes are protected from erosion.

Lord Avenue
This $1.5-million wall was completed in 2003 to protect a handful of homes along Lord Avenue. The flood-reduction project was one of about two dozen in the city paid for out of a $12-million pot from all three levels of government. Residents will pay 10 per cent of the costs back through fees added to their city tax bills.

RIVER ELEVATIONS 2005

Crescent Drive Park, St. Vital Park, Kildonan Park, Bunn’s Creek, Lyndale Drive Park
All five parks are on the list of 11 slumping city parks each needing about $1 million worth of stabilization work. City-owned riverbank collectively needs $80 million worth of stabilization.
In these parks this summer, high water swept off with tress and scraped away at soft banks, some of which collapsed when the river level dropped. At Churchill Park, part of a pathway was swept down the river.

TOP 11 RIVERBANK STABILIZATION PROJECTS ON CITY LAND:

- St. Vital Park
- Lyndale Drive Park
- St. John’s Park
- King’s Park
- Churchill Park
- Red River at Bunn’s Creek
- Fort Rouge Park
- Crescent Drive Park
- King’s Park
- Evans Avenue at Cusson Street
- Granite Curling Club/Mostyn Park